1 A coevolution experiment between Flavobacterium johnsoniae and

2 Burkholderia thailandensis reveals parallel mutations that reduce antibiotic

3 susceptibility

4

- 5 John L. Chodkowski¹ and Ashley Shade^{1,2,3*}
- 6 Department of Microbiology and Molecular Genetics, Michigan State University, East Lansing, MI 48824, USA
- ²Department of Plant, Soil and Microbial Sciences, Michigan State University, East Lansing, MI 48824, USA
- 8 ³Program in Ecology, Evolution and Behavior, Michigan State University, East Lansing, MI 48824, USA
- 9 * Corresponding author and material requests. Email: shadeash@msu.edu; ORCiD: 0000-0002-7189-3067

10

11

13

14

15

Acknowledgements

We thank Dr. Mark McBride for sending us the plasmid pYT354 in DH5aMCR used for recombinant

construction and strain HB101 used for triparental conjugation. We also thank Dr. Yongtao Zhu for his consultation

in creating F. johnsoniae recombinants. Lastly, we thank Dr. Colin Manoil and members of the Manoil laboratory

for providing transposon mutants.

16

17

18

19

20

21

22

23

Abstract

One interference mechanism of bacterial competition is the production of antibiotics. Bacteria exposed to antibiotics can resist antibiotic inhibition through intrinsic or acquired mechanisms. Here, we performed a coevolution experiment to understand long-term consequences of antibiotic production and antibiotic susceptibility for two environmental bacterial strains. We grew five independent lines of the antibiotic-producing environmental strain, *Burkholderia thailandensis* E264, and the antibiotic-inhibited environmental strain, *Flavobacterium johnsoniae* UW101, together and separately on agar plates for 7.5 months (1.5 month incubations), transferring each

line five times to new agar plates. We observed that the F. johnsoniae ancestor could tolerate the B. thailandensisproduced antibiotic through efflux mechanisms, but that the co-evolved lines had reduced susceptibility. We then sequenced genomes from the coevolved and monoculture F. johnsoniae lines, and uncovered mutational ramifications to the long-term antibiotic exposure. The coevolved genomes from F. johnsoniae revealed four potential mutational signatures of reduced antibiotic susceptibility that were not observed in the evolved monoculture lines. Two mutations were found in tolC: one corresponding to a 33 bp deletion and the other corresponding to a nonsynonymous mutation. A third mutation was observed as a 1 bp insertion coding for a RagB/SusD nutrient uptake protein. The last mutation was a G83R nonsynonymous mutation in acetyl-coA carboxylayse carboxyltransferase subunit alpha (AccA). Deleting the 33 bp from tolC in the F. johnsoniae ancestor reduced antibiotic susceptibility, but not to the degree observed in coevolved lines. Furthermore, the accA mutation matched a previously described mutation conferring resistance to B. thailandensis-produced thailandamide. Analysis of B. thailandensis transposon mutants for thailandamide production revealed that thailandamide was bioactive against F. johnsoniae, but also suggested that additional B. thailandensis-produced antibiotics were involved in the inhibition of F. johnsoniae. This study reveals how multi-generational interspecies interactions, mediated through chemical exchange, can result in novel interaction-specific mutations, some of which may contribute to reductions in antibiotic susceptibility.

Key words: *Burkholderia thailandensis* E264, *Flavobacterium johnsoniae* UW101, coevolution, TolC, efflux, thailandamide, interference competition

42

43

44

45

46

47

48

24

25

26

27

28

29

30

31

32

33

34

35

36

37

38

39

40

41

Introduction

Cultivation-independent sequencing of environmental microbial DNA has revealed the prevalence of antibiotic resistance genes in pristine environments (Allen at al. 2010), indicating that antibiotics and their corresponding resistance mechanisms have long-evolved in natural environments that predate their use in medicine (D'Costa et al. 2006). For example, glycopeptide antibiotics and resistance mechanisms have been present in bacterial genomes for at least 150 million years (Waglechner et al. 2019). Thus, it is expected that understanding the

evolution of antibiotic resistance in "natural" settings will provide insights into emerging mechanisms of antibiotic resistance that may be useful for addressing resistance in clinical settings (Walsh 2013).

Microbial antibiotic production in the environment is typically viewed through the lens of competition (van der Meij et al. 2017). Bacteria produce antibiotics that interfere directly with competitors by inflicting cell damage (Hibbing et al. 2010). The DNA blueprints for antibiotics are organized in biosynthetic gene clusters (BSGC), in which locally proximal genes collectively encode the pathway for molecule production (Medema et al. 2015). The activation of BSGCs is typically tied to stress regulation (Baral et al. 2018), suggesting antibiotic production can be deployed as a survival strategy when conditions are not optimal for growth (Granato et al. 2019).

Bacteria can survive antibiotic exposure through the upregulation of intrinsic resistance mechanisms and can achieve antibiotic resistance through acquired mechanisms (e.g. Mutation or horizontal gene transfer; Arzanlou et al. 2017). Multidrug efflux pumps are particularly interesting because they can provide both intrinsic and acquired resistance mechanisms (Poole 2004). For example, low-levels of antibiotic exposure can upregulate intrinsic mechanisms of resistance, such as efflux pumps (Du et al. 2018; Frimodt-Møller and Løbner-Olesen 2019). The survival of bacteria to low levels of antibiotics can facilitate adaptive resistance (Ebbensgaard et al. 2020). This has been demonstrated by clinically relevant antibiotic resistance achieved via efflux pumps (Blair et al. 2014). Therefore, studying multigenerational interactions between antibiotic-producing and antibiotic-inhibited environmental isolates may provide insight into evolutionary dynamics driving antibiotic resistance.

We were interested in the competitive ability of two environmental strains, *B. thailandensis* and *F. johnsoniae*. A previous study examined the competitive ability of *F. johnsoniae* against *B. thailandensis* through contact-dependent mechanisms involving the type VI secretion system (Russel et al. 2014). Given the nature of *B. thailandensis* as a prolific secondary metabolite producer, including various antibiotics (Mao et al. 2017), and the various TolC efflux systems observed in *F. johnsoniae*, we wanted to expand the exploration of interspecies competition between these strains by focusing on contact-independent mechanisms. Preliminary results suggested that *F. johnsoniae* was susceptible to a *B. thailandensis*-produced antibiotic(s), but intrinsic mechanisms, such as efflux systems, allowed *F. johnsoniae* to tolerate the presence of the antibiotic(s) and permit growth on agar. We then tested whether these intrinsic mechanisms of antibiotic(s) tolerance would pave the way for mutational acquisition in *F. johnsoniae* that would make it less susceptible to antibiotic(s).

We performed an agar-based experimental coevolution with B. thailandensis and F. johnsoniae. These strains were co-plated together and, in parallel, also plated in monocultures on M9 minimal medium agar plates containing 0.2% glucose (M9-glucose; % v/v) for over the span of 7.5 months. B. thailandensis and F. johnsoniae were co-plated such that B. thailandensis antibiotic inhibition of F. johnsoniae could occur without intergrowth of the colonies. By comparing outcomes of the coevolved lines to the evolved monoculture lines, we asked: What are the genetic and phenotypic repercussions of coevolution and how consistent are they across independent, replicate lines? What are the genetic signatures of F. johnsoniae of reduced antibiotic susceptibility? What is the antibiotic produced by B. thailandensis that inhibits F. johnsoniae? We found that coevolved F. johnsoniae lines reduced susceptibility to the B. thailandensis-produced antibiotic while evolved monoculture lines remained susceptible. A 33 bp deletion in tolC and a nonsynonymous mutation in accA suggested two different paths to the evolution of reduced antibiotic susceptibility in F. johnsoniae. The ancestor F. johnsoniae strain became less susceptible after we deleted the tolC 33 bp region, but not to an equivalent level observed in the coevolved lines. This result suggests that multiple mutations may contribute to the antibiotic susceptibility. Though genomics from B. thailandensis did not further inform as to the bioactive compound(s), a mutation in F. johnsoniae provided evidence that thailandamide, a previously described antibiotic that inhibits fatty acid synthesis (Wu and Seyedsayamdost 2018), was among the bioactive compounds that inhibited F. johnsoniae. Our data also suggest that multiple antibiotics produced by B. thailandensis contributed to the observed inhibition of F. johnsoniae.

93

94

95

96

97

98

99

100

101

76

77

78

79

80

81

82

83

84

85

86

87

88

89

90

91

92

Results

F. johnsoniae is inhibited by a bioactive compound(s) produced by B. thailandensis

We first observed that *B. thailandensis* inhibited *F. johnsoniae* when co-plated on M9-agar plates (Fig. 1). *B. thailandensis* exhibited radial growth on all edges along the circumference of the colony, while the *F. johnsoniae* colony proximal to *B. thailandensis* was inhibited. However, the distal end of the *F. johnsoniae* colony grew away from *B. thailandensis*, suggesting that *F. johnsoniae* may have intrinsic mechanisms to reduce antibiotic susceptibility. We note that, despite efforts to do so, we were unable to purify and directly link the antibiotic(s) that inhibited *F. johnsoniae*. We still use the terminology antibiotic(s) to refer to any number of compounds that may be

inhibiting *F. johnsoniae*, whether that was an antibiotic derived from a BSGC or a by-product of *B. thailandensis* metabolism that was bioactive against *F. johnsoniae*.

Efflux allows F. johnsoniae to grow in the presence of a B. thailandensis-produced antibiotic

Given the growth pattern of *F. johnsoniae* when co-plated with *B. thailandensis*, we hypothesized that efflux contributed to *F. johnsoniae* as an intrinsic mechanism to reduce antibiotic susceptibility. We collected the organic fraction from spent supernatant of *B. thailandensis* grown in monoculture, which contained the antibiotic(s). We then treated *F. johnsoniae* cultures with the supernatant alone and in combination with daidzein, an efflux pump inhibitor (Aparna et al. 2014). While the supernatant inhibited *F. johnsoniae*, daidzein did not, and the supernatant with daidzein significantly inhibited *F. johnsoniae* more than the supernatant alone (Fig. 2, Supplementary Fig. 1). This suggested that *F. johnsoniae* had intrinsic mechanisms to reduce antibiotic susceptibility via efflux. extrusion and, these intrinsic mechanisms of antibiotic tolerance could allow for mutational acquisition to further decrease antibiotic susceptibility. We tested this hypothesis by performing a coevolution experiment.

Coevolutionary outcomes of B. thailandensis-F. johnsoniae interactions

To better understand the underlying factors contributing to *F. johnsoniae* antibiotic susceptibility, we next asked how the susceptibility to antibiotic(s) in *F. johnsoniae* would change when coevolved with *B. thailandensis*. We performed an agar-based coevolution experiment with 10 μLvolume of two liquid overnight cultures spotted 14 mm apart to allow for extracellular chemical interactions, allowed to grow into colonies, and passaged onto another plate before intergrowth of the colonies could occur (**Fig 3**). The colonies spotted were either one of each of *B. thailandensis* and *F. johnsoniae* ("coevolved"), two of the same *B. thailandensis* colonies, or two of the same *F. johnsoniae* colonies ("monoculture"). All monoculture controls were grown in parallel to the co-evolved lines (**Fig. 3**). We observed that the radial growth increased between the 5th plate passage and the 1st plate passage within both the monoculture evolved and coevolved lines (Wilcoxon Rank-Sum; p-values < 0.01), suggesting increased growth capabilities on the M9-glucose medium over time. The radial growth of *F. johnsoniae* generally increased with each

successive plate passage (Fig. 4, Supplementary Fig. 2). In addition, *B. thailandensis* substantially inhibited *F. johnsoniae* on the first plate (Supplementary Fig. 2), as the radial growth of the coevolved lines was significantly less than the radial growth of the monoculture lines (q-value = 0.039). In successive plate passages, the radial growth in coevolved lines were insignificantly different to the monoculture evolved lines (q-values >=0.15) with the exception of plate passage 4 (q-value= 0.039). This suggested that co-evolved lines of *F. johnsoniae* were becoming less susceptible to *B. thailandensis*-produced antibiotics. Indeed, when a freezer stock from a coevolved *F. johnsoniae* line and a freezer stock from the corresponding monoculture *F. johnsoniae* line were plated with the *B. thailandensis* ancestor, *F. johnsoniae* from the coevolved line displayed more radial growth and thus less antibiotic susceptibility as compared to the evolved monoculture control (Supplementary Fig. 3). Interestingly, colonies from the coevolved *F. johnsoniae* lines were also able to resist colony invasion by *B. thailandensis*, while colonies from the evolved monoculture lines could not (Supplementary Fig. 4). Overall, these results suggest that coevolved *F. johnsoniae* evolved decreased susceptibility to antibiotics as an outcome of long-term exposure to and engagement with *B. thailandensis*.

Whole genome sequencing reveals genetic signatures of reduced antibiotic susceptibility

We performed whole genome sequencing to discover mutations that may have contributed to reduced antibiotic susceptibility in the *F. johnsoniae* coevolved lines. We sequenced a clonal isolate from the *F. johnsoniae* ancestor and clonal isolates from each of the 5 independent coevolved and monoculture evolved lines from the final (fifth) plate passage. We detected mutations in all coevolved and monoculture evolves isolate genomes compared to the ancestor (Table 1, Supplemental File 1). *F. johnsoniae* lines coevolved with *B. thailandensis* acquired mutations that were distinct from acquired mutations in *F. johnsoniae* lines grown in monocultures (Table 2, Supplementary Fig. 5).

Table 1. Summary of mutation types observed in F. johnsoniae from the (co)evolution experiment. Mutations are from five representative clonal isolates after the final (5^{th}) plate passage and the ancestor.

F. johnsoniae						
isolate	Total	Insertion	Deletion	Nonsynonymous	Synonymous	Nonsense

Coevolved rep 1	6	2	1	3	0	0
Coevolved rep 2	5	0	2	3	0	0
Coevolved rep 3	6	0	0	5	1	0
Coevolved rep 4	5	1	1	3	0	0
Coevolved rep 5	5	1	2	2	0	0
Evolved monoculture rep 1	6	1	3	2	0	0
Evolved monoculture rep 2	7	1	3	2	0	1
Evolved monoculture rep 3	6	0	4	2	0	0
Evolved monoculture rep 4	6	2	1	3	0	0
Evolved monoculture rep 5	3	0	2	0	0	1
Ancestora	2	0	1	1	0	0

^aAncestor mutations that were also observed in evolved line(s) were not included in the tally of evolved line mutations.

be evidence of an acquired mutation that would reduce antibiotic susceptibility (Table 2). A *tolC* mutation was observed in 4 out of the 5 coevolved lines. While *F. johnsoniae* contains 16 *tolC* genes (Supplementary Table 1), the same gene was mutated in 4 independent replicates. Though, the TolC harboring mutations in coevolved isolates (FJOH_RS06580) only had 24.2% or less protein sequence identity with all other TolC proteins in *F. johnsoniae* (Supplementary Table 2). Furthermore, there was evidence of parallel evolution at the nucleotide level, as 3/5 of the coevolved lines had the same *tolC* 33 bp deletion at the same *tolC* locus (Supplemental File 1). This deletion was from nucleotides 261-293 in the FJOH_RS06580 coding sequence, resulting in an in-frame deletion (Fig. 5). This deletion affected one of the extracellular loops of TolC. The WT sequence revealed a 11 bp direct repeat, occurring

before the deletion and representing the last 11 bp of the 33 bp deletion. This suggests that the deletion may have

F. johnsoniae evolved isolates harbored mutations in an efflux outer membrane protein, TolC, and could

occurred during a replication deletion event. The other mutation in FJOH_RS06580 (coevolved line 3) was a single nucleotide polymorphism (G247A in the coding sequence) that resulted in a nonsynonymous mutation (G83R). Protein modeling suggested that this mutation resulted in a decreased diameter of the efflux channel (Supplementary Fig. 6). Coevolved line 4 did not harbor a mutation in FJOH_RS06580 but instead had a unique bp insertion in a *ragB/susD* nutrient uptake outer membrane protein (FJOH_RS24865). Guanine was inserted between nucleotide positions 792 and 793 in the coding sequence for FJOH_RS24865. This frameshift mutation resulted in a premature termination codon 6 bp downstream of the insertion, likely rendering the protein nonfunctional. Mutations were also uniquely found in regulators of coevolved isolates including, a small insertion in a TetR/AcrR family transcriptional regulator in coevolved isolate 1, a nonsynonymous mutation in an OmpR family response regulator in coevolved isolate 2, and a nonsynonymous mutation in a LytTR family response regulator within the same loci of coevolved isolates 2 and 5. These regulators may have indirect effects on antibiotic susceptibility (e.g. up/downregulation of efflux pumps).

Table 2. Distinctions and overlaps of loci with mutations unique to the *F. johnsoniae* lines that were coevolved with *B. thailandensis*. These mutations were detected (+) in at least one coevolved line and not present (-) in any of the evolved *F. johnsoniae* monocultures

F. johnsoniae

Locus	Annotation	Rep 1	Rep 2	Rep 3	Rep 4	Rep 5
FJOH_RS00255	acetyl-CoA carboxylase carboxyltransferase subunit alpha	-	-	C479A	-	-
FJOH_RS02320	aminomethyl-transferring glycine dehydrogenase	-	-	-	-	Δ1 bp (504)
FJOH_RS04780	hypothetical protein	G329C	-	-	-	-
FJOH_RS06580	TolC family protein	Δ33 bp (261-293)	Δ33 bp (261- 293)	G247A	-	Δ33 bp (261- 293)
FJOH_RS07830	NAD(P)/FAD-dependent oxidoreductase	-	C148A	-	-	-
FJOH_RS09515	LyTR family DNA-binding domain-containing protein	-	G46A	-	-	C44T
FJOH_RS09520	Histidine kinase	825insG	-	G496A	Δ1 bp (621)	-
FJOH_RS11170	Gfo/Idh/MocA family oxidoreductase	-	-	G273C	-	-
FJOH_RS12240	AIR synthase-related protein	-	-	C791T	-	-
FJOH_RS14175	response regulator transcription factor	-	С269Т	-	-	-
FJOH_RS20510	TetR/AcrR family transcriptional regulator	201insT	-	-	-	-
FJOH_RS21875	glycoside hydrolase	T1489C	-	-	-	-
FJOH_RS24865	RagB/SusD family nutrient uptake outer membrane protein	-	-	-	793insG	-
FJOH_RS25290	phosphoribosylanthranilate isomerase	-	-	-	T50C	-

Mutations were also observed in (co)evolved *B. thailandensis* lines (Supplemental File 1). Most mutations were unique to individually sequenced isolates. Exact mutational parallelism was present, (e.g. flagellar assembly protein FilH, TetR/AcrR transcriptional regulator, and efflux periplasmic adaptor subunit) but was observed across both monoculture evolved lines and coevolved lines, indicating that these mutations were not acquired due to the presence of *F. johnsoniae*.

One mutation of interest was observed in *B. thailandensis* coevolved line 4: a 7 bp insertion in BTH_II1238. This gene codes for *btaP*, a metallo-β-lactamase involved in the production of the bactobolin

antibiotic (Duerkop et al. 2009). The insertion resulted in a premature stop codon, rendering the protein non-functional. A previous study showed abrogated bactobolin production in a *btaP* knockout (Carr et al. 2011), meaning that the insertion observed in our study likely abrogated bactobolin production as well. To ascertain that *F. johnsoniae* inhibition persists in the presence of *B, thailandensis* with abrogated bactobolin production, we co-plated *F. johnsoniae* with a *B. thailandensis btaK*::T23 transposon mutant. We had possession of this transposon mutant, and, similar to the *btaP* mutant, the *btaK* (BTH_II1233) mutant has been confirmed to abrogate bactobolin production (Duerkop et al. 2009). As expected, we found that the *B. thailandensis btaK*::T23 transposon mutant inhibited *F. johnsoniae* despite the inability to produce bactobolin (Supplementary Fig. 7), suggesting either that bactobolin was ineffective against *F. johnsoniae* or that multiple antibiotics were involved in *F. johnsoniae* inhibition. Overall, there was no mutational genomic evidence to help to inform the *B. thailandensis*-produced antibiotic(s) that inhibits *F. johnsoniae*.

The FJOH RS06580 tolC 33 bp deletion reduces antibiotic susceptibility

We asked whether the mutations in tolC or the mutation in ragB/susD observed in coevolved F. johnsoniae lines would reduce antibiotic susceptibility to the B. thailandensis-produced antibiotic(s). These mutations were amplified from the coevolved F. johnsoniae lines and recombined into the ancestor so that the ancestor would only harbor one of these mutations and not any of the additional mutations observed in the coevolved lines. Strains and plasmids used to make recombinant F. johnsoniae are outlined in Table 3. Ancestor B. thailandensis inhibited the F. johnsoniae ancestor and recombinant strains reG247A_tolC and re792_793insG_ragB (Fig. 6). In fact, reG247A_tolC appeared more inhibited compared to the F. johnsoniae ancestor, suggesting that a decreased diameter to the TolC efflux channel (inferred from protein structure predicted by SWISS-MODEL) is detrimental to fitness. In contrast, recombinant strain $re\Delta33$ _tolC was the least inhibited when plated with ancestor B. thailandensis, suggesting that the 33 bp deletion reduces susceptibility to an antibiotic(s) (Fig. 6B). Thus, it appears that F. johnsoniae uses intrinsic mechanisms to reduce antibiotic susceptibility (e.g. efflux pumps, Fig. 2) but also acquired a mutation in the outer membrane protein of an efflux system that further reduced susceptibility to a B. thailandensis-produced antibiotic(s). The acquired mutation evolved independently in 3/5 of the coevolved isolates at the same tolC locus. However, the 33 bp deletion in tolC alone did not reduce antibiotic susceptibility to the same degree observed in the coevolved lines, as the coevolved lines harboring the tolC 33 bp deletion with

additional mutations less susceptible to *B. thailandensis*-produced antibiotic(s) compared to the recombinant strain $re\Delta 33_tolC$ (Supplementary Fig. 8). This suggests that coevolved lines harboring the tolC 33 bp mutation may contain synergistic mutations contributing to further reductions in antibiotic susceptibility.

Table 3. Strains and plasmids used in this study.

^aAbbreviations: Ap^r-ampicillin resistance, 100 micrograms per ml; Km^r kanamycin resistance 30 micrograms per

Strain or plasmid	Description ^a	Source or reference	
Escherichia coli strains			
DH5αMCR	Strain used for general cloning	Life Technologies (Grand Island, NY)	
HB101	Strain used with pRK2013 for triparental conjugation		
DH5αMCR_pYT354	pYT354 in DH5amcr; sacB-containing suicide vector	Helinski 1979 Zhu et al. 2017	
B. thailandensis strain			
E264 (ATCC 700388)	Wild type	Brett et al. 1998	
F. johnsoniae strains			
UW101 (ATCC 17061)	Wild type	McBride et al. 2009	
CoE_\Delta33_tolC	Coevolved strain containing a 33 bp (261-293) deletion in <i>tolC</i> (FJOH_RS06580)	This study	
CoE_G247A_tolC	Coevolved strain containing a nonsynonymous mutation (G247A) in <i>tolC</i> (FJOH RS06580)	This study	
CoE_792_793insG_ <i>ragB</i>	Coevolved strain containing an insertion (G) between bps 792 and 793 in <i>ragB/susD</i> (FJOH RS24865)	This study	
reΔ33_tolC	tolC (FJOH_RS06580) 33 bp deletion placed in ancestor	This study	
reG247A_tolC	tolC (FJOH_RS06580) G247A mutation placed in ancestor	This study	
re792_793insG_ragB	ragB/susD (FJOH_RS24865) bp (G) insertion placed between bps 792 and 793 in ancestor	This study	
Plasmids			
pYT354	sacB-containing suicide vector; Apr (Emr). pYT354 is modified from pYT313 with different multiple cloning site	Zhu et al. 2017	
pJC101	Construct used to replace ancestral native <i>tolC</i> (FJOH_RS06580) with <i>tolC</i> 33 bp deletion	This study	
pJC102	Construct used to replace ancestral native <i>tolC</i> (FJOH_RS06580) with <i>tolC</i> G247A	This study	
pJC103	Construct used to replace ancestral native $ragB/susD$ This study (FJOH RS24865) with $ragB/susD$ 792 793insG		
pRK2013	Helper plasmid for triparental conjugation; Km ^r	Figurski and Helinski 1979	

ml; (Em^r-erythromycin resistance, 100 micrograms per ml for *F. johnsoniae*). Antibiotics resistance phenotypes

listed in parentheses (Em) are those expressed in F. johnsoniae but not in E. coli. Antibiotics resistance phenotypes

listed not in parentheses (Ap, Km) are those expressed in E. coli but not in F. johnsoniae.

We then quantified the extent of F. johnsonaie antibiotic susceptibility. We grew B. thailandensis in spent F. johnsoniae medium and extracted the organic fraction from the spent B. thailandensis medium. The organic layer contained unknown compound(s) that were bioactive against F. johnsoniae. A Kirby-Bauer disk diffusion assay was performed to quantify the zone of inhibition (ZOI) of our F. johnsoniae strains (Table 4). The ZOIs in coevolved strains were significantly less than the ZOI's in monoculture evolved strains (Wilcoxon Rank-Sum; p-value <0.001). However, the ZOIs in coevolved replicates were not significantly different from the ZOI in the ancestor (Wilcoxon Rank-Sum; q-values >= 0.6). In addition, the ZOI in the recombinant strain, re $\Delta 33_tolC$, did not significantly differ from the ZOI in the ancestor (Wilcoxon Rank-Sum; q-value = 1.0). Despite this observation, all coevolved strains and the re $\Delta 33_tolC$ recombinant strain grew better than the ancestor when plated together on the same plate with B. thailandensis (Supplementary Fig. 9). Coevolved strains, but not the recombinant strain, grew better than the monoculture evolved strains, consistent with the Kirby-Bauer results. Taken together, these data suggest that coevolved strains are less susceptible to antibiotic(s) produced by B. thailandensis.

Table 4. Results of antimicrobial activity observed in spent *B. thailandensis* medium against *F. johnsoniae* strains represented by zone of inhibition (ZOI).

Strain		ZOI (mm)	
Ancestor	2.62	2.63	3.10
Evolved monoculture rep 1	5.50	5.39	6.20
Evolved monoculture rep 2	4.90	5.55	4.61
Evolved monoculture rep 3	5.90	5.53	3.25
Evolved monoculture rep 4	3.96	4.72	4.75
Evolved monoculture rep 5	5.41	5.17	5.14
Coevolved rep 1	1.31	2.14	1.33
Coevolved rep 2	2.00	2.00	2.17
Coevolved rep 3	0	0	0
Coevolved rep 4	2.06	2.04	2.07
Coevolved rep 5	1.97	3.08	2.31
reΔ33_tolC	2.48	3.17	3.11

Thailandamide is one of the bioactive molecules that inhibits F. johnsoniae

The nonsynonymous mutation in *F. johnsoniae* coevolved line 3 *tolC* did not reduce susceptibility to the *B. thailandensis*-produced antibiotic(s). But, *F. johnsoniae* coevolved line 3 displayed reduced antibiotic(s)

susceptibility despite harboring this mutation (Fig. 7A). This *F. johnsoniae* coevolved line 3 also contained a unique nonsynonymous mutation in acetyl-CoA carboxylase carboxyltransferase subunit alpha (*accA*, Table 2). This was a C479A nonsynonymous mutation in the coding sequence of *accA* that resulted in a P160Q alteration in AccA. This mutation was similar to a P164Q mutation in AccA from *Salmonella enterica* serovar Typhimurium strain LT2 that conferred resistance to thailandamide from *B. thailandensis* (Wozniak et al. 2018). The P164Q mutation from *S. enterica* aligned with the P160Q mutation observed in our coevolved line (Fig. 7). Thus, we hypothesized that thailandamide was one of the antibiotics responsible for inhibition of *F. johnsoniae*.

We plated the *F. johnsoniae* ancestor with *B. thailandensis thaF* (BTH_II1675), *thaA* (BTH_II1681), and *atsR* (BTH_I0633) transposon mutants. *thaF* encodes a polyketide synthetase trans-AT domain directly involved in the biosynthesis of thailandamide, *thaA* encodes a LuxR-type regulator in the thailandamide biosynthetic gene cluster, and *astR* encodes a global regulator. ThaA positively regulates the thailandamide biosynthetic gene cluster while AtsR negatively regulates the thailandamide biosynthetic gene cluster. We found that *thaF*::T23 and *thaA*::T23 mutants decreased inhibition of *F. johnsoniae* (Fig. 7B, Fig. 7C) while the *atsR*::T23 mutant increased inhibition of *F. johnsoniae* (Fig. 7D). This suggests that thailandamide is bioactive against *F. johnsoniae*. However, *F. johnsoniae* was still slightly inhibited when plated with *thaF*::T23 and *thaA*::T23 mutants, which also suggests that in addition to thailandamide, there may be another *B. thailandensis*-produced antibiotic that is inhibiting *F. johnsoniae*. However, we were unable to determine this molecule.

Discussion

We performed an experimental coevolution study between a strain capable of antibiotic production (*B. thailandensis*) and an antibiotic-susceptible strain (*F. johnsoniae*). Our findings show how long-term interspecies interactions facilitated through chemical exchange via diffusion in agar can result in the acquisition of mutations that reduce antibiotic susceptibility. Analysis of mutations of *F. johnsoniae* coevolved lines as compared to lines evolved in monoculture revealed that reduced antibiotic susceptibility was achieved via a mutation in an efflux outer membrane protein. Specifically, a 33 bp deletion in *tolC*, which eliminated 11 amino acids that were part of an extracellular loop in TolC, reduced antibiotic susceptibility in coevolved *F. johnsoniae* lines. Parallel evolution was

observed for this mutation, as 3/5 coevolved isolates harbored the same 33 bp deletion within the same *tolC* locus. Decreased antibiotic susceptibility was also achieved through a nonsynonymous mutation in *accA*. While the *accA* mutation was not directly assessed for antibiotic susceptibility in our study, the same mutation was spontaneously derived in a *Salmonella* strain that conferred resistance to *B. thailandensis*-derived thailandamide (Wozniak et al. 2018). This led us to hypothesize that thailandamide was the antibiotic inhibiting *F. johnsoniae*. *B. thailandensis* transposon mutants with abrogated thailandamide production confirmed that thailandamide was bioactive against *F. johnsoniae*, but slight inhibition was observed, again suggesting that multiple antibiotics are inhibiting *F. johnsoniae*.

Performing the experimental coevolution on agar plates created a heterogenous environment that facilitated the evolution of decreased antibiotic susceptibility. *F. johnsoniae* growth at the distal end of the colony was permitted because of an antibiotic concentration gradient that was established via diffusion. Low-dose antibiotics likely upregulated intrinsic mechanisms of resistance (e.g. efflux pumps) that conferred low-levels of resistance (Sandoval-Motta and Aldana 2016). The ability to survive exposure to antibiotics via intrinsic mechanisms (Frimodt-Møller et al. 2018; Meouche & Dunlop 2018) can provide the opportunity for mutational acquisition of resistance (Frimodt-Møller and Løbner-Olesen 2019; Ebbensgaard et al. 2020). This was demonstrated experimentally in a seminal study that found that a heterogenous environment increased the rate of adaptation to antibiotics with as few at 100 bacteria in the initial inoculum (Zhang et al. 2011). This approach has been expanded to show how the initial adaptation to low levels of antibiotics facilitate adaptations to high levels of resistance (Baym et al. 2016). Thus, evolutionary adaptations to antibiotic resistance can be fostered in heterogenous environments that would otherwise not be achieved in a uniform environment (Hermsen and Hwa 2010; Hermsen et al. 2012).

Reduced susceptibility to the *B. thailandensis* antibiotic(s) was observed in *F. johnsoniae* coevolved lines that had a 33 bp deletion in *tolC*. The occurrence of the 11 bp directed repeats may support a replication misalignment event that led to the 33 bp deletion (Kong and Masker 1994; Bzymek and Lovett 2001). TolC forms the outer membrane channel part of resistance nodulation division (RND) efflux transporters (Nishino et al. 2003; Anes et al. 2015). *tolC* (FJOH_RS06580) is located in an operon that includes the remaining components necessary for a functional efflux pump. This includes a TetR/AcrR family transcriptional regulator (FJOH_RS06575), an

efflux transporter periplasmic adaptor subunit (FJOH_RS06585), and a multidrug efflux pump permease subunit (FJOH_RS0690). We note that we were unable to confirm the RND-type transport system of this operon. Elimination of 11 amino acids from an extracellular loop in TolC may result in TolC more frequently adopting an open conformation, which could increase the rate of antibiotic extrusion. "Leaky" TolC mutants have been characterized, but these mutations occurred at the periplasmic end of TolC (Bavro et al. 2008; Pei et al. 2011). In fact, mutational studies of the TolC extracellular loops appear uncommon but may present a novel mechanism for antibiotic resistance (Krishnamoorthy et al. 2013). One study carried out a mutational analysis in OprM, a TolC homolog. Two separate insertion mutants were created in external loops of the OprM β -barrel. Modest reductions in channel conductance were observed for these mutants, but this was correlated with either unchanged or reduced MICs to an array of antimicrobials. Regardless, the authors demonstrated that external loops contribute to the control of passage of certain substrates (Wong et al. 2001).

The *F. johnsoniae* recombinant strain harboring the 33 bp deletion in *tolC* had reduced antibiotic susceptibility, but not to the same degree as the *F. johnsoniae* coevolved lines to the *B. thailandensis*-produced antibiotic(s). Additional mutations in the coevolved lines are likely to provide further reductions in antibiotic susceptibility. For example, coevolved line 1 also harbored a 1 bp insertion (T) at position 4734734 in FJOH_RS20510, annotated as a TetR/AcrR family transcriptional regulator. This results in a nonsense mutation that would render the protein nonfunctional. TetR regulators are typically negative regulators, so a nonfunctional TetR regulator would lead to increased expression of efflux pump systems (Cuthbertson and Nodwell 2013). We note that this occurred in FJOH_RS20510 and not FJOH_RS06575, but some TetR regulators have multiple targets and TetR from FJOH_RS20510 could also be negatively regulating the FJOH_RS06580-FJOH_RS06585-FJOH_RS06590 efflux system (Colclough et al. 2019). The remaining coevolved lines with the 33 bp deletion in *tolC* (line 2 and line 5) also had mutations in transcriptional regulators (OmpR and LytTR). Mutations in OmpR may have a potential link to antibiotic resistance by altering expression of the major porin, OmpF, or other genes controlled under the EnvZ/OmpR two-component regulatory system (Card et al. 2021). The potential contributions of mutations in LytTR to reduced antibiotic susceptibility is unknown.

While it was clear that differences in antibiotic susceptibility emerged between the monoculture and coevolved lines, there were both congruencies and discrepancies between Kirby-Bauer assay results (Table 4) and

qualitative plate assays (Supplementary Fig. 9). To start, the decreased antibiotic susceptibility in coevolved strains was consistent between both assays. Quantitatively, the coevolved strains had a modest decrease in ZOIs compared to the ancestor and a significant decrease compared to monoculture evolved strains. Qualitatively, the coevolved strains were the least susceptible to the B. thailandensis-produced antibiotic(s). The monoculture evolved strains had a modest increase in ZOIs compared to the ancestor despite qualitatively being less susceptible to the B. thailandensis antibiotic(s). Lastly, the ZOI of the recombinant strain, re $\Delta 33$ tolC was not different from the ancestor but was qualitatively less susceptible to the B. thailandensis antibiotic(s). These differences in quantitative vs qualitative outcomes could have arisen for a few reasons. The Kirby-Bauer assays were performed from antibiotic(s) concentrated from spent liquid culture. The antibiotic profile of B. thailandensis in liquid culture could be different from the profile on agar medium. Similarly, the spent supernatant from the Kirby-Bauer assay was obtained from strains that did not directly interact with one another. There could be a dynamic, chemical interactions between F. johnsonaie and B. thailandensis when co-plated that leads to a unique antibiotic profile not achieved by growing B. thailandensis in filtered spent F. johnsoniae culture. Lastly, the Kirby-Bauer assays were performed on TSA50 medium and not M9-glucose agar (see Materials and Methods section: Extraction of B. thailandensis bioactive compound(s) and Kirby-Bauer assays). Differences in nutrient composition between TSA50 and M9-glucose could have affected the overall expression of and/or functionality of mechanisms to reduce antibiotic susceptibility F. johnsoniae.

TolC also has a multifaceted role beyond antibiotic export. TolC has been found to be the outer membrane protein part of type I secretion systems (Lee et al. 2012), involved in the export of siderophores (Bleuel et al. 2005), and an importer of toxins such as bacteriocins (Housden et al. 2021). Furthermore, mutations that make TolC nonfunctional have pleiotropic consequences. For example, a gene expression analysis of a non-functional TolC mutant showed upregulation of nutrient transporters, stress response genes, and central metabolism, while genes involved in nitrogen metabolism and transport were downregulated (Santos et al. 2010). We cannot completely rule out these alternative explanations, such as nutrient acquisition, as a reason why *F. johnsoniae* could grow better in the presence of *B. thailandensis*. The Kirby-Bauer results show that there was a significant difference between monoculture evolved and coevolved lines ZOIs. This result provides credence to mutational acquisition in coevolved lines related to decreased antibiotic susceptibility. Additional functional assays would need to be performed, specifically with the *tolC* 33 bp mutant, to better understand its role in antibiotic susceptibility. In addition, further

effots to isolate the bioactive compound(s) and test their effects on strains in isolation would improve MIC assays and establish mutations that lead to resistance.

A nonsynonymous mutation in *accA* in coevolved line 3 also reduced susceptibility to the *B. thailandensis*produced antibiotic(s). In addition, this mutation guided our efforts to uncover that thailandamide was one of the
antibiotics produced in *B. thailandensis* that inhibited *F. johnsoniae*. Thailandamide resistance was characterized in
spontaneous mutants from *S. enterica* (Wozniak et al. 2018). Wozniak and colleagues found 6 unique mutations for
3 different amino acid positions in AccA that conferred thailandamide resistance. One of these mutations was also
spontaneously generated in our study (P160Q in *F. johnsoniae*, P164Q in *S. enterica*). Thailandamide is speculated
to inhibit fatty acid synthesis by competitively inhibiting the binding of carboxy-biotin to acetyl-CoA carboxylase
(Wu and Seyedsayamdost 2018). Protein modeling shows that the P164Q mutation in *S. enterica* is located in a loop
region of AccA that forms the channel to the active site where carboxy-biotin binds. The authors speculate that this
mutation may alter the shape of the channel, thereby limiting the accessibility of thailandamide to the active site
(Wozniak et al. 2018).

B. thailandensis transposon mutants with abrogated thailandamide production effectively reduced inhibition of F. johnsoniae. But, we still observed inhibition with the thailandamide transposon mutants. It is likely that F. johnsoniae was subjected to multiple antibiotics but other mutations conferring reduced antibiotic susceptibility in the coevolved lines did not provide insight into other B. thailandensis-produced antibiotics affecting F. johnsoniae. Futhermore, genome sequencing of B. thailandensis coevolved isolates did not provide insights into the B. thailandensis-produced antibiotic(s) affecting F. johnsoniae. The only possible mutation of interest was a 7 bp insertion that abrogated bactobolin production. But, a B. thailandensis transposon mutant with abrogated bactobolin production still inhibited F. johnsoniae, suggesting that there are other bioactive compounds inhibiting F. johnsoniae.

F. johnsoniae coevolved line 4 did not harbor a mutation in tolC or accA. However, the ragB/susD mutation was unique to coevolved line 4 and we hypothesized that this may provide an alternative mechanism for reduced antibiotic susceptibility. Some antibiotics enter bacterial cells via nutrient transporters (Yoneyama and Nakae 1993; Castañeda-García et al. 2009). Since the ragB/susD, rendered the protein nonfunctional, reduced antibiotic susceptibility could have been conferred to coevolved line 4 by the reduction of antibiotic uptake. We did

not find this to be the case, as the *F. johnsoniae* recombinant strains with the *ragB/susD* nonsynonymous mutation had equivalent susceptibility to the *B. thailandensis*-produced antibiotic(s) as the *F. johnsoniae* ancestor. The other mutations in coevolved line 4 may reduce antibiotic susceptibility or, it is possible that mutations did not fixate in the population, and we chose an isolate for sequencing that did not acquire a mutation conferring reduced antibiotic susceptibility. Bacterial population sequencing could shed light on this discrepancy.

The diversity of antibiotics (Rutledge and Challis 2015) and corresponding resistance mechanisms (Mungan et al. 2020) demonstrate the breadth of genetic novelties that have arisen from millions of years of bacterial competition. Our results provide a case study of bacterial interspecies chemical engagements that can lead to evolution in a heterogeneous environment, with insights into understanding the complex and potentially interacting mutational paths to decreased antibiotic susceptibility.

Materials and Methods

Extraction of B. thailandensis supernatant containing antibiotic activity

A freezer stock of *B. thailandensis* was plated on 50% trypticase soy agar (TSA50) and grown for \sim 16 h at 27 °C. A loopful of lawn growth was transferred to 7 mL of M9 minimal salts-0.2% glucose (M9-glucose; % v/v) medium to achieve an initial OD590 of \sim 0.2 as measured on an Evolution 60S UV-Visible Spectrophotometer (Thermo Scientific). The culture was incubated with shaking at 200 rpm for \sim 16 h at 27 °C. The next day, 1 mL of culture was transferred to 50 mL fresh M9-glucose medium. The culture was incubated with shaking at 200 rpm for 24 h at 27 °C. The culture was transferred to a falcon tube and centrifuged at 5000 rpm for 20 min at 4 °C. The supernatant was removed, filtered with a 0.22 μ M PES filter, and transferred to a separatory funnel. Ten mL of dichloromethane (DCM) was added to the separatory funnel. The separatory funnel was agitated three times and the DCM layer was removed. The addition, agitation, and removal of DCM was repeated twice more. The collected DCM layer was dried under nitrogen gas. The dried DCM extracts were reconstituted in 1 mL of a 50:50 methanol:water (% v/v) mixture. This mixture was used for the efflux pump inhibitor experiment.

Efflux pump inhibitor experiment

A freezer stock of F. johnsoniae was plated on TSA50 and grown for ~16 h at 27 °C. Five individual colonies were then inoculated in 5 mL of 50% trypticase soy broth (TSB50) and incubated with shaking at 200 rpm for ~16 h at 27 °C. The following day, 50 μL of culture was diluted into 4.95 mL of fresh TSB50 for each independent replicate. Then, 650 µL aliquots were dispensed in each of seven tubes for each independent replicate. Seven conditions were prepared across the seven tubes as follows: 1) F. johnsoniae culture control 2) F. johnsoniae with DMSO control 3) F. johnsoniae with 50:50 methanol:water (% v/v) control 4) F. johnsoniae with DMSO + 50:50 methanol:water (% v/v) control 5) F. johnsoniae with daidzein + 50:50 methanol:water (% v/v) 6) F. johnsoniae with DMSO + B. thailandensis supernatant and 7) F. johnsoniae with daidzein + B. thailandensis supernatant. A volume of 1.04 μL was added to tubes containing Daidzein (10 mg/ml) or DMSO and a volume of 16.25 μL was added to tubes containing B. thailandensis supernatant or 50:50 methanol:water (% v/v). After additions of solvent or components, 200 µL aliquots from each tube was placed in a 96 well plate (Supplementary Fig. 1). The plate contained 5 independent replicates, 2 technical replicates/independent replicate for conditions 1-3 and 3 tech reps/independent replicate for conditions 4-7 (90 samples). For the remaining 6 wells, 200 µL TSB50 was added to each well as a negative control. An initial OD590 reading was measured on a Tecan Infinite® F500 Multimode Microplate Reader (Tecan Group Ltd., Männedorf, Switzerland). The plate was then incubated with shaking at 200 rpm for 24 h at 27 °C. A final OD590 reading was taken after 24 h of incubation. A Wilcoxon Rank-Sum test was used to compare all the controls to the F. johnsonaie culture control. All comparisons were insignificantly different (q-values >= 0.82). For this reason, we only used the F. johnsoniae culture control (with no added solvents) to serve as a control for a follow-up Wilcoxon Rank-Sum test with FDR correction that compared final OD590 across test conditions. Analyses were performed in R using the stats package (R Core Team 2021). Measurements were uploaded to R to generate boxplots using ggplot2 (Wickham 2016).

428

429

430

431

432

433

434

407

408

409

410

411

412

413

414

415

416

417

418

419

420

421

422

423

424

425

426

427

Experimental evolution

B. thailandensis E264 and F. johnsoniae UW101 were plated from freezer stocks onto TSA50. Plates were incubated for \sim 16 h at 27 °C. A single, isolated colony of B. thailandensis and of F. johnsoniae were inoculated as separate cultures in 7 mL of TSB50 to serve as the ancestral cultures. Cultures were incubated with shaking at 200 rpm for \sim 16 h at 27 °C. The following day, the cultures were pelleted by centrifugation at 5000 rpm for 10 min at room temperature, the supernatant was removed, and the cultures were resuspended in 1X phosphate buffered saline

(PBS). This process was repeated once more. The cultures were resuspended in PBS at a final volume of 5 mL. Ancestral freezer stocks were prepared by adding 750 mL of each overnight culture to 750 mL of 70% glycerol (% v/v). All freezer stocks were stored at -80 °C. From the remaining cultures containing ancestral *B. thailandensis* and ancestral *F. johnsonaie*, the OD590 was measured on an Evolution 60S UV-Visible Spectrophotometer (Thermo Scientific) and each culture was diluted to an OD590 of 0.1 in PBS to prepare the evolution experiments. Ten μL of a culture (OD590 0.1) was spotted onto M9 minimal salts agar plates containing 0.2% glucose (M9-glucose; % v/v). Both strains were plated in isolation and co-plated (Fig. 3). When co-plated together, *B. thailandensis* and *F. johnsoniae* were spotted 14 mm apart. This allowed sufficient time for the strains to chemically interact without intergrowth of colonies. Five independent replicates were prepared, resulting in 15 plates total. The plates were wrapped with parafilm and incubated at 27 °C for 1.5 months.

After incubation, we performed a plate passage. Sterilized toothpicks were used for the collection of lawn growth. These cells were resuspended in 1 mL of PBS. For *B. thailandensis*, we preferentially collected radial colony growth that was growing toward *F. johnsoniae*. A section of radial colony growth was collected for *B. thailandensis* colonies in monocultures. The entirety of the *F. johnsoniae* was removed from each plate. First plate passage freezer stocks were prepared by adding 500 mL of each resuspended culture to 500 mL of 70% glycerol (% v/v). From the remaining cultures, the OD590 was measured on an Evolution 60S UV-Visible Spectrophotometer (Thermo Scientific) and each culture was diluted to an OD590 of 0.1 in PBS. The plating scheme was repeated as previously described while preserving the previous replicate partnerships of the last coevolved experiment (e.g. *B. thailandensis* coevolved replicate 1 was re-plated with *F. johnsoniae* coevolved replicate 1). The plates were wrapped with parafilm and incubated at 27 °C for 1.5 months. This process was repeated for a total of 5 plate passages, resulting in a total experimentation time of 7.5 months.

Measurements of radial colony growth of (co)evolved plates

Prior to a setting up another plate passage (after a 1.5 mos incubation period), plates were imaged using an Epson Perfection V370 Photo Scanner. A ruler was placed in the scanner to scale pixels to mm for radial growth measurements. Images were uploaded to ImageJ2 for analysis (Rueden et al. 2017; Schneider et al. 2012). Radial

growth was determined by measuring the distance from the center of the colony to the furthest point of radial growth. Measurements were uploaded to R to generate boxplots using ggplot2 (Wickham 2016).

463

464

465

466

467

468

469

470

471

472

473

474

475

476

477

478

479

480

481

482

483

461

462

Whole genome sequencing

All F. johnsoniae replicates (monoculture and coevolution experiments) from the 5th plate passage and the F. johnsoniae ancestor were plated from freezer stocks onto TSA50 (11 freezer stocks total). Plates were incubated for ~16 h at 27 °C. The following night, isolated colonies were inoculated into TSB50 medium and incubated with shaking at 200 rpm for ~16 h at 27 °C. The following morning, DNA was extracted from all 11 cultures using the E.Z.N.A.® Bacterial DNA Kit (Omega Bio-tek, Norcross, GA) according to the manufacturer's instructions. DNA integrity was assessed from 260/280 and 260/230 ratios using a NanoDrop® ND-1000 UV-Vis Spectrophotometer (Thermo Fisher Scientific, Waltham, MA) and quantified using a Qubit 2.0 fluorometer (Invitrogen, Carlsbad, CA, USA). DNA samples were sent to the Microbial Genome Sequencing Center (MiGS, Pittsburgh, PA) for whole genome sequencing. Illumina DNA library preparations were performed at the MiGS facility according to standard operating protocols. Sequencing (2x151bp) was performed on a NextSeq 2000 platform. A minimum of 200 Mbp of sequencing data was obtained with >O30 reads. Low-quality bases were removed with Trimmomatic (Bolger et al. 2014) using a sliding-window approach; reads were trimmed if the average Phred quality score was <20 in a 4-bp window. Reads were also removed if read length was < 70 bp. Average Phred quality scores of trimmed reads were assessed using FastQC (Andrews 2010). Mutations were identified using breseq version0.37.0 with default parameters (Deatherage and Barrick 2014) B. thailandensis E264 (accession numbers NC 007651 & NC 007650) and F. johnsoniae UW101 (accession number NC 009441) were used as reference sequences. The summary files from post-breseq analysis were used to determine total reads, percentage of reads mapped to reference sequences, and average genome coverage. Sequencing statistics from whole genome sequencing are provided in Supplemental File 2.

484

485

486

487

TolC model prediction

The *F. johnsoniae* TolC protein sequence of interest (FJOH_RS06580) was downloaded from NCBI. The protein FASTA file was manually edited to remove 11 amino acids associated with the 33 bp deletion (amino acids

87-97). The protein FASTA file was also manually edited to create the nonsynonymous mutation (G83R). Then all three files were placed into SWISS-MODEL to model the protein structure of TolC (Waterhouse et al. 2018). The template used for rendering all models was SWISS-MODEL Template Library (SMTL) ID: 6wxi.1 (Budiardjo et al. 2022). The model from TolC wild-type was downloaded and uploaded into Swiss-PdbViewer to highlight amino acids associated with the 33 bp deletion (Guex and Peitsch 1997). The SWISS-MODEL homology target-template modeling reports are available at [https://github.com/ShadeLab/Paper Chodkowski Coevolution 2022].

Construction of mutants in F. johnsoniae ancestral strain

Single mutations of interest observed in the coevolved lines were engineered into the genome of the ancestral strain. These mutants were constructed following the previously described method (Zhu et al. 2017), with the exception a nested PCR step. All primers used in this study are listed in Supplementary Table 3.

Nested PCR

DNA extracted from coevolved lines for whole genome sequencing was used as templates for PCR. Coevolved line 1 (CoE_Δ33_tolC) was used to amplify the 33 bp deletion in tolC (F. johnsoniae locus FJOH_RS06580; 261-293 in coding sequence), coevolved line 3 (CoE_G247A_tolC) was used to amplify the nonsynonymous mutation in tolC (F. johnsoniae locus FJOH_RS06580; G247A in coding sequence), and coevolved line 4 (CoE_792_793insG_ragB) was used to amplify the base insertion sequence in ragB/susD (F. johnsoniae locus FJOH_RS24865; 792_793insG in coding sequence). Nested PCR was performed to obtain enough DNA for downstream methods. For the first round of nested PCR, a 3.3-kbp fragment containing tolCΔ33 or tolC(G247A) was amplified using primers 1001 and 1002. A 3.5-kbp fragment containing ragB792_793insG was amplified using primers 1010 and 1011. The PCR reactions contained reagents and volumes outlined in Supplementary Table 4.

PCR conditions were as follows: 98 °C for 30 s, 98 °C for 10 s, 56 °C for 15 s, and 72 °C for 70 s, repeated 29 times from step 2, followed by 72 °C for 10 min and hold at 4 °C. PCR products were run on a 0.8% agarose (% w/v) gel at 100V for 60 min. PCR bands at the correct fragment sizes were excised from the gel and extracted using Wizard® SV Gel and PCR Clean-Up System (Promega Corporation, Madison WI). PCR products were quantified using a Qubit 2.0 fluorometer (Invitrogen, Carlsbad, CA, USA).

For the second round of PCR, a 3.2-kbp fragment containing *tolC*Δ33 or *tolC*(G247A) was amplified using primers 1003 (engineered XbaI site) and 1004 (engineered BamHI site). A 3.1-kbp fragment containing *ragB*792_793insG was amplified using primers 1012 (engineered XbaI site) and 1013 (engineered BamHI site). The PCR reactions contained reagents and volumes outlined in Supplementary Table 5. PCR conditions were as follows: 98 °C for 30 s, 98 °C for 10 s, 56 °C for 15 s, and 72 °C for 70 s, repeated 29 times from step 2, followed by 72 °C for 10 min and hold at 4 °C. PCR products were run on a 0.8% agarose (% w/v) gel at 100V for 60 min. PCR bands at the correct fragment sizes were excised from the gel and extracted using Wizard® SV Gel and PCR Clean-Up System (Promega Corporation, Madison WI). PCR products were quantified using a Qubit 2.0 fluorometer (Invitrogen, Carlsbad, CA, USA).

Plasmid isolation and purification

A *E. coli* DH5αmcr_pYT354 freezer stock was plated on lysogeny broth (LB) agar with ampicillin (100 μg/mL) and incubated for ~16 h at 37 °C. A single colony was inoculated into 5 mL LB with ampicillin (100 μg/mL) and incubated with shaking at 200 rpm for ~16 h at 37 °C. Plasmid pYT354 was extracted *E. coli* DH5αmcr_pYT354and purified the following morning using the E.Z.N.A.® Plasmid DNA Mini Kit I Q-spin (Omega Bio-tek, Norcross, GA) according to the manufacturer's instructions.

Restriction enzyme digestion and ligation

Separately prepared restriction enzyme double digestions were performed on purified PCR products from nested PCR round 2 and pYT354. The reaction reagents and volumes are outlined in Supplementary Table 6. Reactions were incubated at 37 °C for 15 min. Reactions were then run on a 0.8% agarose (% w/v) gel at 100V for 60 min. Bands at the correct fragment sizes were excised from the gel and extracted using Wizard® SV Gel and PCR Clean-Up System (Promega Corporation, Madison WI). PCR products were quantified using a Qubit 2.0 fluorometer (Invitrogen, Carlsbad, CA, USA).

The PCR fragment containing $tolC\Delta33$ was ligated into pYT354 to form pJC101, the PCR fragment containing tolC (G247A) was ligated into pYT354 to form pJC102, and the PCR fragment containing

*ragB*792_793insG was ligated into pYT354 to form pJC103. Ligation reagents are outlined in Supplementary Table 7. The reactions were incubated at room temperature for 10 min and then heat inactivated for 10 min at 65 °C.

Preparation of heat shock competent cells

A *E. coli* DH5amcr freezer stock was plated on lysogeny broth (LB) agar and incubated ~16 h at 37 °C. A single colony was inoculated into 5 mL LB and incubated with shaking at 200 rpm for ~16 h at 37 °C. One mL of the overnight culture was diluted into 100 mL LB and incubated with shaking at 37 °C until the OD590 reached 0.3 (~2 h), as measured on an Evolution 60S UV-Visible Spectrophotometer (Thermo Scientific). The culture was placed on ice for 15 min. Two 45 mL aliquots were placed into 2, 50 mL falcon tubes and centrifuged at 4000 rpm for 10 min at 4 °C. Supernatant was decanted, and the pellets were resuspended in 45 mL ice-cold 0.1 M CaCl₂. The resuspended cultures were placed on ice for 30 min. Cultures were then centrifuged at 4000 rpm for 10 min at 4 °C. Supernatant was decanted, and the pellets were resuspended in 4.5 mL ice-cold 0.1 M CaCl₂ with 15% glycerol (% v/v). The cultures were then distributed as 50 μ L aliquots into microcentrifuge tubes. Competent cells were stored as freezer stocks at -80 °C until ready for use.

Heat shock transformation

Heat shock competent cells (50 μ L) were removed from the freezer and placed on ice for 20 min (4 tubes, 1 for each ligation product and 1 pYT354 plasmid control). Two μ L of ligation products (and 1 μ L of 10 ng/ μ L pYT354 plasmid) were added to each tube and placed on ice for an additional 20 min. Cells were then heat shocked for 45 s at 42 °C. Heat shocked cells were placed on ice for 2 min. One mL of super optimal broth (SOC) medium was added to each tube and the tubes were incubated with shaking at 200 rpm at 37 °C for 1 h. Cells were pelleted by centrifugation at 4000 g for 2 min at 4 °C. The supernatant was removed (950 μ L) and the remaining culture was plated on LB agar containing ampicillin (100 μ g/mL). Plates were incubated ~16 h at 37 °C. Successful transformants were inoculated into LB containing ampicillin (100 μ g/mL) and incubated ~16 h at 37 °C. Freezer stocks were made the following morning for triparental conjugation.

Triparental conjugation and recombinant confirmation

pJC101, pJC103, and pJC104 in recombinant *E. coli* DH5αMCR needed to be transferred to the *F. johnsoniae* ancestral strain. This was introduced into *F. johnsoniae* by triparental conjugation as previously described (Rhodes et al. 2011) using recombinant *E. coli* DH5αMCR, *F. johnsoniae* ancestor, and *E. coli* HB101 (carrying the helper plasmid pRK2013), except that the *sacB* and *ermF*-containing suicide vector was used to select for successful *F. johnsoniae* recombinants (Zhu et al. 2017). F. johnsoniae recombinants (reΔ33_tolC, reG247A_tolC, re792_793insG_ragB) were confirmed by Sanger sequencing at the Michigan State Genomics Core using primers 1005 and 1006 for tolCΔ33 or tolC(G247A) recombinants and primers 1014 and 1014 for the ragB792_793insG_recombinant.

Acetyl-CoA carboxylase carboxyl transferase subunit alpha (AccA) protein alignment

AccA sequences were download from *F. johnsoniae* UW101 (protein ID: WP_011921560.1) and from *Salmonella enterica* serovar Typhimurium strain LT2 (protein ID: NP_459237.1) on NCBI and concatenated as a text file. The text file was uploaded to T-Coffee (Version_11.00) for protein alignment using default parameters (Di Tommaso et al. 2011). The FASTA alignment file from T-Coffee output was download and used as input for BoxShade (version 3.21) using default parameters. The protein alignment was then uploaded to Inkscape for final edits.

Extraction of B. thailandensis bioactive compound(s) and Kirby-Bauer assays

A freezer stock of *F. johnsoniae* was plated on TSA50 and grown for ~16 h at 27 °C. A loopful of lawn growth was transferred to 7 mL of M9 minimal salts-0.2% glucose (M9-glucose; % v/v) medium to achieve an initial OD590 of ~0.2 as measured on an Evolution 60S UV-Visible Spectrophotometer (Thermo Scientific). The culture was incubated with shaking at 200 rpm for ~16 h at 27 °C. The next day, 5 mL of culture was transferred to 50 mL fresh M9-glucose medium in a 250 mL Erlenmeyer flask. The culture was incubated with shaking at 200 rpm for 48 h at 27 °C. On the second day of the *F. johnsoniae* 48 h incubation, a freezer stock of *B. thailandensis* was plated on TSA50 and grown for ~16 h at 27 °C. A loopful of *B. thailandensis* lawn growth was transferred to 7 mL of M9-glucose medium to achieve an initial OD590 of ~0.2 as measured on an Evolution 60S UV-Visible

Spectrophotometer (Thermo Scientific). The *B. thailandensis* culture was incubated with shaking at 200 rpm for \sim 16 h at 27 °C.

At the completion of the *F. johnsoniae* 48 h incubation, the culture was transferred to a falcon tube and centrifuged at 5000 rpm for 20 min at 4 °C. The supernatant was removed, filtered with a 0.22 μM PES filter, and ~50 mL was transferred to a 250 mL Erlenmeyer flask. Five mL of the overnight *B. thailandensis* culture was transferred to the 50 mL filtered spent *F. johnsoniae* M9-glucose medium. In addition, 250 μL 40% glucose (% w/v) was added to the culture to re-achieve ~0.2% glucose (% v/v) in the M9-medium. The culture was incubated with shaking at 200 rpm for 48 h at 27 °C. At the completion of the *B. thailandensis* 48 h incubation in the filtered spent *F. johnsoniae* medium, the culture was transferred to a falcon tube and centrifuged at 5000 rpm for 20 min at 4 °C. The supernatant was removed, filtered with a 0.22 μM PES filter, and transferred to a separatory funnel. Ten mL of dichloromethane (DCM) was added to the separatory funnel. The separatory funnel was agitated three times and the DCM layer was removed. The addition, agitation, and removal of DCM was repeated twice more. The collected DCM layer was dried under nitrogen gas. The dried DCM extracts were reconstituted in 1 mL of a 50:50 methanol:water (% v/v) mixture. This mixture was used for the Kirby-Bauer assays.

Freezer stocks of the *F. johnsoniae* ancestor, co(evolved) strains from the fifth plate passage, and recombinant strain, re $\Delta 33_tolC$, were plated on TSA50 and grown for ~16 h at 27 °C. A loopful of lawn growth was transferred and resuspended in 500 μ L of 1X PBS. The cultures were pelleted by centrifugation at 5000 rpm for 10 min at room temperature, the supernatant was removed, and the cultures were resuspended in 500 μ L 1X PBS. The OD590 of the cultures were measured on an Evolution 60S UV-Visible Spectrophotometer (Thermo Scientific). From the OD590 values, we calculated the volume of PBS to remove to achieve an OD590 of 10. The cultures were pelleted by centrifugation at 5000 rpm for 10 min at room temperature, the calculated volumes of supernatant were removed, and the cultures were resuspended in the remaining volume of 1X PBS. One-hundred μ L of each culture was placed on TSA50 using a cell spreader. TSA50 plates were used instead of M9-glucose agar plates because *F. johnsoniae* was incapable of growing overnight on this medium. Once dried, 3, 6 mm blank paper discs (BD BBLTM) we placed on each plate. Each disc received 20 μ L of one of the following solutions: 1) *B. thailandensis* filtered spent medium grown in *F. johnsoniae* filtered spent medium (described above), 2) 50:50 methanol:water (%

v/v) control, or 3) water control. Plates were incubated at ~16 h at 27 °C. Three independent replicates were prepared for each strain.

The following day, each plate was imaged using an Epson Perfection V370 Photo Scanner. A ruler was placed in the scanner to scale pixels to mm for zone of inhibition (ZOI) measurements. Images were uploaded to ImageJ2 for analysis (Rueden et al. 2017; Schneider et al. 2012). ZOIs were measured as the length between the outer perimeter of the disc to the point of observable growth. Measurements were uploaded to R to test for differences in ZOIs between strains using Wilcoxon Rank-Sum test. Plate images have been uploaded to GitHub [https://github.com/ShadeLab/Paper_Chodkowski_Coevolution_2022].

Re-plating experiments

Strains of interest ((co)evolved strains, ancestor strains, recombinants, and transposon mutants; see Figs. 6 & 7 and Supplementary Figs. 3,4, 8, and 9) were plated from freezer stocks onto TSA50. Plates were incubated for ~16 h at 27 °C. A loopful of lawn growth for each strain was inoculated as separate cultures in 7 mL TSB50. Cultures were incubated with shaking at 200 rpm for ~16 h at 27 °C. The following day, the cultures were pelleted by centrifugation at 5000 rpm for 10 min at room temperature, the supernatant was removed, and the cultures were resuspended in 1X PBS. This process was repeated once more. The cultures were resuspended in PBS at a final volume of 5 mL. The OD590 was measured on an Evolution 60S UV-Visible Spectrophotometer (Thermo Scientific) and each culture was diluted to an OD590 of 0.1 in PBS. Ten μL of a culture (OD590 0.1) was spotted onto M9 minimal salts agar plates containing 0.2% glucose (M9-glucose; % v/v). Strains were either plated in isolation or co-plated together. When co-plated together, strains were spotted 14 mm apart. Plates were incubated at 27 °C for various amounts of time (see Figs. 6 & 7 and Supplementary Figs. 3,4,8, and 9 legends for details). *B. thailandensis* transposon mutants were acquired from the Manoil lab (Gallagher et al. 2013).

Statements and Declarations

Funding

646	This work was supported by Michigan State University and NSF CAREER award DEB #1749544.
647	
648	Conflicts of interest
649	The authors declare that there is no conflict of interest
650	
651	Data and code availability
652	Supplemental files, Sanger sequencing files, and our breseq pipeline are available at
653	[https://github.com/ShadeLab/Paper_Chodkowski_Coevolution_2022]. F. johnsoniae and B. thailandensis whole
654	genome raw sequences files are deposited in the NCBI Sequence Read Archive (BioProject ID PRJNA812898).
655	
656	Authors' contributions
657	JLC and AS conceived the project. JLC carried out the experiments and data analysis. JLC and AS wrote the
658	manuscript.
659	
660	References
661 662 663	Allen, H. K., Donato, J., Wang, H. H., Cloud-Hansen, K. A., Davies, J., & Handelsman, J. (2010). Call of the wild: Antibiotic resistance genes in natural environments. <i>Nature Reviews Microbiology</i> , 8(4), 251–259. https://doi.org/10.1038/nrmicro2312
664 665	Andrews, S. (2010). FastQC: a quality control tool for high throughput sequence data. Available online at: http://www.bioinformatics.babraham.ac.uk/projects/fastqc
666 667	Anes, J., McCusker, M. P., Fanning, S., & Martins, M. (2015). The ins and outs of RND efflux pumps in Escherichia coli. <i>Frontiers in Microbiology</i> , <i>6</i> , 587. https://doi.org/10.3389/FMICB.2015.00587
668 669 670 671	Aparna, V., Dineshkumar, K., Mohanalakshmi, N., Velmurugan, D., & Hopper, W. (2014). Identification of natural compound inhibitors for multidrug efflux pumps of Escherichia coli and Pseudomonas aeruginosa using In Silico high-throughput virtual screening and In Vitro validation. <i>PLoS ONE</i> , <i>9</i> (7), e101840. https://doi.org/10.1371/journal.pone.0101840
672 673	Arzanlou, M., Chai, W. C., & Venter, H. (2017). Intrinsic, adaptive and acquired antimicrobial resistance in Gramnegative bacteria. <i>Essays in Biochemistry</i> , 61(1), 49–59. https://doi.org/10.1042/EBC20160063
674 675 676	Baral, B., Akhgari, A., & Metsä-Ketelä, M. (2018). Activation of microbial secondary metabolic pathways: Avenues and challenges. <i>Synthetic and Systems Biotechnology</i> , <i>3</i> (3), 163–178. https://doi.org/10.1016/j.synbio.2018.09.001

- Bavro, V. N., Pietras, Z., Furnham, N., Pérez-Cano, L., Fernández-Recio, J., Pei, X. Y., ... Luisi, B. (2008).
- Assembly and Channel Opening in a Bacterial Drug Efflux Machine. *Molecular Cell*, 30(1), 114–121.
- https://doi.org/10.1016/j.molcel.2008.02.015
- Baym, M., Lieberman, T. D., Kelsic, E. D., Chait, R., Gross, R., Yelin, I., & Kishony, R. (2016). Spatiotemporal
- microbial evolution on antibiotic landscapes. *Science*, *353*(6304), 1147–1151.
- https://doi.org/10.1126/science.aag0822
- Blair, J. M. A., Richmond, G. E., & Piddock, L. J. V. (2014). Multidrug efflux pumps in Gram-negative bacteria and
- their role in antibiotic resistance. *Http://Dx.Doi.Org/10.2217/Fmb.14.66*, *9*(10), 1165–1177.
- https://doi.org/10.2217/FMB.14.66
- Bleuel, C., Große, C., Taudte, N., Scherer, J., Wesenberg, D., Krauß, G. J., ... Grass, G. (2005). TolC Is Involved in
- Enterobactin Efflux across the Outer Membrane of Escherichia coli. *Journal of Bacteriology*, 187(19), 6701.
- https://doi.org/10.1128/JB.187.19.6701-6707.2005
- Bolger, A. M., Lohse, M., & Usadel, B. (2014). Trimmomatic: a flexible trimmer for Illumina sequence data. Bioinformatics (Oxford, England), 30(15), 2114–2120. https://doi.org/10.1093/bioinformatics/btu170
- Bolivar, F., & Backman, K. (1979). Plasmids of Escherichia coli as cloning vectors. *Methods in Enzymology*, 68(C),
 245–267. https://doi.org/10.1016/0076-6879(79)68018-7
- Brett, P. J., DeShazer, D., & Woods, D. E. (1998). Burkholderia thailandensis sp. nov., a Burkholderia
- pseudomallei-like species. *International Journal of Systematic Bacteriology*, 48(1), 317–320.
- 695 https://doi.org/10.1099/00207713-48-1-317
- Budiardjo, S. J., Stevens, J. J., Calkins, A. L., Ikujuni, A. P., Wimalasena, V. K., Firlar, E., ... Slusky, J. S. G.
 (2022). Colicin E1 opens its hinge to plug TolC. *eLife*, 11, e73297. https://doi.org/10.7554/ELIFE.73297
- Bzymek, M., & Lovett, S. T. (2001). Instability of repetitive DNA sequences: The role of replication in multiple
 mechanisms. *Proceedings of the National Academy of Sciences of the United States of America*, 98(15), 8319–
- 700 8325. https://doi.org/10.1073/pnas.111008398
- Card, K. J., Thomas, M. D., Graves, J. L., Barrick, J. E., & Lenski, R. E. (2021). Genomic evolution of antibiotic
- resistance is contingent on genetic background following a long-term experiment with Escherichia coli.
- *Proceedings of the National Academy of Sciences of the United States of America, 118*(5), e2016886118.
- 704 https://doi.org/10.1073/pnas.2016886118
- Carr, G., Seyedsayamdost, M. R., Chandler, J. R., Greenberg, E. P., & Clardy, J. (2011). Sources of diversity in
- bactobolin biosynthesis by burkholderia thailandensis E264. *Organic Letters*, 13(12), 3048–3051.
- 707 https://doi.org/https://doi.org/10.1021/ol200922sCastañeda-García, A., Rodríguez-Rojas, A., Guelfo, J. R., &
- 708 Blázquez, J. (2009). The glycerol-3-phosphate permease GlpT is the only fosfomycin transporter in
- Pseudomonas aeruginosa. *Journal of Bacteriology*, 191(22), 6968–6974. https://doi.org/10.1128/JB.00748-09
- 710 Colclough, A. L., Scadden, J., & Blair, J. M. A. (2019). TetR-family transcription factors in Gram-negative bacteria:
- 711 Conservation, variation and implications for efflux-mediated antimicrobial resistance. *BMC Genomics*, 20(1),
- 712 1–12. https://doi.org/10.1186/s12864-019-6075-5
- Cuthbertson, L., & Nodwell, J. R. (2013). The TetR Family of Regulators. *Microbiology and Molecular Biology Reviews*, 77(3), 440–475. https://doi.org/10.1128/mmbr.00018-13
- 715 D'Costa, V. M., McGrann, K. M., Hughes, D. W., & Wright, G. D. (2006). Sampling the antibiotic resistome.
- 716 *Science*, 311(5759), 374–377. https://doi.org/10.1126/science.1120800

- 717 Deatherage, D. E., & Barrick, J. E. (2014). Identification of mutations in laboratory-evolved microbes from next-
- 718 generation sequencing data using breseq. Methods in Molecular Biology, 1151, 165–188.
- 719 https://doi.org/10.1007/978-1-4939-0554-6 12
- 720 Di Tommaso, P., Moretti, S., Xenarios, I., Orobitg, M., Montanyola, A., Chang, J. M., ... Notredame, C. (2011). T-
- 721 Coffee: A web server for the multiple sequence alignment of protein and RNA sequences using structural
- information and homology extension. *Nucleic Acids Research*, 39((Web Server issue)), W13-7.
- 723 https://doi.org/10.1093/nar/gkr245
- 724 Du, D., Wang-Kan, X., Neuberger, A., van Veen, H. W., Pos, K. M., Piddock, L. J. V., & Luisi, B. F. (2018).
- Multidrug efflux pumps: structure, function and regulation. *Nature Reviews Microbiology*, 16(9), 523–539.
- 726 https://doi.org/10.1038/s41579-018-0048-6
- Duerkop, B. A., Varga, J., Chandler, J. R., Peterson, S. B., Herman, J. P., Churchill, M. E. A., ... Greenberg, E. P.
- 728 (2009). Quorum-sensing control of antibiotic synthesis in Burkholderia thailandensis. *Journal of Bacteriology*,
- 729 *191*(12), 3909–3918. https://doi.org/10.1128/JB.00200-09
- 730 Ebbensgaard, A. E., Løbner-Olesen, A., & Frimodt-Møller, J. (2020). The role of efflux pumps in the transition from
- low-level to clinical antibiotic resistance. *Antibiotics*, 9(12), 1–7. https://doi.org/10.3390/antibiotics9120855
- 732 Figurski, D. H., & Helinski, D. R. (1979). Replication of an origin-containing derivative of plasmid RK2 dependent
- 733 on a plasmid function provided in trans. Proceedings of the National Academy of Sciences of the United States
- 734 of America, 76(4), 1648–1652. https://doi.org/10.1073/pnas.76.4.1648
- Frimodt-Møller, J., & Løbner-Olesen, A. (2019). Efflux-Pump Upregulation: From Tolerance to High-level
- Antibiotic Resistance? *Trends in Microbiology*, 27(4), 291–293. https://doi.org/10.1016/j.tim.2019.01.005
- 737 Frimodt-Møller, J., Rossi, E., Haagensen, J. A. J., Falcone, M., Molin, S., & Johansen, H. K. (2018). Mutations
- 738 causing low level antibiotic resistance ensure bacterial survival in antibiotic-treated hosts. *Scientific Reports*,
- 739 *8*(1), 1–13. https://doi.org/10.1038/s41598-018-30972-y
- 740 Gallagher, L. A., Ramage, E., Patrapuvich, R., Weiss, E., Brittnacher, M., & Manoil, C. (2013). Sequence-defined
- transposon mutant library of Burkholderia thailandensis. *MBio*, 4(6), e00604-13.
- 742 https://doi.org/10.1128/mBio.00604-13
- 743 Granato, E. T., Meiller-Legrand, T. A., & Foster, K. R. (2019). The Evolution and Ecology of Bacterial Warfare.
- 744 *Current Biology*, 29(11), R521–R537. https://doi.org/10.1016/j.cub.2019.04.024
- Guex, N., & Peitsch, M. C. (1997). SWISS-MODEL and the Swiss-PdbViewer: An environment for comparative
- 746 protein modeling. *Electrophoresis*, 18(15), 2714–2723. https://doi.org/10.1002/elps.1150181505
- Hermsen, R., Deris, J. B., & Hwa, T. (2012). On the rapidity of antibiotic resistance evolution facilitated by a
- 748 concentration gradient. Proceedings of the National Academy of Sciences of the United States of America,
- 749 109(27), 10775–10780. https://doi.org/10.1073/pnas.1117716109
- Hermsen, R., & Hwa, T. (2010). Sources and sinks: A stochastic model of evolution in heterogeneous environments.
- 751 *Physical Review Letters*, 105(24), 248104. https://doi.org/10.1103/PhysRevLett.105.248104
- 752 Hibbing, M. E., Fuqua, C., Parsek, M. R., & Peterson, S. B. (2010). Bacterial competition: Surviving and thriving in
- 753 the microbial jungle. *Nature Reviews Microbiology*, 8(1), 15–25. https://doi.org/10.1038/nrmicro2259

- Housden, N. G., Webby, M. N., Lowe, E. D., El-Baba, T. J., Kaminska, R., Redfield, C., ... Kleanthous, C. (2021).
- Toxin import through the antibiotic efflux channel TolC. *Nature Communications*, 12, 4625.
- 756 https://doi.org/10.1038/s41467-021-24930-y
- Kong, D., & Masker, W. (1994). Deletion between direct repeats in T7 DNA stimulated by double-strand breaks.
- 758 *Journal of Bacteriology*, 176(19), 5904–5911. https://doi.org/10.1128/jb.176.19.5904-5911.1994
- 759 Krishnamoorthy, G., Tikhonova, E. B., Dhamdhere, G., & Zgurskaya, H. I. (2013). On the role of TolC in multidrug
- 760 efflux: The function and assembly of AcrAB-TolC tolerate significant depletion of intracellular TolC protein.
- 761 *Molecular Microbiology*, 87(5), 982–997. https://doi.org/10.1111/mmi.12143
- Lee, M., Jun, S. Y., Yoon, B. Y., Song, S., Lee, K., & Ha, N. C. (2012). Membrane fusion proteins of type I
- 763 secretion system and tripartite efflux pumps share a binding motif for TolC in gram-negative bacteria. *PloS*
- 764 *One*, 7(7), e40460. https://doi.org/10.1371/journal.pone.0040460
- Mao, D., Bushin, L. B., Moon, K., Wu, Y., & Seyedsayamdost, M. R. (2017). Discovery of scmR as a global
- regulator of secondary metabolism and virulence in Burkholderia thailandensis E264. *Proceedings of the*
- National Academy of Sciences of the United States of America, 114(14), E2920–E2928.
- 768 https://doi.org/10.1073/pnas.1619529114
- McBride, M. J., Xie, G., Martens, E. C., Lapidus, A., Henrissat, B., Rhodes, R. G., ... Stein, J. L. (2009). Novel
- features of the polysaccharide-digesting gliding bacterium Flavobacterium johnsoniae as revealed by genome
- 771 sequence analysis. Applied and Environmental Microbiology, 75(21), 6864–6875.
- 772 https://doi.org/10.1128/AEM.01495-09
- 773 Medema, M. H., Kottmann, R., Yilmaz, P., Cummings, M., Biggins, J. B., Blin, K., ... Glöckner, F. O. (2015).
- 774 Minimum Information about a Biosynthetic Gene cluster. *Nature Chemical Biology*, 11(9), 625–631.
- 775 https://doi.org/10.1038/nchembio.1890
- Meouche, I. E., & Dunlop, M. J. (2018). Heterogeneity in efflux pump expression predisposes antibiotic-resistant
- 777 cells to mutation. Science, 362(6415), 686–690. https://doi.org/10.1126/SCIENCE.AAR7981Mungan, M. D.,
- 778 Alanjary, M., Blin, K., Weber, T., Medema, M. H., & Ziemert, N. (2020). ARTS 2.0: Feature updates and
- expansion of the Antibiotic Resistant Target Seeker for comparative genome mining. *Nucleic Acids Research*,
- 780 48(W1), W546–W552. https://doi.org/10.1093/NAR/GKAA374
- 781 Nishino, K., Yamada, J., Hirakawa, H., Hirata, T., & Yamaguchi, A. (2003). Roles of TolC-Dependent Multidrug
- 782 Transporters of Escherichia coli in Resistance to β-Lactams. *Antimicrobial Agents and Chemotherapy*, 47(9),
- 783 3030. https://doi.org/10.1128/AAC.47.9.3030-3033.2003
- Pei, X. Y., Hinchliffe, P., Symmons, M. F., Koronakis, E., Benz, R., Hughes, C., & Koronakis, V. (2011). Structures
- of sequential open states in a symmetrical opening transition of the TolC exit duct. *Proceedings of the*
- National Academy of Sciences of the United States of America, 108(5), 2112–2117.
- 787 https://doi.org/10.1073/pnas.1012588108
- 788 Poole, K. (2004). Efflux-mediated multiresistance in Gram-negative bacteria. Clinical Microbiology and Infection:
- 789 The Official Publication of the European Society of Clinical Microbiology and Infectious Diseases, 10(1), 12–
- 790 26. https://doi.org/10.1111/J.1469-0691.2004.00763.X
- 791 R Core Team (2021). R: A language and environment for statistical computing, R Foundation for
- 792 Statistical Computing, Vienna, Austria. URL https://www.R-project.org/.

- Rhodes, R. G., Pucker, H. G., & McBride, M. J. (2011). Development and use of a gene deletion strategy for Flavobacterium johnsoniae to identify the redundant gliding motility genes remF, remG, remH, and remI.
- Journal of Bacteriology, 193(10), 2418–2428. https://doi.org/10.1128/JB.00117-11
- Rueden, C. T., Schindelin, J., Hiner, M. C., DeZonia, B. E., Walter, A. E., Arena, E. T., & Eliceiri, K. W. (2017).
 ImageJ2: ImageJ for the next generation of scientific image data. *BMC Bioinformatics*, 18(1), 529.
 https://doi.org/10.1186/s12859-017-1934-z
- Russell, A. B., Wexler, A. G., Harding, B. N., Whitney, J. C., Bohn, A. J., Goo, Y. A., ... Mougous, J. D. (2014). A
 type VI secretion-related pathway in Bacteroidetes mediates interbacterial antagonism. *Cell Host & Microbe*,
 16(2), 227. https://doi.org/10.1016/j.chom.2014.07.007
- Rutledge, P. J., & Challis, G. L. (2015). Discovery of microbial natural products by activation of silent biosynthetic gene clusters. *Nature Reviews Microbiology*, *13*(8), 509–523. https://doi.org/10.1038/nrmicro3496
- Sandoval-Motta, S., & Aldana, M. (2016). Adaptive resistance to antibiotics in bacteria: A systems biology perspective. *Wiley Interdisciplinary Reviews: Systems Biology and Medicine*, 8(3), 253–267. https://doi.org/10.1002/wsbm.1335
- Santos, M. R., Cosme, A. M., Becker, J. D., Medeiros, J. M., Mata, M. F., & Moreira, L. M. (2010). Absence of functional TolC protein causes increased stress response gene expression in Sinorhizobium meliloti. *BMC Microbiology*, 10, 180. https://doi.org/10.1186/1471-2180-10-180
- Schneider, C. A., Rasband, W. S., & Eliceiri, K. W. (2012). NIH Image to ImageJ: 25 years of image analysis.
 Nature Methods. https://doi.org/10.1038/nmeth.2089
- van der Meij, A., Worsley, S. F., Hutchings, M. I., & van Wezel, G. P. (2017). Chemical ecology of antibiotic
 production by actinomycetes. *FEMS Microbiology Reviews*, *41*(3), 392–416.
 https://doi.org/10.1093/femsre/fux005
- Waglechner, N., McArthur, A. G., & Wright, G. D. (2019). Phylogenetic reconciliation reveals the natural history of glycopeptide antibiotic biosynthesis and resistance. *Nature Microbiology*, *4*(11), 1862–1871.
 https://doi.org/10.1038/s41564-019-0531-5
- Walsh, F. (2013). Investigating antibiotic resistance in non-clinical environments. *Frontiers in Microbiology*, *4*, 19.
 https://doi.org/10.3389/fmicb.2013.00019
- Waterhouse, A., Bertoni, M., Bienert, S., Studer, G., Tauriello, G., Gumienny, R., ... Schwede, T. (2018). SWISS MODEL: Homology modelling of protein structures and complexes. *Nucleic Acids Research*, 46(W1), W296–W303. https://doi.org/10.1093/nar/gky427
- Wickham, H. (2016). ggplot2: Elegant Graphics for Data Analysis. Springer-Verlag New York.
- Wong, K. K. Y., Brinkman, F. S. L., Benz, R. S., & Hancock, R. E. W. (2001). Evaluation of a structural model of
 Pseudomonas aeruginosa outer membrane protein OprM, an efflux component involved in intrinsic antibiotic
 resistance. *Journal of Bacteriology*, 183(1), 367–374. https://doi.org/10.1128/JB.183.1.367-374.2001
- Wozniak, C. E., Lin, Z., Schmidt, E. W., Hughes, K. T., & Liou, T. G. (2018). Thailandamide, a fatty acid synthesis antibiotic that is coexpressed with a resistant target gene. *Antimicrobial Agents and Chemotherapy*, *62*(9), e00463-18. https://doi.org/10.1128/AAC.00463-18

830 Wu, Y., & Seyedsayamdost, M. R. (2018). The Polyene Natural Product Thailandamide A Inhibits Fatty Acid 831 Biosynthesis in Gram-Positive and Gram-Negative Bacteria. *Biochemistry*, 57(29), 4247–4251. 832 https://doi.org/10.1021/acs.biochem.8b00678 833 Yoneyama, H., & Nakae, T. (1993). Mechanism of efficient elimination of protein D2 in outer membrane of 834 imipenem-resistant Pseudomonas aeruginosa. Antimicrobial Agents and Chemotherapy, 37(11), 2385–2390. 835 https://doi.org/10.1128/AAC.37.11.2385 836 Zhang, Q., Lambert, G., Liao, D., Kim, H., Robin, K., Tung, C. K., ... Austin, R. H. (2011). Acceleration of 837 emergence of bacterial antibiotic resistance in connected microenvironments. Science, 333(6050), 1764–1767. 838 https://doi.org/10.1126/science.1208747 839 Zhu, Y., Thomas, F., Larocque, R., Li, N., Duffieux, D., Cladière, L., ... McBride, M. J. (2017). Genetic analyses unravel the crucial role of a horizontally acquired alginate lyase for brown algal biomass degradation by 840 Zobellia galactanivorans. Environmental Microbiology, 19(6), 2164-2181. https://doi.org/10.1111/1462-841 842 2920.13699 843 844 Figure legends 845 846 Fig. 1 A bioactive compound is produced by B. thailandensis that inhibits F. johnsoniae. B. thailandensis (right) 847 and F. johnsoniae (left) were co-plated on M9-glucose agar at a distance that allowed for chemical interactions. An 848 unidentified antibiotic(s) inhibited *F. johnsoniae*. 849 850 Fig. 2 F. johnsoniae efflux system contributes to the extrusion of a B. thailandensis-produced antibiotic(s). An end-851 point growth measurement (n=5) was taken after F. johnsoniae 24 h incubation with either B. thailandensis culture 852 supernatant (Supernatant), with the efflux pump inhibitor (Daidzein), or with a combination of the supernatant and 853 daidzein. An untreated F. johnsoniae culture (Culture control), a F. johnsoniae culture with dimethyl sulfoxide 854 (DMSO), a F. johnsoniae culture with methanol (MeOH), a F. johnsoniae culture with both solvents (DMSO + 855 MeOH), and blank TSB50 medium served as controls. The bottom and top of each boxplot are the first and third 856 quartiles, respectively, and the line inside the box is the median. The whiskers extend from their respective hinges to 857 the largest value (top), and smallest value (bottom) was no further away than 1.5 times the interquartile range. Black 858 points on a boxplot represent outliers that were greater than 1.5 times the interquartile range. AWilcoxon Rank-Sum 859 test was performed comparing all treatments to the culture control. * q-value <0.05, n.s.: not significant.

Fig. 3 Schematic of (co)evolution experiment.

Fig. 4 *F. johnsoniae* trends toward increased growth success with each plate passage in the presence of *B. thailandensis*. Images were taken at the end of each plate passage (1.5 mos) to quantify radial growth for both *F. johnsoniae* monoculture evolved (gray bars) lines and *F. johnsoniae* coevolved (white bars) lines (n=5 independent replicated per time point). Radial colony growth was measured from the center of the colony to the point of furthest growth on the agar plate. The bottom and top of each box are the first and third quartiles, respectively, and the line inside the box is the median. The whiskers extend from their respective hinges to the largest value (top), and smallest value (bottom) no further away than 1.5× the interquartile range. Black points on a boxplot represent outliers that were greater than 1.5 times the interquartile range.

Fig. 5 A *tolC* 33 bp deletion is located on a TolC extracellular loop. The TolC protein (A) contains a α-helical transperiplasmic tunnel, a β-barrel channel embedded in the outer membrane, and extracellular loops at the cell surface. The yellow box represents the inset in (B), where the 11 amino acids corresponding to the 33 bp deletion are highlighted in blue. These amino acids are part of one of the extracellular loops. The nucleotide sequence is shown below the image, representing bps 247-294 (amino acids 83-98) in the FJOH_RS06580 coding sequence. The corresponding amino acids are shown above each codon. Nucleotides highlighted in blue represent the 33 bp deletion. Nucleotides highlighted in orange show how the deletion was in-frame. The 11 bp direct repeats are in bold and underlined. The nucleotide highlighted in green is associated with the nonsynonymous mutation (G247A in the coding sequence, G83R in TolC). TolC from *E. coli* was used as the template (SMTL ID: 6wxi.1) to construct the target *F. johnsoniae* WT TolC model (SWISS-MODEL: GMQE= 0.6, Seq ID=19.06) shown in the figure. The *F. johnsoniae* TolC model generated from removal of 33 bp still maintains equivalent modeling quality (SWISS-MODEL: GMQE=0.61, Seq ID=19.06).

Fig. 6 The *tolC* 33 bp deletion reduces antibiotic susceptibility. The ancestor (A) and recombinant strains of *F. johnsoniae* ancestor (C-D) were co-plated with the *B. thailandensis* ancestor. The recombinant strain with the *tolC*

33 bp deletion (B) is the least inhibited by *B. thailandensis* compared to the *F. johnsoniae* ancestor and other *F. johnsoniae* recombinant strains. Plates were imaged after a week of incubation.

Fig. 7 Thailandamide is bioactive against *F. johnsoniae*. While the nonsynonymous mutation in *tolC* did not reduce antibiotic susceptibility (present in *F. johnsoniae* coevolved line 3), *F. johnsoniae* coevolved line 3 still displayed a reduction in antibiotic susceptibility at the end of plate passage five (A). *B. thailandensis* transposon mutants in *thaF* (B) and *thaA* (C) have decreased inhibition toward *F. johnsoniae* while an *atsR* transposon mutant has increased inhibition of *F. johnsoniae* (D). Below the panels is an amino acid sequence alignment between the *F. johnsoniae* AccA and S. enterica AccA. The asterisks indicate positions within the proteins that were identical. The blue box highlights the alignment of P160 in *F. johnsoniae* and P164 in *S. enterica*.

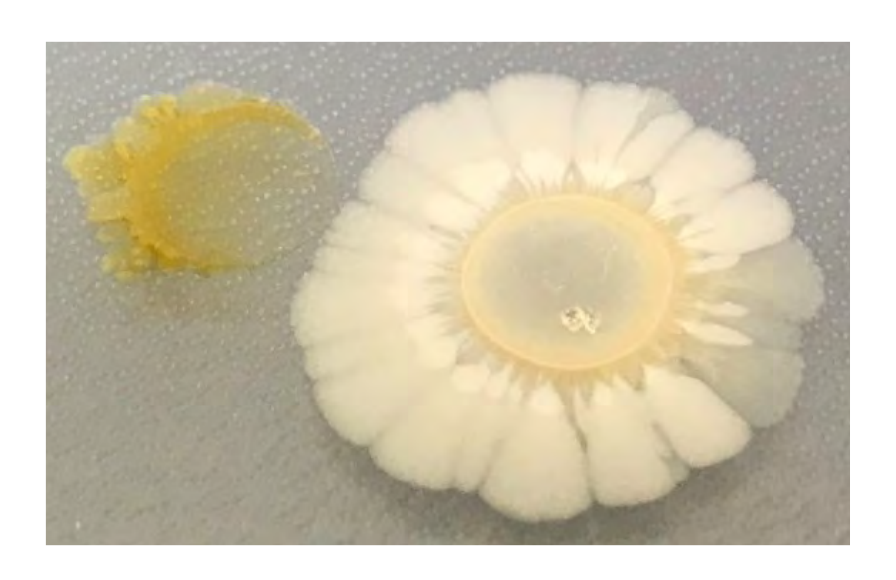


Fig. 1 B. thailandensis-produced antibiotic(s) inhibits F. johnsoniae. B. thailandensis (right) and F. johnsoniae (left) were co-plated on M9-glucose agar at a distance that allowed for chemical interactions. An unidentified antibiotic(s) inhibited F. johnsoniae.

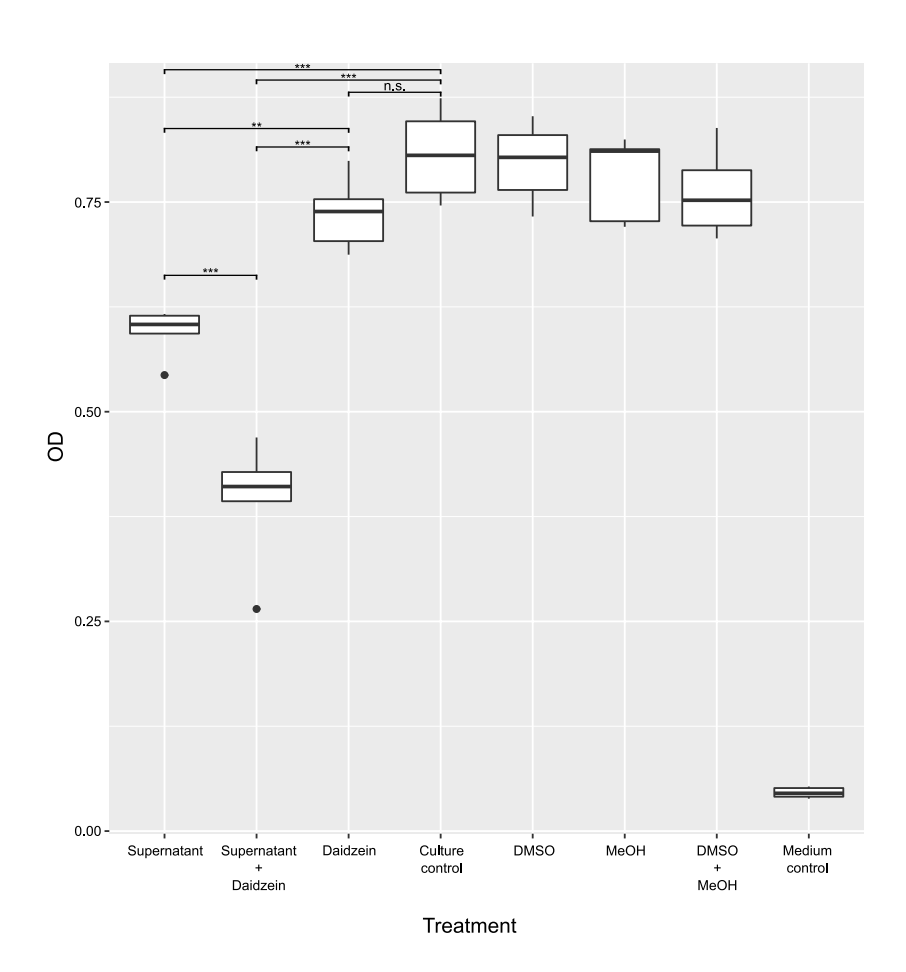
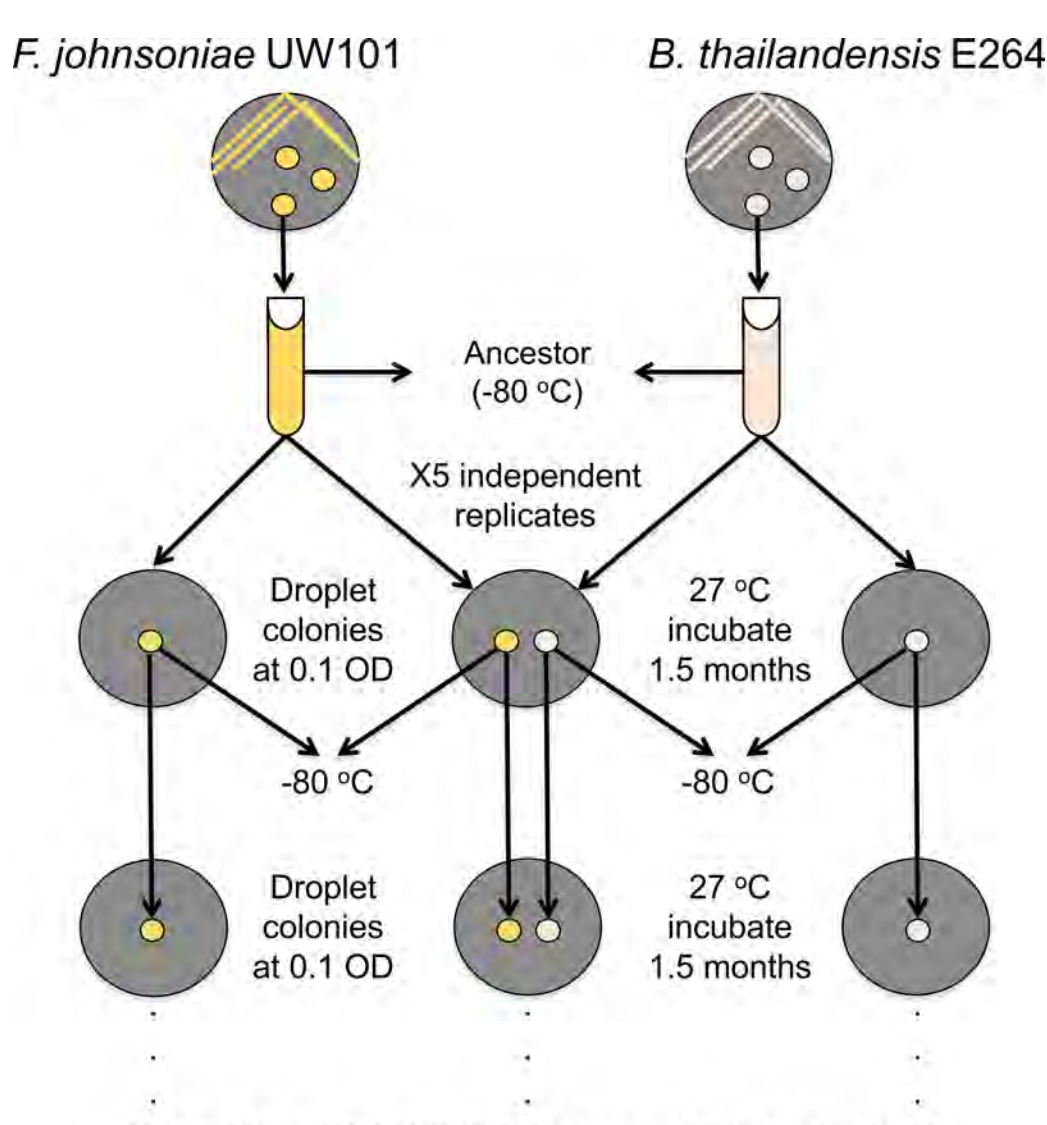


Fig. 2 F. johnsoniae efflux system contributes to the extrusion of a B. thailandensis-produced antibiotic(s). An end-point growth measurement was taken after F. johnsoniae incubation with B. thailandensis culture supernatant, with the efflux pump inhibitor (daidzein), or with a combination of the supernatant and daidzein. An untreated F. johnsoniae culture, a F. johnsoniae culture with dimethyl sulfoxide (DMSO), a F. johnsoniae culture with methanol (MeOH), a F. johnsoniae culture with combined solvents, and blank medium served as controls. An ANOVA was performed comparing all treatments to the culture control. A Tukey HSD post-hoc analysis was performed for pairwise comparisons. Data shown are representative of 5 independent experiments; * p<0.05, ** p<0.001, ***p<0.0001, n.s.: not significant



Repeat for a total of 5 plate passages (7.5 months total)

Fig. 3 Schematic of (co)evolution experiment.

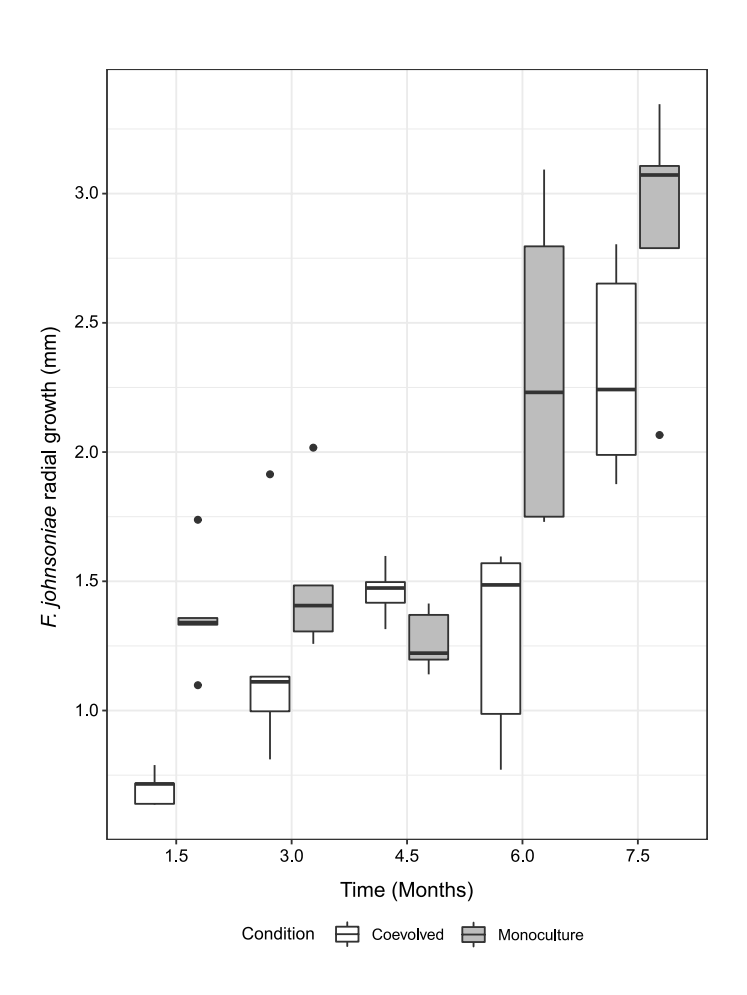


Fig. 4 F. johnsoniae trends toward increased growth success with each plate passage in the presence of B. thailandensis. Radial colony growth of coevolved F. johnsoniae was measured from the center of the colony to point of furthest growth on the agar plate. Measurements were taken at the end of each plate passage

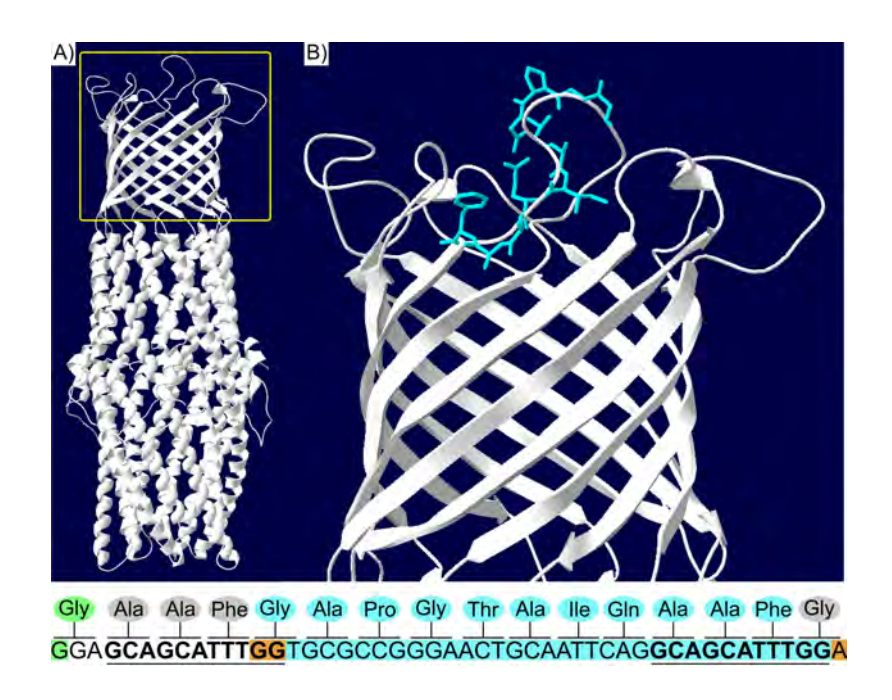


Fig. 5 A toIC 33 bp deletion is located on a ToIC extracellular loop. The ToIC protein (A) contains a α -helical trans-periplasmic tunnel, a β -barrel channel embedded in the outer membrane, and extracellular loops at the cell surface. The yellow box represents the inset in (B), where the 11 amino acids corresponding to the 33 bp deletion are highlighted in blue. These amino acids are part of one of the extracellular loops. The nucleotide sequence is shown below the image, representing bps 247-294 in the FJOH_RS06580 coding sequence. The corresponding amino acids are shown above each codon. Nucleotides highlighted in blue represent the 33 bp deletion. Nucleotides highlighted in orange show how the deletion was in-frame. The 11 bp direct repeats are in bold and underlined. The nucleotide highlighted in green is associated with the nonsynonymous mutation (G247A in the coding sequence, G83R in ToIC).

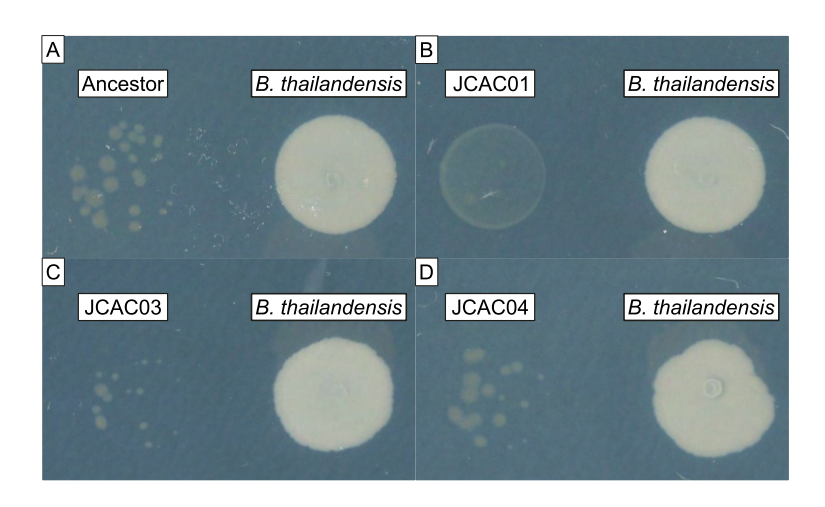


Fig. 6 The toIC 33 bp deletion confers antibiotic resistance. The ancestor (A) and recombinant strains of F. johnsoniae ancestor (C-D) were co-plated with B. thailandensis. The recombinant strain with the toIC 33 bp deletion (B) is the least inhibited by B. thailandensis compared to the ancestor and other recombinant strains. Plates were imaged after a week of incubation.

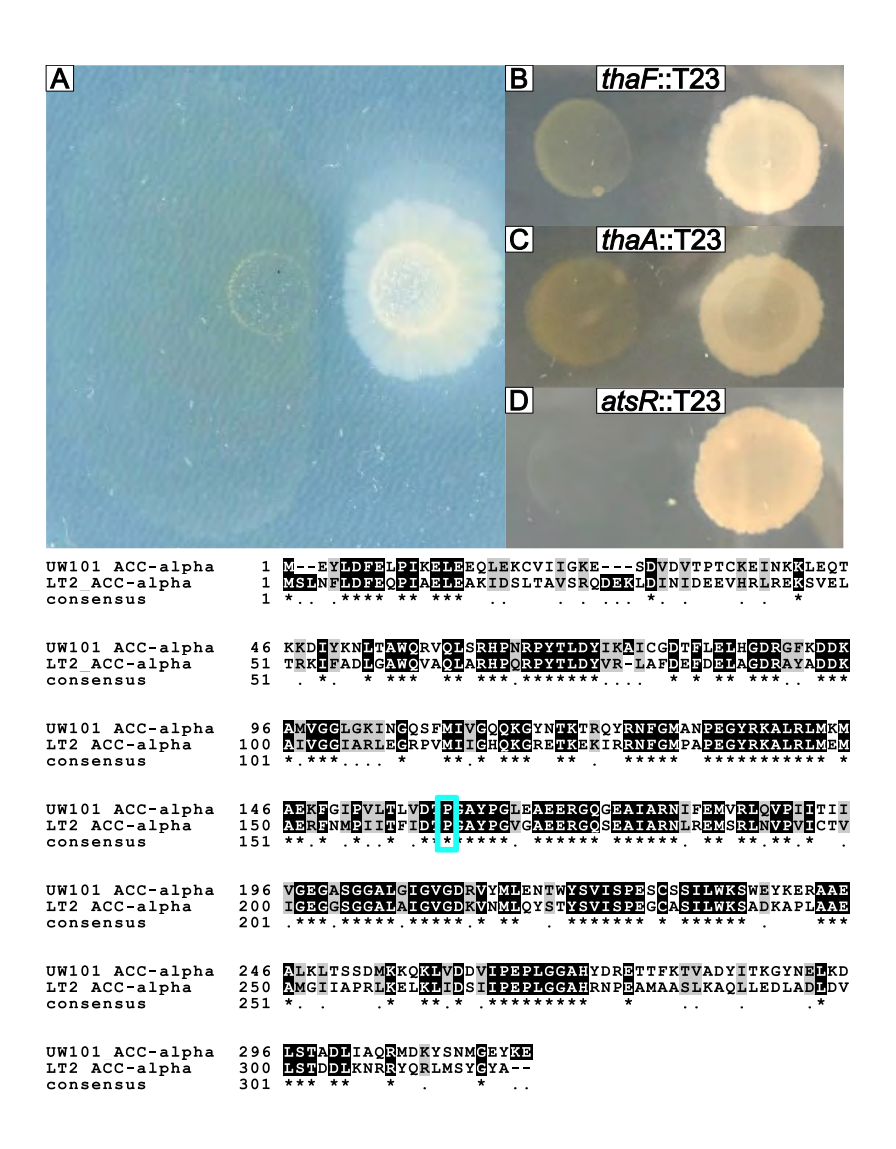


Fig. 7 Thailandamide is bioactive against F. johnsoniae. While the nonsynonymous mutation in tolC did not confer antibiotic resistance (present in F. johnsoniae coevolved line 3), F. johnsoniae coevolved line 3 still displayed antibiotic resistance at the end of plate passage five (A). B. thailandensis transposon mutants in thaF (B) and thaA (C) have decreased inhibition toward F. johnsoniae while an atsR transposon mutant has increased inhibition of F. johnsoniae (D). Below the panels is an amino acid sequence alignment between the F. johnsoniae AccA and S. enterica AccA. The asterisks indicate positions within the proteins that were identical. The blue box highlights the alignment of P160 in F. johnsoniae and P164 in S. enterica.

1	Supplementary material for
2	
3	A coevolution experiment between Flavobacterium johnsoniae and Burkholderia
4	thailandensis reveals parallel mutations that reduce antibiotic susceptibility
5	
6	John L. Chodkowski ¹ and Ashley Shade ^{1,2,3*}
7	¹ Department of Microbiology and Molecular Genetics, Michigan State University, East Lansing, MI 48824, USA
8	² Department of Plant, Soil and Microbial Sciences, Michigan State University, East Lansing, MI 48824, USA
9	³ Program in Ecology, Evolution and Behavior, Michigan State University, East Lansing, MI 48824, USA
10	* Corresponding author and material requests. Email: shadeash@msu.edu ; ORCiD: 0000-0002-7189-3067
11	
12	Data and code availability: https://github.com/ShadeLab/Paper_Chodkowski_Coevolution_2022
13	

14 Supplementary Tables

Supplementary Table 1 Summary of *tolC* loci in *F. johnsoniae*

Locus	Protein ID	Top blastp hit	AA length
FJOH_RS06580	WP_012023347.1	TolC family protein	444
FJOH_RS07030	WP_012023433.1	cc	451
FJOH_RS08665	WP_012023747.1	cc	461
FJOH_RS14165	WP_012024794.1	cc	415
FJOH_RS15250	WP_012025000.1	cc	436
FJOH_RS15955	WP_008463753.1	٠,	415
FJOH_RS16725	WP_012025212.1	٠,	469
FJOH_RS16800	WP_012025225.1	٠,	484
FJOH_RS17335	WP_044047818.1	٠,	426
FJOH_RS20485	WP_012025935.1	٠,	472
FJOH_RS22150	WP_044048008.1	٠,	461
FJOH_RS22200	WP_012026267.1	cc	412
FJOH_RS22240	WP_012026275.1	cc	472
FJOH_RS23175	WP_012026451.1	cc	417
FJOH_RS25120	WP_012026826.1	cc	479
FJOH_RS25325	WP_012026867.1	cc	439

- **Supplementary Table 2** Percent identity matrix for all TolC proteins annotated in *F. johnsoniae*. Mutations in
- 20 coevolved isolates were found in RS06580. Multiple sequence alignments were made using Clustal Omega

RS06580	100															
RS15250	24.2	100														
RS20485	15.99	15.5	100													
RS15955	13.94	11.86	13.51	100												
RS16800	16.46	15.21	14.84	16.19	100											
RS25120	15.15	14.65	12.29	18.49	31.99	100										
RS16725	19.07	18.78	11.62	18.09	32.03	29.68	100									
RS22240	15.46	15.08	13.89	16.71	28.6	34.48	40.51	100								
RS17335	17.71	19.84	14.68	16.48	15.38	13.95	15.61	15.3	100							
RS22150	18.02	17.5	15.11	11.83	14.15	15.82	15.92	15.42	16.67	100						
RS23175	16.84	15.3	13.35	14.48	18.53	17.26	15.84	15.32	15.95	13.57	100					
RS14165	17.36	14.82	13.66	16.49	17.05	18.09	14.51	14.78	13.06	18.25	23.08	100				
RS22200	17.05	17.69	12.37	17.21	15.37	14.11	14.8	15.82	18.68	15.17	22.19	28.1	100			
RS07030	20.15	18.72	14.77	14.66	14.63	14.11	14.5	14	17.95	16.1	15.38	12.94	14.21	100		
RS25325	20.54	19.55	15.84	12.87	13.51	13.51	16.12	15.62	12.5	21.22	16.71	15.4	14.86	24.65	100	
RS08665	22	21.84	17.36	14.33	14.47	16.2	19.01	16.41	18.59	18.76	15.03	18.16	18.59	20.15	20.35	100

22 Supplementary Table 3 Primers used in this study

Primer	Sequence (5' > 3')	Description
1001	TTGCTTATTTGGGAG GAACAACA	Used to amplify tolC for nested PCR round 1
1002	CATCTGCTTTTGCAG CGATGA	Used to amplify tolC for nested PCR round 1
1003	GCTAGTCTAGAGCA TCAGTTGAGTTTTCA CTGGA	Used for nested PCR round 2 to construct pJC101 and pJC102; XbaI site underlined
1004	GCTAGGGATCCAAG CTTGCAACCTGGCTT TC	Used for nested PCR round 2 to construct pJC101 and pJC102; BamHI site underlined
1005	AAATGACGGTCCCA TCTCAAA	Used to amplify tolC to confirm successful mutant construction
1006	CCCATGTAAAACTTC AATGCGT	Used to amplify tolC to confirm successful mutant construction
1010	TGAGAACCAAAGGC TGGGAA	Used to amplify ragB/susD for nested PCR round 1
1011	GGTACATTGTTTTCG GCGCA	Used to amplify ragB/susD for nested PCR round 1
1012	GCTAGTCTAGATGG GGATTAACCAGCGA CAG	Used for nested PCR round 2 to construct pJC103; XbaI site underlined
1013	GCTAGGGATCCTTCA CCTGCATCGGCAGTT C	Used for nested PCR round 2 to construct pJC103; BamHI site underlined
1014	ATGCTCCCGCAAAA CCAAGA	Used to amplify ragB/susD to confirm successful mutant construction
1015	ATCAGGACCAGTTG TTGCCG	Used to amplify ragB/susD to confirm successful mutant construction

25 Supplementary Table 4 PCR conditions for nested PCR round 1

Reagent	Volume (µL)
Template (6.25 ng/μL)	10
Forward/Reverse primers (10 μM)	2.5
10 mM dNTPs (Sigma-Aldrich, St. Louis, MO)	1
Phusion DNA polymerase (New England BioLabs,	0.5
Ipswich, MA)	
Phusion 5X buffer (HF buffer for <i>tolC</i> and GC buffer	9.5
for ragB/susD)	
Nuclease-free water	24

Supplementary Table 5 PCR conditions for nested PCR round 2

Reagent	Volume (µL)
Template (1 ng/μL; PCR product from R1)	0.5
Forward/Reverse primers (10 μM)	2.5
10 mM dNTPs	1
Phusion DNA polymerase	0.5
Phusion 5X buffer (HF buffer for <i>tolC</i> and GC buffer for	9.5
ragB/susD)	
Nuclease-free water	33.5

31 Supplementary Table 6 Reagents and reaction volumes for restriction enzyme digestion

Reagent	Volume (µL)
Nested PCR R2 products or pYT354 (1 μg/μL)	1
10X cutsmart buffer (New England BioLabs, Ipswich, MA)	5
BamHI-HF (New England BioLabs, Ipswich, MA)	1 (20 units)
XbaI (New England BioLabs, Ipswich, MA)	1 (20 units)
Nuclease-free water	42

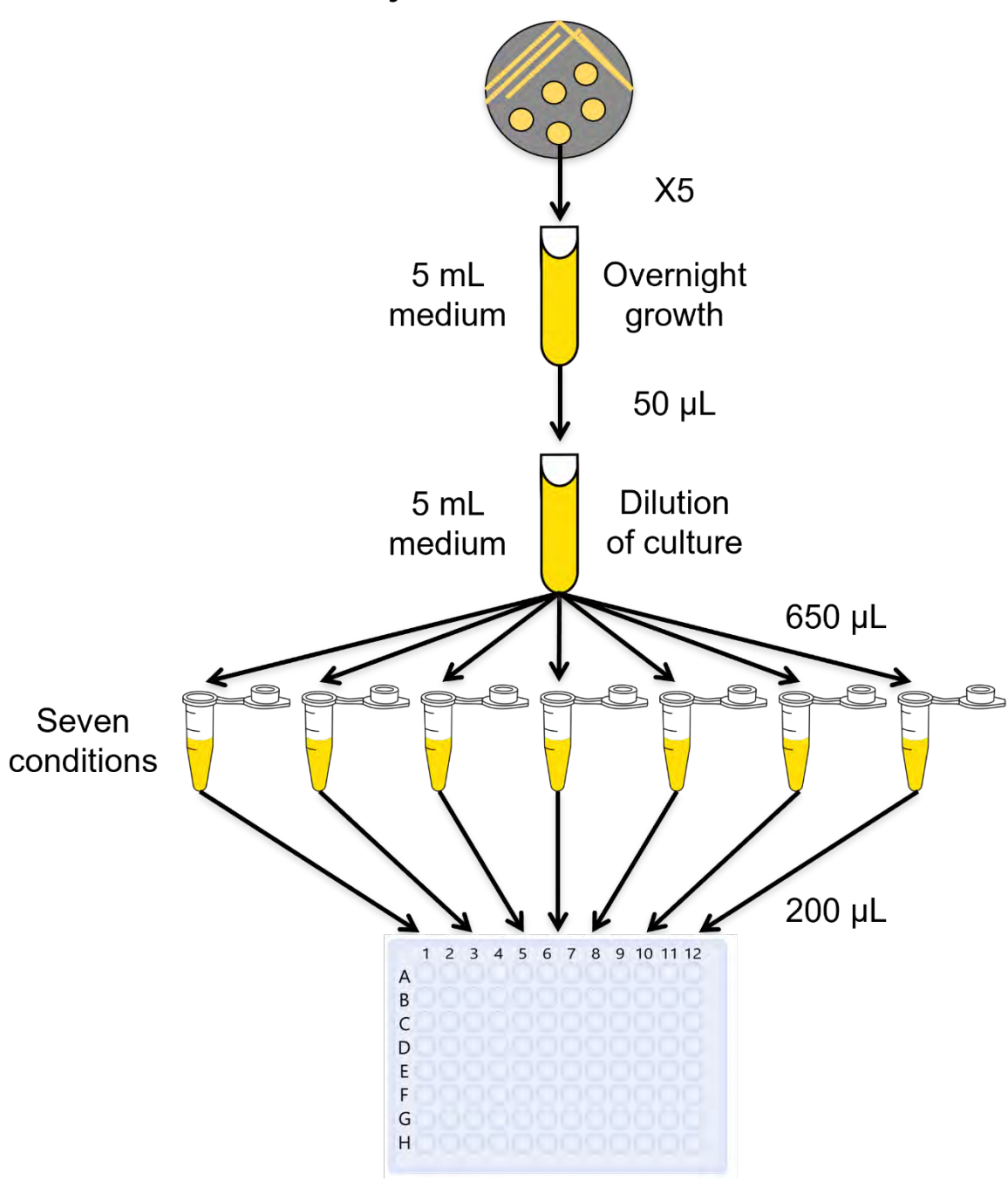
Supplementary Table 7 Reagents and reaction volumes/mass for ligation reactions

Reagent	Volume/Mass
Insert (\sim 3.2 for <i>tolC</i> , \sim 3.1 kbp for <i>ragB/susD</i>)	Varied ^a
Vector (~7.7 kbp)	50 ng
T4 DNA ligase (New England BioLabs, Ipswich, MA)	1 μL
10 X T4 DNA ligase buffer (New England BioLabs, Ipswich, MA)	2 μL
Nuclease-free water	Up to 20 μL

^aTo achieve a 1:3 vector:insert molar ratio, 61.49 ng was used from *tolC*-containing PCR products and 59.37 ng used from *ragB/susD*-containing PCR products.

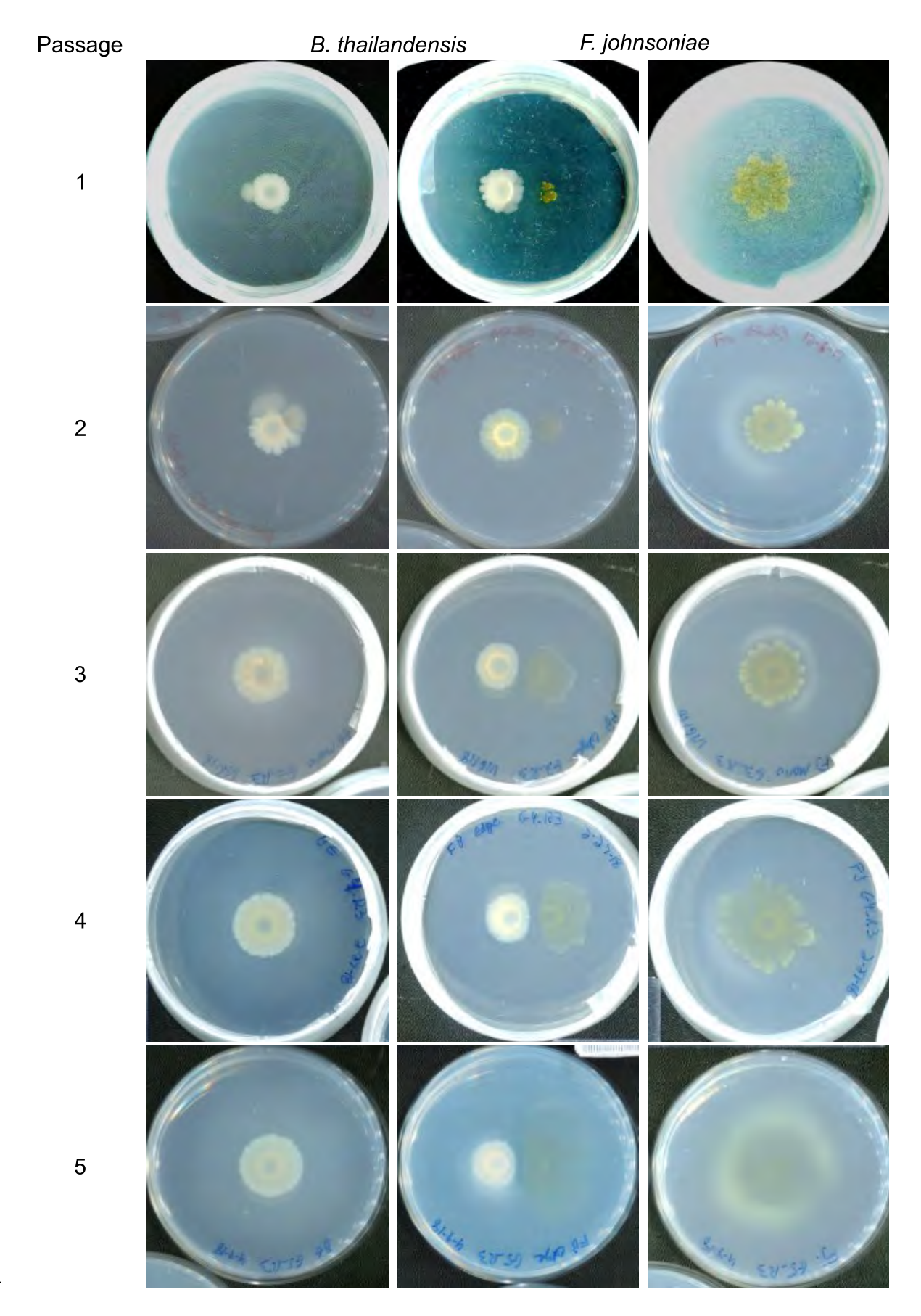
38 Supplementary Figures

F. johnsoniae UW101



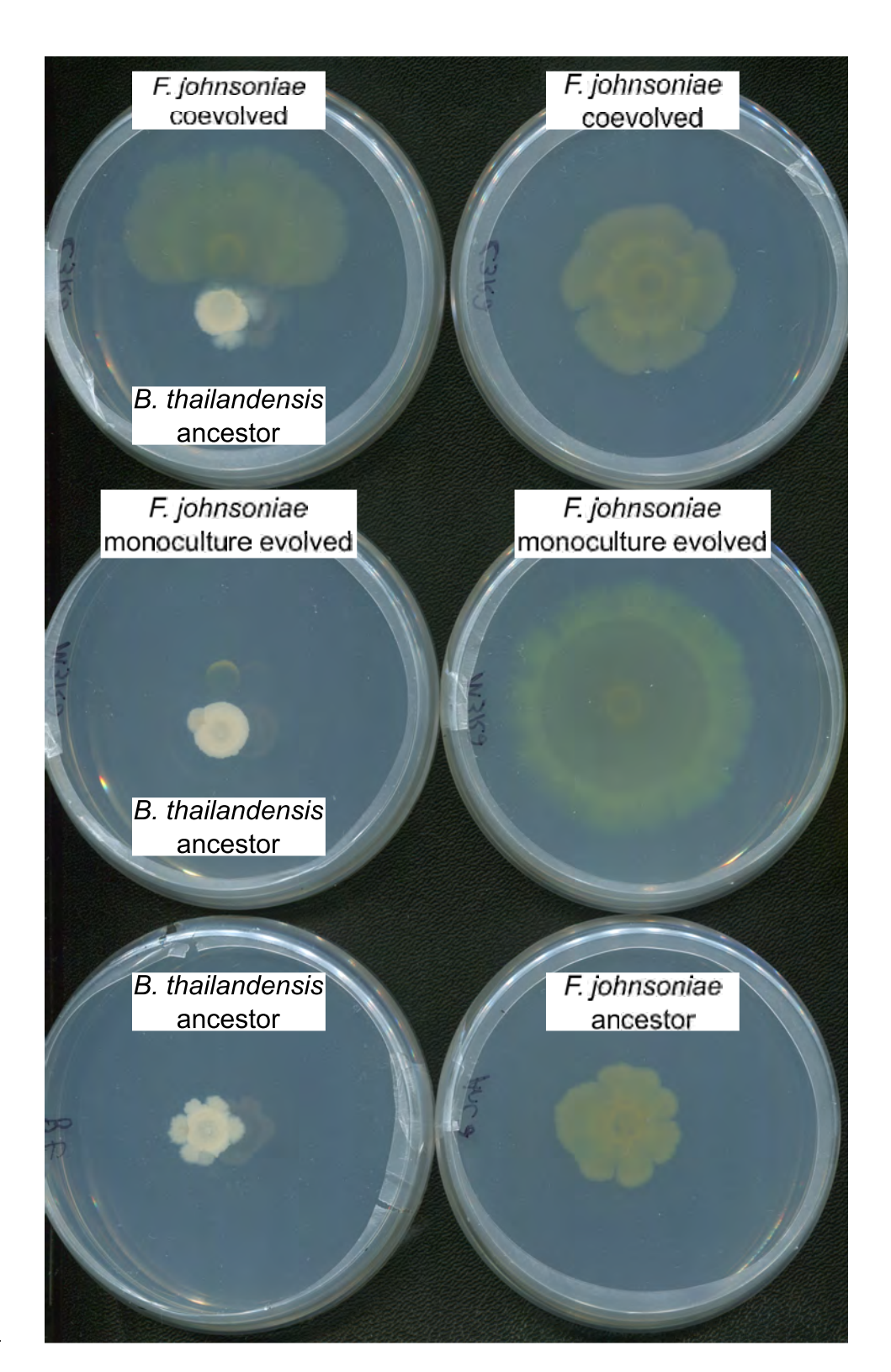
Supplementary Fig. 1 Schematic of preparation for efflux pump inhibitor experiment.

40 41

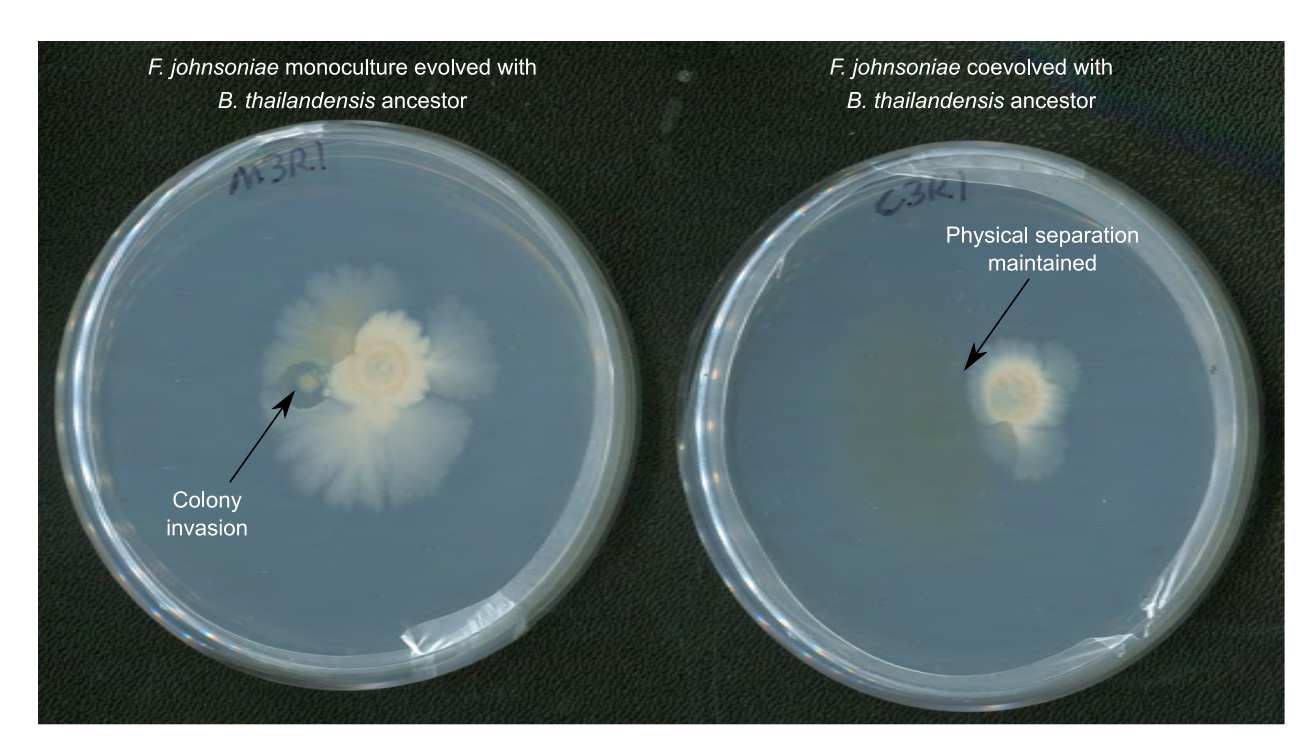


Supplementary Fig. 2 Colony morphologies and growth success over the (co)evolution experiment. Plate images were taken at 1.5 months after each plate passage. Shown are colony morphologies and growth success of *B*.

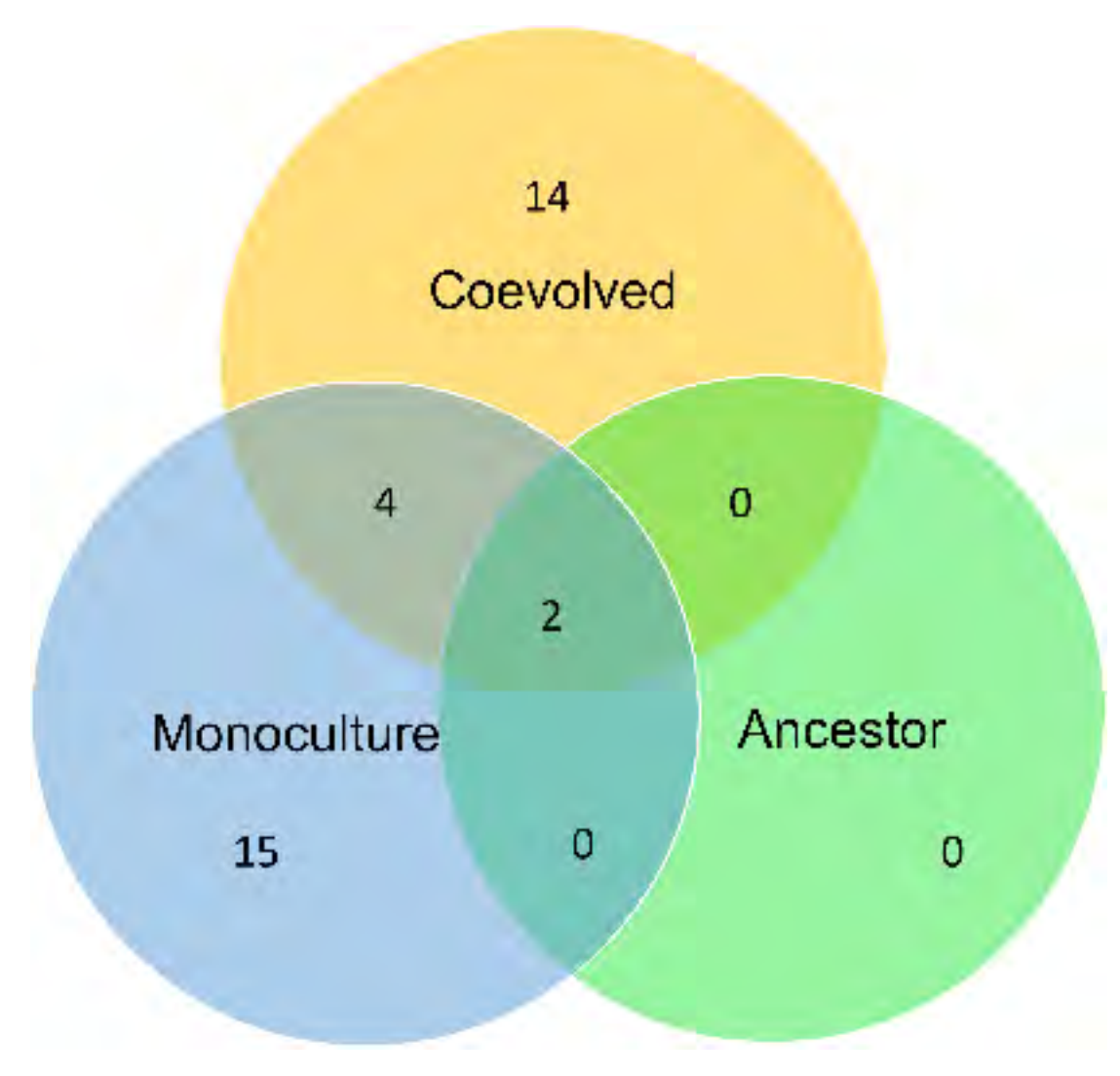
thailandensis monoculture (column 1), co-plated *B. thailandensis-F. johnsoniae* (column 2), and *F. johnsoniae* monoculture (column 3) for a representative independent replicate (rep 3). Each row is plate passage



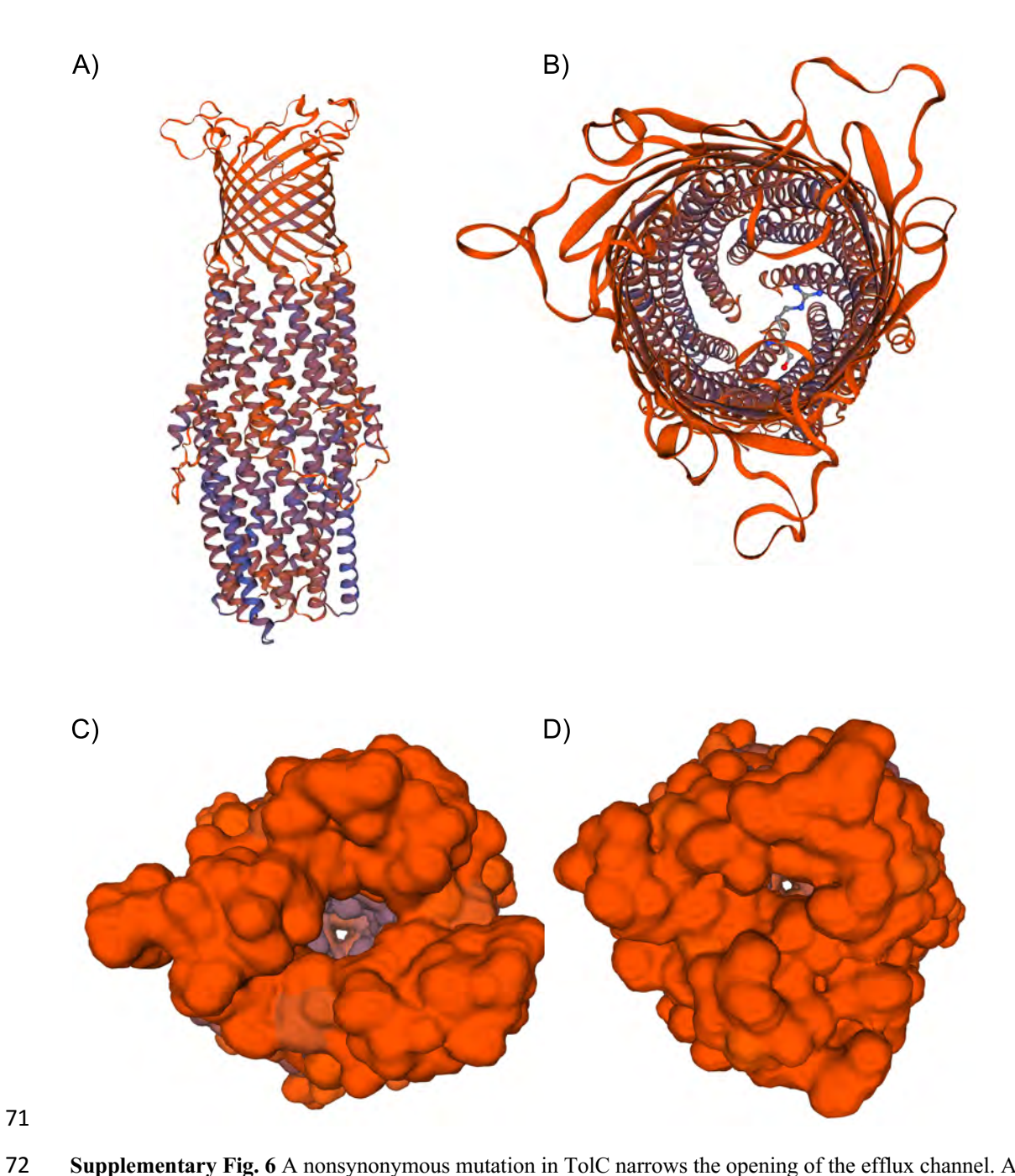
Supplementary Fig. 3 Coevolved *F. johnsoniae* has reduced susceptibility to a *B. thailandensis*-produced antibiotic(s). Coevolved *F. johnsoniae* can grow better in the presence of *B. thailandensis* (column 1, top row) compared to the monoculture evolved *F. johnsoniae* (column 1, middle row). Monocultures are shown as a growth control (column 2, top and middle rows). Shown are evolved lines from one of the independent replicates (rep 3) from the fifth plate passage. Ancestor *F. johnsoniae* and ancestor *B. thailandensis* are shown as additional monoculture controls (bottom row). Images were taken after incubation for 1.5 months



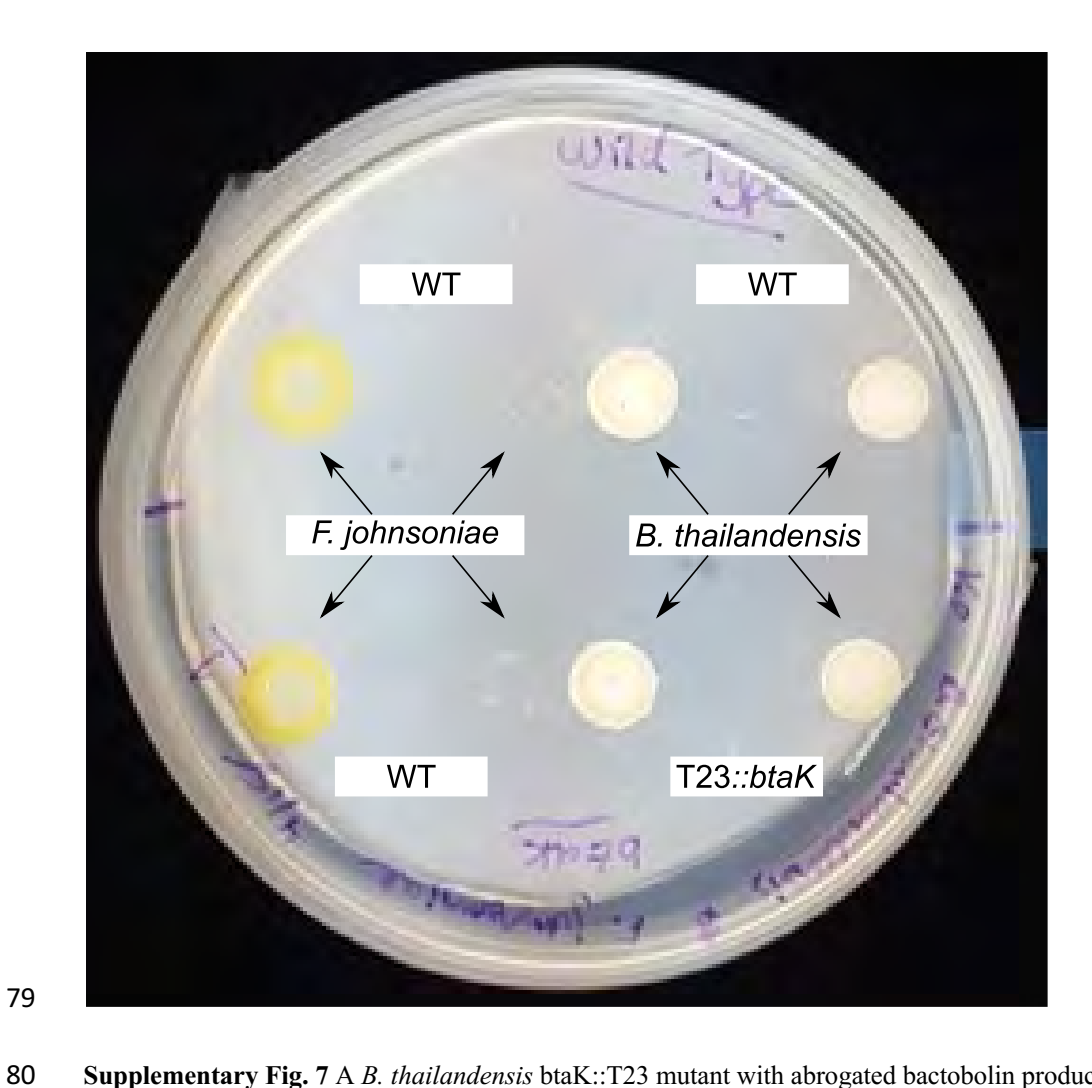
Supplementary Fig. 4 Coevolved *F. johnsoniae* can resist colony invasion. On each plate, *F. johnsoniae* is on the left and *B. thailandensis* (right) is on the right. The *B. thailandensis* ancestor was co-plated with *F. johnsoniae* evolved monoculture (left plate) and *F. johnsoniae* coevolved (right plate) from the fifth plate passage. Plates were incubated for 2.5 months to allow the chance for physical interactions to occur



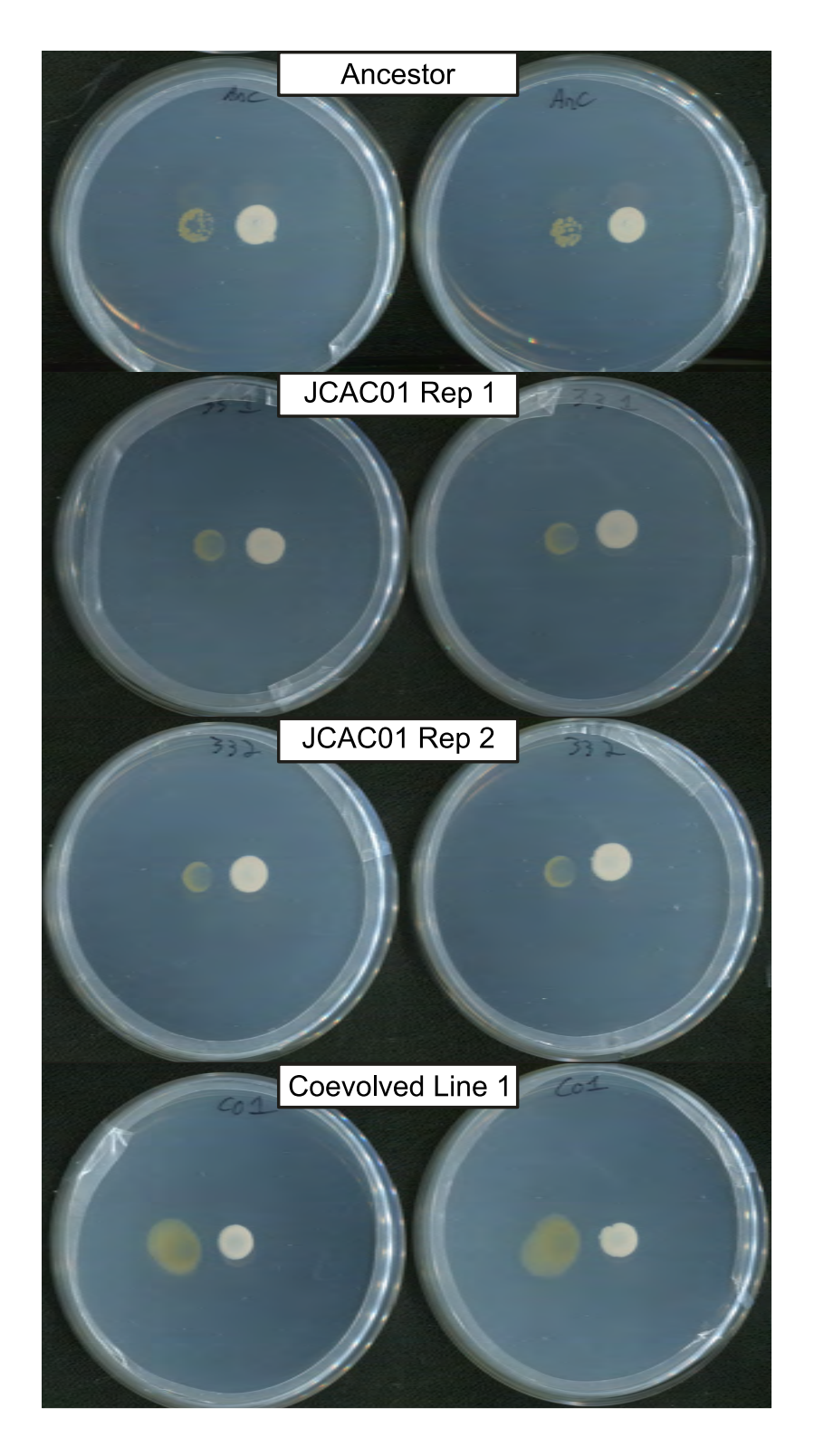
Supplementary Fig. 5 Coevolved lines acquire unique mutations as a result of interspecies interactions. Shown is a Venn diagram comparing distinctions and overlaps of gene loci where mutations were observed in the ancestor, monoculture evolved lines, and coculture evolved lines



Supplementary Fig. 6 A nonsynonymous mutation in TolC narrows the opening of the efflux channel. A model of TolC (A) with the G83R nonsynonymous mutation. TolC is rotated +90 about the x-axis in panels B-D such that TolC is viewed from top looking down the channel. The G83R residue (B) is located on one of the extracellular loops of TolC. The opening of the efflux channel in WT TolC (C) is predicted to narrow due to the G83R mutation (D). TolC from *E. coli* was used as the template (SMTL ID: 6wxi.1) to construct the target *F. johnsoniae* WT TolC (SWISS-MODEL: GMQE=0.6, Seq ID=19.06) and G83R TolC (SWISS-MODEL: GMQE=0.59, Seq ID=19.06) models.

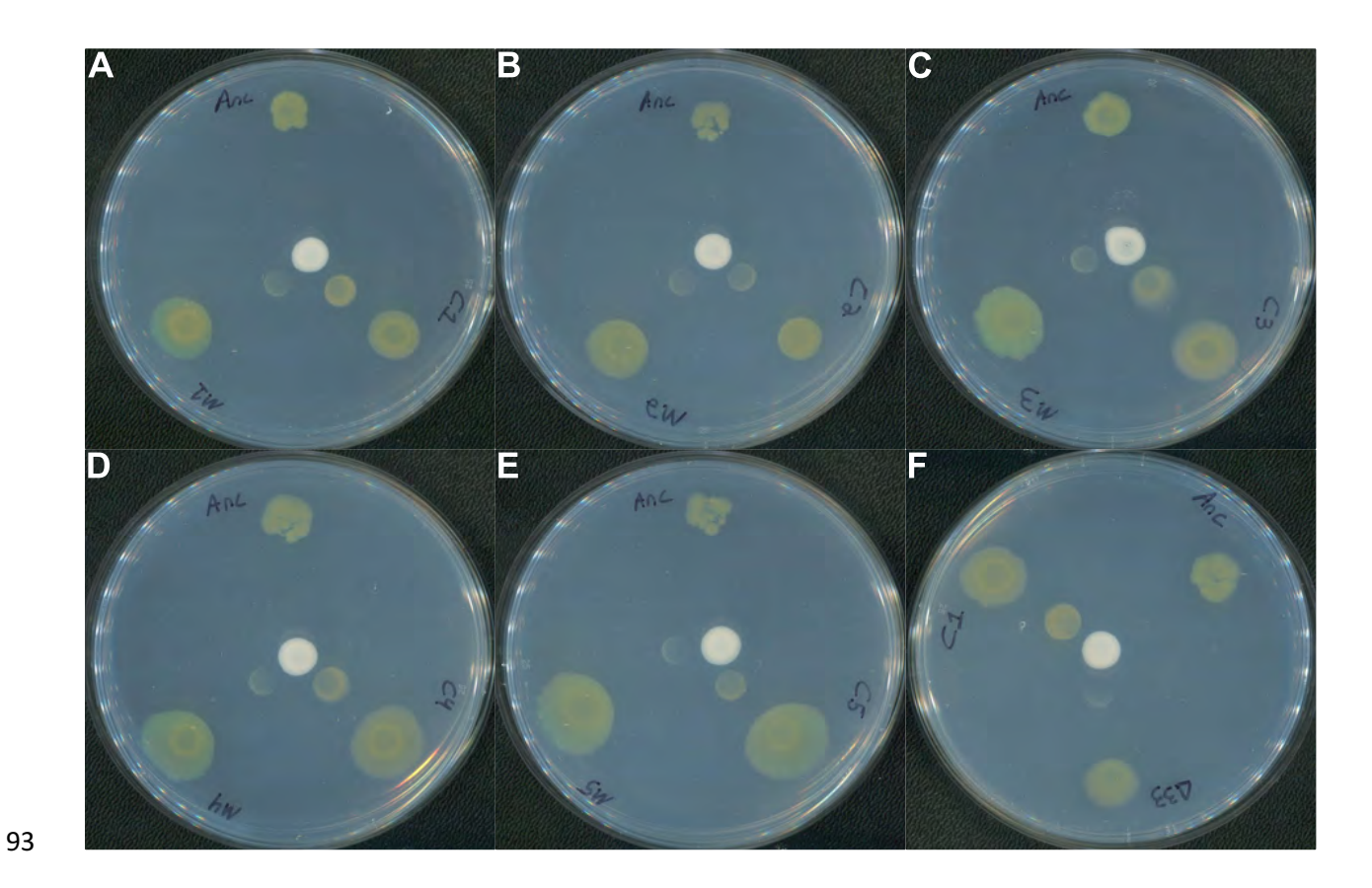


Supplementary Fig. 7 A *B. thailandensis* btaK::T23 mutant with abrogated bactobolin production still inhibits *F.* johnsoniae. B. thailandensis WT (top) and B. thailandensis btaK::T23 (bottom) was co-plated with F. johnsoniae WT. Strains were also plated outside the interspecies interaction zone as controls



Supplementary Fig. 8 *F. johnsoniae* recombinants display a reduction in antibiotic susceptibility, but not to the same degree observed in coevolved lines. The 33 bp deletion in FJOH_RS06580 was placed into the *F. johnsoniae* ancestor and co-plated with *B. thailandensis*. Two confirmed successful recombinants (re $\Delta 33_tolC$, replicates 1&2)

are less inhibited by *B. thailandensis* compared to the *F. johnsoniae* ancestor but are more inhibited compared to the coevolved line from which FJOH_RS06580 was amplified to create the recombinants. All strains were co-plated with the *B. thailandensis* ancestor. Plates were imaged after a month of incubation



Supplementary Fig. 9 Growth success of *F. johnsoniae* strains when co-plated with *B. thailandensis. F. johnsoniae* strains (yellow) were plated in the vicinity of the *B. thailandensis* ancestor (beige, middle colony) to observe growth inhibition. In each panel, the *F. johnsoniae* ancestor (Anc; panels A-F), the *F. johnsoniae* coevolved replicates from the 5th plate passage (C1, panels A-F; C2-C5, panels A-E), the *F. johnsoniae* evolved monocultures from the 5th plate passage (M1-M5, panels A-E), and the *F. johnsoniae* recombinant strain, re $\Delta 33_tolC$ ($\Delta 33$, panel F), were plated in a triangular formation around *B. thailandensis*. Duplicate colonies were spotted at the exterior of the plates as a growth control. Plates were imaged after a week of incubation

Summary of results from breseq

Organism	Evolved line and replicate	gene_name
----------	----------------------------	-----------

Organism	Evolved line and replicate	gene_name
F. johnsoniae	Coevolved replicate 1	FJOH_RS04780
F. johnsoniae	Coevolved replicate 1	FJOH_RS06580
F. johnsoniae	Coevolved replicate 1	FJOH_RS09520
F. johnsoniae	Coevolved replicate 1	FJOH_RS14155
F. johnsoniae	Coevolved replicate 1	FJOH_RS20510
F. johnsoniae	Coevolved replicate 1	FJOH_RS21875
F. johnsoniae	Coevolved replicate 2	FJOH_RS06580
F. johnsoniae	Coevolved replicate 2	FJOH_RS07830
F. johnsoniae	Coevolved replicate 2	FJOH_RS09515
F. johnsoniae	Coevolved replicate 2	FJOH_RS14175
F. johnsoniae	Coevolved replicate 2	FJOH_RS15020
F. johnsoniae	Coevolved replicate 3	FJOH_RS00255
F. johnsoniae	Coevolved replicate 3	FJOH_RS06580
F. johnsoniae	Coevolved replicate 3	FJOH_RS09520
F. johnsoniae	Coevolved replicate 3	FJOH_RS11170
F. johnsoniae	Coevolved replicate 3	FJOH_RS12240
F. johnsoniae	Coevolved replicate 3	FJOH_RS14155
F. johnsoniae	Coevolved replicate 4	FJOH_RS09520
F. johnsoniae	Coevolved replicate 4	FJOH_RS14155
F. johnsoniae	Coevolved replicate 4	FJOH_RS24860
F. johnsoniae	Coevolved replicate 4	FJOH_RS24865
F. johnsoniae	Coevolved replicate 4	FJOH_RS25290
F. johnsoniae	Coevolved replicate 5	gcvP
F. johnsoniae	Coevolved replicate 5	FJOH_RS06580
F. johnsoniae	Coevolved replicate 5	FJOH_RS07435
F. johnsoniae	Coevolved replicate 5	FJOH_RS09515
F. johnsoniae	Coevolved replicate 5	FJOH_RS14155
F. johnsoniae	Monoculture replicate 1	[FJOH_RS00780]
F. johnsoniae	Monoculture replicate 1	FJOH_RS07435
F. johnsoniae	Monoculture replicate 1	FJOH_RS07490
F. johnsoniae	Monoculture replicate 1	FJOH_RS12480
F. johnsoniae	Monoculture replicate 1	FJOH_RS14155
F. johnsoniae	Monoculture replicate 1	FJOH_RS26065
F. johnsoniae	Monoculture replicate 2	FJOH_RS01300/ffh
F. johnsoniae	Monoculture replicate 2	rpsL
F. johnsoniae	Monoculture replicate 2	FJOH_RS07435
F. johnsoniae	Monoculture replicate 2	FJOH_RS13650
F. johnsoniae	Monoculture replicate 2	FJOH_RS14155
F. johnsoniae	Monoculture replicate 2	FJOH_RS26355
F. johnsoniae	Monoculture replicate 2	FJOH_RS24860
F. johnsoniae	Monoculture replicate 3	FJOH_RS07435

F. johnsoniae	Monoculture replicate 3	FJOH_RS07495
F. johnsoniae	Monoculture replicate 3	
F. johnsoniae	Monoculture replicate 3	FJOH_RS14155
F. johnsoniae	Monoculture replicate 3	FJOH_RS15020
F. johnsoniae	Monoculture replicate 3	FJOH_RS24860
F. johnsoniae	Monoculture replicate 4	FJOH_RS05090
F. johnsoniae	Monoculture replicate 4	FJOH_RS07435
F. johnsoniae	Monoculture replicate 4	FJOH_RS07495
F. johnsoniae	Monoculture replicate 4	FJOH_RS14155
F. johnsoniae	Monoculture replicate 4	FJOH_RS20925
F. johnsoniae	Monoculture replicate 4	FJOH_RS24860
F. johnsoniae	Monoculture replicate 5	FJOH_RS02110
F. johnsoniae	Monoculture replicate 5	FJOH_RS14170
F. johnsoniae	Monoculture replicate 5	FJOH_RS15030/FJC
F. johnsoniae	tolc 33 bp deltion recombin	FJOH_RS06580
F. johnsoniae	tolc 33 bp deltion recombin	FJOH_RS19625/FJO

gene_position gene_product

gene_position	gene_product
329	hypothetical protein
coding (261-293/1335 nt)	TolC family protein
coding (825/999 nt)	histidine kinase
2476	CusA/CzcA family heavy metal efflux RND transporter
coding (201/594 nt)	TetR/AcrR family transcriptional regulator
1489	glycoside hydrolase
coding (261-293/1335 nt)	TolC family protein
148	NAD(P)/FAD-dependent oxidoreductase
46	LytTR family DNA-binding domain-containing protein
269	response regulator transcription factor
coding (747-758/3714 nt)	SusC/RagA family TonB-linked outer membrane protei
479	acetyl-CoA carboxylase carboxyltransferase subunit alp
247	7 TolC family protein
496	histidine kinase
273	Gfo/Idh/MocA family oxidoreductase
79:	AIR synthase-related protein
278	CusA/CzcA family heavy metal efflux RND transporter
coding (621/999 nt)	histidine kinase
2476	CusA/CzcA family heavy metal efflux RND transporter
328	TonB-dependent receptor
coding (793/1734 nt)	RagB/SusD family nutrient uptake outer membrane pr
50	phosphoribosylanthranilate isomerase
coding (504/2850 nt)	aminomethyl-transferring glycine dehydrogenase
coding (261-293/1335 nt)	TolC family protein
coding (353/2184 nt)	carboxy terminal-processing peptidase
44	LytTR family DNA-binding domain-containing protein
699	CusA/CzcA family heavy metal efflux RND transporter
	[FJOH_RS00780]
coding (786/2184 nt)	carboxy terminal-processing peptidase
coding (584-597/747 nt)	response regulator transcription factor
coding (719/774 nt)	carboxypeptidase-like regulatory domain-containing pr
	CusA/CzcA family heavy metal efflux RND transporter
838	sigma-54 dependent transcriptional regulator
intergenic (-39/+50)	bifunctional 5,10-methylene-tetrahydrofolate dehydrog
	7 30S ribosomal protein S12
coding (817/2184 nt)	carboxy terminal-processing peptidase
coding (1064/1260 nt)	site-specific integrase
2297	CusA/CzcA family heavy metal efflux RND transporter
	T9SS type A sorting domain-containing protein
coding (2054-2056/3288 nt)	TonB-dependent receptor
coding (995/2184 nt)	carboxy terminal-processing peptidase

coding (103/1731 nt)	ATP-binding protein
2071	DNA-directed RNA polymerase subunit beta'
2476	CusA/CzcA family heavy metal efflux RND transporter
coding (973-1245/3714 nt)	SusC/RagA family TonB-linked outer membrane protei
coding (603-605/3288 nt)	TonB-dependent receptor
124	DUF4837 family protein
coding (735-779/2184 nt)	carboxy terminal-processing peptidase
coding (1606/1731 nt)	ATP-binding protein
2476	CusA/CzcA family heavy metal efflux RND transporter
coding (137/540 nt)	tail fiber protein
1673	TonB-dependent receptor
coding (3112-3204/3252 nt)	SusC/RagA family TonB-linked outer membrane protei
158	HAMP domain-containing histidine kinase
intergenic (-108/+243)	sigma-70 family RNA polymerase sigma factor/hypoth
coding (261-293/1335 nt)	TolC family protein
intergenic (-402/-451)	hypothetical protein/Crp/Fnr family transcriptional reg

mutation_ca new_seq	position	position_end	position_star	size	SNP_type
snp_nonsyno C	1032329	1032329	1032329		nonsynonymo
small_indel	1442876	1442908	1442876	33	
small_indel T	2115383	2115383	2115383		
snp_nonsyno A	3254087	3254087	3254087		nonsynonymo
small_indel T	4734734	4734734	4734734		
snp_nonsyno C	5103192	5103192	5103192		nonsynonymo
small_indel	1442876	1442908	1442876	33	
snp_nonsyno A	1735676	1735676	1735676		nonsynonymo
snp_nonsyno T	2115191	2115191	2115191		nonsynonymo
snp_nonsyno A	3260769	3260769	3260769		nonsynonymo
small_indel	3437168	3437179	3437168	12	
snp_nonsyno T	48770	48770	48770		nonsynonymo
snp_nonsyno A	1442862	1442862	1442862		nonsynonymo
snp_nonsyno T	2115712	2115712	2115712		nonsynonymo
snp_synonym C	2593409	2593409	2593409		synonymous
snp_nonsyno T	2825359	2825359	2825359		nonsynonymo
snp_nonsyno G	3256285	3256285	3256285		nonsynonymo
small_indel	2115587	2115587	2115587	1	
snp_nonsyno A	3254087	3254087	3254087		nonsynonymo
snp_nonsyno C	5823750	5823750	5823750		nonsynonymo
small_indel G	5827528	5827528	5827528		
snp_nonsyno C	5916920	5916920	5916920		nonsynonymo
small_indel	461783	461783	461783	1	
small_indel	1442876	1442908	1442876	33	
small_indel A	1639597	1639597	1639597		
snp_nonsyno A	2115193	2115193	2115193		nonsynonymo
snp_nonsyno A	3255868	3255868	3255868		nonsynonymo
large_deletion	149160	149449	149160	290	
small_indel	1640030	1640030	1640030	1	
small_indel	1654068	1654081	1654068	14	
small_indel A	2874473	2874473	2874473		
snp_nonsyno A	3255194	3255194	3255194		nonsynonymo
snp_nonsyno T	6085864	6085864	6085864		nonsynonymo
large_deletion	257856	257906	257856	51	
snp_nonsyno A	411121	411121	411121		nonsynonymo
small_indel A	1640061	1640061	1640061		
small_indel	3132257	3132257	3132257	1	
snp_nonsyno T	3254266	3254266	3254266		nonsynonymo
snp_nonsens A	4834921	4834921	4834921		nonsense
small_indel	5825476	5825478	5825476	3	
small_indel	1640239	1640239	1640239	1	

small_indel	1656294	1656294	1656294	1	
snp_nonsyno A	2249614	2249614	2249614		nonsynonymo
snp_nonsyno A	3254087	3254087	3254087		nonsynonymo
large_deletion	3436681	3436953	3436681	273	
small_indel	5824025	5824027	5824025		
snp_nonsyno C	1091086	1091086	1091086		nonsynonymo
small_indel	1639979	1640023	1639979	45	
small_indel T	1654791	1654791	1654791		
snp_nonsyno A	3254087	3254087	3254087		nonsynonymo
small_indel GG	4828379	4828379	4828379		
snp_nonsyno C	5825095	5825095	5825095		nonsynonymo
large_deletion	416734	416826	416734	93	
snp_nonsens T	3260203	3260203	3260203		nonsense
small_indel	3440151	3440164	3440151	14	
small_indel	1442876	1442908	1442876	33	
small_indel CTAA	4493481	4493481	4493481		

Type

Туре
SNP
DEL
INS
SNP
INS
SNP
DEL
SNP
SNP
SNP
DEL
SNP
DEL
SNP
SNP
INS
SNP
DEL
DEL
INS
SNP
SNP
DEL
DEL
DEL
INS
SNP
SNP
DEL
SNP
INS
DEL
SNP
SNP
DEL
DEL

DEL
SNP
SNP
DEL
DEL
SNP
DEL
INS
SNP
INS
SNP
DEL
SNP
DEL
DEL
INS

•	ults from breseq				
Organism	Evolved line and replicate				codon_new_:
F. johnsoniae	Coevolved replicate 1	А	110	G	GCA
F. johnsoniae	Coevolved replicate 1				
F. johnsoniae	Coevolved replicate 1				
F. johnsoniae	Coevolved replicate 1	С	826	R	TGT
F. johnsoniae	Coevolved replicate 1				
F. johnsoniae	Coevolved replicate 1	Н	497	Υ	CAT
F. johnsoniae	Coevolved replicate 2				
F. johnsoniae	Coevolved replicate 2	T	50	Р	ACA
F. johnsoniae	Coevolved replicate 2	Т	16	А	ACG
F. johnsoniae	Coevolved replicate 2	F	90	S	TTC
F. johnsoniae	Coevolved replicate 2				
F. johnsoniae	Coevolved replicate 3	Q	160	Р	CAG
F. johnsoniae	Coevolved replicate 3	R	83	G	AGA
F. johnsoniae	Coevolved replicate 3	R	166	G	AGA
F. johnsoniae	Coevolved replicate 3	G	91	G	GGC
F. johnsoniae	Coevolved replicate 3	L	264	S	TTA
F. johnsoniae	Coevolved replicate 3	S	93		TCA
F. johnsoniae	Coevolved replicate 4			_	
F. johnsoniae	Coevolved replicate 4	С	826	R	TGT
F. johnsoniae	Coevolved replicate 4	Р	110		CCT
F. johnsoniae	Coevolved replicate 4		110	3	CCI
F. johnsoniae	Coevolved replicate 4	A	17	V	GCA
F. johnsoniae	Coevolved replicate 5	A	17	V	GCA
F. johnsoniae	Coevolved replicate 5				
F. johnsoniae	Coevolved replicate 5				
F. johnsoniae	Coevolved replicate 5	L	15	D	CTG
F. johnsoniae		V	232		GTT
	Coevolved replicate 5	V	232	d	GII
F. johnsoniae	Monoculture replicate 1				
F. johnsoniae	Monoculture replicate 1				
F. johnsoniae	Monoculture replicate 1				
F. johnsoniae	Monoculture replicate 1	C	457	•	TCT
F. johnsoniae	Monoculture replicate 1	S	457		TCT
F. johnsoniae	Monoculture replicate 1	Τ	280	А	ACA
F. johnsoniae	Monoculture replicate 2				
F. johnsoniae	Monoculture replicate 2	I	49	M	ATT
F. johnsoniae	Monoculture replicate 2				
F. johnsoniae	Monoculture replicate 2				
F. johnsoniae	Monoculture replicate 2	Q	766	R	CAA
F. johnsoniae	Monoculture replicate 2	*	1331	S	TAA
F. johnsoniae	Monoculture replicate 2				
F. johnsoniae	Monoculture replicate 3				
F. johnsoniae	Monoculture replicate 3				
F. johnsoniae	Monoculture replicate 3		691		AGT
F. johnsoniae	Monoculture replicate 3				
F. johnsoniae	Monoculture replicate 3				
F. johnsoniae	Monoculture replicate 3				

F. johnsoniae	Monoculture replicate 4	E	42	Q	GAA
F. johnsoniae	Monoculture replicate 4				
F. johnsoniae	Monoculture replicate 4				
F. johnsoniae	Monoculture replicate 4	С	826	R	TGT
F. johnsoniae	Monoculture replicate 4				
F. johnsoniae	Monoculture replicate 4	P	558	H	CCC
F. johnsoniae	Monoculture replicate 5				
F. johnsoniae	Monoculture replicate 5	*	53	L	TAG
F. johnsoniae	Monoculture replicate 5				
F. johnsoniae	tolc 33 bp deltion recombine				
F. johnsoniae	tolc 33 bp deltion recombine				

codon_numb codon_positiccodon_ref_segene_name

codon_numb	codon_positi	codon_rei_s	egene_	name
110	2	GGA	FJOH_	RS04780
			FJOH	RS06580
			FJOH	RS09520
826	1	CGT	FJOH	RS14155
			FJOH	RS20510
497	1	TAT	_	RS21875
				RS06580
50	1	CCA	_	RS07830
16	1			RS09515
90	2		_	RS14175
	_		_	RS15020
160	2	CCG		RS00255
83	1	GGA		RS06580
166	1	GGA		RS09520
91	3			RS11170
264	2	TCA		RS12240
93	2	TTA		RS14155
33	2	IIA	_	RS09520
826	1	CGT		RS14155
	1			
110	1	TCT		RS24860
47	2	CT A		RS24865
17	2	GTA		_RS25290
			gcvP	
				_RS06580
				_RS07435
15	2			_RS09515
232	2	GGT		_RS14155
				_RS00780]
			FJOH_	_RS07435
				_RS07490
			FJOH_	_RS12480
457	1	GCT	FJOH_	_RS14155
280	1	GCA	FJOH_	_RS26065
			FJOH_	_RS01300/ffh
49	3	ATG	rpsL	
			FJOH_	_RS07435
			FJOH	_RS13650
766	2	CGA	FJOH_	_RS14155
1331	2	TCA	FJOH	RS26355
			FJOH	RS24860
			FJOH	RS07435
			FJOH	RS07495
691	1		rpoC	
826	1			RS14155
				RS15020
			FJOH	RS24860

42	1	CAA	FJOH_RS05090
			FJOH_RS07435
			FJOH_RS07495
826	1	CGT	FJOH_RS14155
			FJOH_RS20925
558	2	CAC	FJOH_RS24860
			FJOH_RS02110
53	2	TTG	FJOH_RS14170
			FJOH_RS15030/FJOH_RS1
			FJOH_RS06580
			FJOH_RS19625/FJOH_RS1

gene_position gene_product

320	by mothetical protein
	hypothetical protein
coding (261-293/1335 nt)	TolC family protein
coding (825/999 nt)	histidine kinase
	CusA/CzcA family heavy metal efflux RND transporter
coding (201/594 nt)	TetR/AcrR family transcriptional regulator
	glycoside hydrolase
coding (261-293/1335 nt)	TolC family protein
	NAD(P)/FAD-dependent oxidoreductase
	LytTR family DNA-binding domain-containing protein
	response regulator transcription factor
coding (747-758/3714 nt)	SusC/RagA family TonB-linked outer membrane protei
	acetyl-CoA carboxylase carboxyltransferase subunit alp
	TolC family protein
	histidine kinase
	Gfo/Idh/MocA family oxidoreductase
	AIR synthase-related protein
	CusA/CzcA family heavy metal efflux RND transporter
coding (621/999 nt)	histidine kinase
	CusA/CzcA family heavy metal efflux RND transporter
	TonB-dependent receptor
coding (793/1734 nt)	RagB/SusD family nutrient uptake outer membrane pr
	phosphoribosylanthranilate isomerase
coding (504/2850 nt)	aminomethyl-transferring glycine dehydrogenase
coding (261-293/1335 nt)	TolC family protein
coding (353/2184 nt)	carboxy terminal-processing peptidase
	LytTR family DNA-binding domain-containing protein
695	CusA/CzcA family heavy metal efflux RND transporter
li (706/0404 i)	[FJOH_RS00780]
coding (786/2184 nt)	carboxy terminal-processing peptidase
coding (584-597/747 nt)	response regulator transcription factor
coding (719/774 nt)	carboxypeptidase-like regulatory domain-containing pr
	CusA/CzcA family heavy metal efflux RND transporter
	sigma-54 dependent transcriptional regulator
intergenic (-39/+50)	bifunctional 5,10-methylene-tetrahydrofolate dehydrog
	30S ribosomal protein S12
coding (817/2184 nt)	carboxy terminal-processing peptidase
coding (1064/1260 nt)	site-specific integrase
	CusA/CzcA family heavy metal efflux RND transporter
	T9SS type A sorting domain-containing protein
coding (2054-2056/3288 nt)	TonB-dependent receptor
coding (995/2184 nt)	carboxy terminal-processing peptidase
coding (103/1731 nt)	ATP-binding protein
	DNA-directed RNA polymerase subunit beta'
	CusA/CzcA family heavy metal efflux RND transporter
coding (973-1245/3714 nt)	SusC/RagA family TonB-linked outer membrane protei
coding (603-605/3288 nt)	TonB-dependent receptor

124	DUF4837 family protein
coding (735-779/2184 nt)	carboxy terminal-processing peptidase
coding (1606/1731 nt)	ATP-binding protein
2476	CusA/CzcA family heavy metal efflux RND transporter
coding (137/540 nt)	tail fiber protein
1673	TonB-dependent receptor
coding (3112-3204/3252 nt)	SusC/RagA family TonB-linked outer membrane protei
158	HAMP domain-containing histidine kinase
intergenic (-108/+243)	sigma-70 family RNA polymerase sigma factor/hypoth
coding (261-293/1335 nt)	TolC family protein
intergenic (-402/-451)	hypothetical protein/Crp/Fnr family transcriptional reg

gene_strand genes_inacti genes_overlagenes_promainsert_positialocus_tag locus_tags_ir FJOH RS04780 FJOH RS04780 FJOH RS06580 FJOH RS065 FJOH RS065 FJOH_RS09520 FJOH RS09520 **FJOH RS14155** FJOH RS14155 FJOH RS20510 FJOH RS205 FJOH RS205 FJOH RS21875 FJOH RS21875 FJOH RS06580 FJOH RS065 FJOH RS065 **FJOH RS07830 FJOH RS07830 FJOH RS09515 FJOH RS09515 FJOH RS14175 FJOH RS14175** FJOH RS15020 FJOH RS150 FJOH RS1502 FJOH RS00255 FJOH RS00255 **FJOH RS06580 FJOH RS06580** FJOH RS09520 FJOH RS09520 **FJOH RS11170 FJOH RS11170 FJOH RS12240 FJOH RS12240 FJOH RS14155 FJOH RS14155** FJOH RS09520 FJOH RS095 FJOH RS0952 < **FJOH RS14155 FJOH RS14155** FJOH RS24860 FJOH RS24860 FJOH RS24865 FJOH RS248 FJOH RS2486 **FJOH RS25290** FJOH RS25290 gcvP FJOH RS023 FJOH RS0232 **FJOH RS06580** FJOH RS065 FJOH RS0658 FJOH RS07435 1 FJOH RS074 FJOH RS0743 **FJOH RS09515 FJOH RS09515 FJOH RS14155** FJOH RS14155 **FJOH RS00780** [FJOH RS00] FJOH RS0078 **FJOH RS07435** FJOH RS074 FJOH RS0743 **FJOH RS07490** FJOH RS074 FJOH RS0749 1 FJOH RS12480 **FJOH RS12480** < **FJOH RS14155 FJOH RS14155 FJOH RS26065 FJOH RS26065** FJOH RS01300/FJOH RS0 **FJOH RS01300** </< FJOH RS02100 rpsL FJOH RS07435 FJOH RS074 FJOH RS0743 **FJOH RS13650** FJOH RS13650 FJOH RS14155 **FJOH RS14155** FJOH_RS263 FJOH_RS263 FJOH_RS26355 **FJOH RS24860** FJOH_RS248 FJOH_RS2486

<		FJOH_RS05090			FJOH_RS050	90
>	FJOH_RS074	35			FJOH_RS074	FJOH_RS0743
<		FJOH_RS074	95	1	FJOH_RS074	95
<		FJOH_RS141	55		FJOH_RS141	55
>	FJOH_RS209	OH_RS20925		1	FJOH_RS209	FJOH_RS2092
>		FJOH_RS248	60		FJOH_RS248	60
>		FJOH_RS021	FJOH_RS02110		FJOH_RS021	10
<	FJOH_RS141	70			FJOH_RS141	FJOH_RS141
<</td <td></td> <td></td> <td>FJOH_RS150</td> <td>30</td> <td>FJOH_RS150</td> <td>30/FJOH_RS1</td>			FJOH_RS150	30	FJOH_RS150	30/FJOH_RS1
>	FJOH_RS065	80			FJOH_RS065	FJOH_RS0658
				1	FJOH_RS196	25/FJOH_RS1

locus_tags_o	locus_tags_p	mutation_ca	new_seq	position	position_end	position_star
FJOH_RS047	80	snp_nonsyno	С	1032329	1032329	1032329
30		small_indel		1442876	1442908	1442876
FJOH_RS095	20	small_indel	Т	2115383	2115383	2115383
FJOH_RS141	55	snp_nonsyno	Α	3254087	3254087	3254087
10		small_indel	Т	4734734	4734734	4734734
FJOH_RS218	75	snp_nonsyno	С	5103192	5103192	5103192
30		small_indel		1442876	1442908	1442876
FJOH_RS078	30	snp_nonsyno	Α	1735676	1735676	1735676
FJOH_RS095	15	snp_nonsyno	Т	2115191	2115191	2115191
FJOH_RS141	75	snp_nonsyno	Α	3260769	3260769	3260769
20		small_indel		3437168	3437179	3437168
FJOH_RS002	55	snp_nonsyno	Т	48770	48770	48770
FJOH_RS065	80	snp_nonsyno	Α	1442862	1442862	1442862
FJOH_RS095	20	snp_nonsyno	T	2115712	2115712	2115712
FJOH_RS111	70	snp_synonym	С	2593409	2593409	2593409
FJOH_RS122	40	snp_nonsyno	Т	2825359	2825359	2825359
FJOH_RS141	55	snp_nonsyno	G	3256285	3256285	3256285
20		small_indel		2115587	2115587	2115587
FJOH_RS141	55	snp_nonsyno	Α	3254087	3254087	3254087
FJOH_RS248	60	snp_nonsyno		5823750	5823750	5823750
5 5		small_indel	G	5827528	5827528	5827528
FJOH_RS252	90	snp_nonsyno	С	5916920	5916920	5916920
20		small_indel		461783	461783	461783
30		small_indel		1442876	1442908	1442876
35		small_indel	А	1639597	1639597	1639597
FJOH_RS095		snp_nonsyno		2115193	2115193	2115193
FJOH_RS141	55	snp_nonsyno		3255868	3255868	3255868
30		large_deletic	n	149160		
35		small_indel		1640030	1640030	
90		small_indel		1654068	1654081	1654068
FJOH_RS124		small_indel	Α	2874473	2874473	2874473
FJOH_RS141		snp_nonsyno		3255194	3255194	3255194
FJOH_RS260		snp_nonsyno		6085864	6085864	6085864
1305		large_deletic		257856	257906	257856
FJOH_RS021	00	snp_nonsyno		411121	411121	411121
35		small_indel	Α	1640061	1640061	1640061
FJOH_RS136		small_indel	т	3132257	3132257	3132257
FJOH_RS141	55	snp_nonsyno		3254266	3254266	3254266
55		snp_nonsens	A	4834921	4834921	4834921
50		small_indel		5825476	5825478	5825476
35				1640239	1640239	1640239
95 FIOLURE 101	1.5		۸	1656294	1656294	1656294
FJOH_RS101				2249614	2249614	2249614
FJOH_RS141				3254087	3254087	3254087
20		large_deletic		3436681	3436953	3436681
50		small_indel		5824025	5824027	5824025

FJOH_RS050	90	snp_nonsyno	C	1091086	1091086	1091086
35		small_indel		1639979	1640023	1639979
FJOH_RS074	95	small_indel	Т	1654791	1654791	1654791
FJOH_RS141	55	snp_nonsyno	Α	3254087	3254087	3254087
25		small_indel	GG	4828379	4828379	4828379
FJOH_RS248	60	snp_nonsyno	С	5825095	5825095	5825095
FJOH_RS021	10	large_deletic	on	416734	416826	416734
70		snp_nonsens	Т	3260203	3260203	3260203
5035	FJOH_RS150	small_indel		3440151	3440164	3440151
30		small_indel		1442876	1442908	1442876
		small_indel	СТАА	4493481	4493481	4493481

repeat_	lengt	repeat_new_	repeat_ref_c	repeat_seq	seq_id	size	SNP_type
					NC_009441		nonsynonym
					NC_009441	33	
	1	7	6	Т	NC_009441		
					NC 009441		nonsynonymo
	1	8	7	Т	NC 009441		
					NC 009441		nonsynonym
					NC_009441	33	
					NC 009441		nonsynonym
					NC 009441		nonsynonymo
					NC 009441		nonsynonym
					NC 009441	12	,,,,,,,,,,,,,,,,,,,,,,,,,,,,,,,,,,,,,,,
					NC 009441		nonsynonymo
					NC 009441		nonsynonym
					NC 009441		nonsynonymo
					NC 009441		synonymous
					NC 009441		nonsynonymo
					NC 009441		nonsynonymo
	1	6	7	Т	NC 009441	1	Horisynonymic
		0	/	1	NC 009441	1	noncymonymy
					NC 009441		nonsynonymo
							nonsynonymo
					NC_009441		D O D C \ (12 O D \ (120)
					NC_009441	1	nonsynonymo
					NC_009441	1	
					NC_009441	33	
					NC_009441		
					NC_009441		nonsynonymo
					NC_009441	200	nonsynonym
					NC_009441	290	
					NC_009441	1	
					NC_009441	14	
					NC_009441		
					NC_009441		nonsynonymo
					NC_009441		nonsynonymo
					NC_009441	51	
					NC_009441		nonsynonymo
					NC_009441		
	1	8	9	Α	NC_009441	1	
					NC_009441		nonsynonymo
					NC_009441		nonsense
					NC_009441	3	
					NC_009441	1	
	1			Т	NC_009441	1	
					NC_009441		
					NC_009441		
					NC_009441	273	
					NC_009441	3	

				NC_009441		nonsynonymo
				NC_009441	45	
				NC_009441		
				NC_009441		nonsynonym
				NC_009441		
				NC_009441		nonsynonymo
				NC_009441	93	
				NC_009441		nonsense
				NC_009441	14	
				NC_009441	33	
4	17	16	СТАА	NC_009441		

Type SNP

туре	
SNP	
DEL	
INS	
SNP	
INS	
SNP	
DEL	
SNP	
SNP	
SNP	
DEL	
SNP	
DEL	
SNP	
SNP	
INS	
SNP	
DEL	
DEL	
INS	
SNP	
SNP	
DEL	
DEL	
DEL	
INS	
SNP	
SNP	
DEL	
SNP	
INS	
DEL	
SNP	
SNP	
DEL	
DEL	
DEL	
SNP	
SNP	
DEL	
DEL	

Summary of result	Summary of results from breseq								
Organism	Evolved line and replicate	gene_name							
B. thailandensis	Coevolved replicate 1	BTH_RS35420							
B. thailandensis	Coevolved replicate 2	tssH							
B. thailandensis	Coevolved replicate 2	BTH_RS04590							
B. thailandensis	Coevolved replicate 2	BTH_RS06525/BTH_RS065							
B. thailandensis	Coevolved replicate 2	tssF/BTH_RS15400							
B. thailandensis	Coevolved replicate 3	BTH_RS04590							
B. thailandensis	Coevolved replicate 3	fliH							
B. thailandensis	Coevolved replicate 3	BTH_RS13245/BTH_RS132							
B. thailandensis	Coevolved replicate 4	BTH_RS06340							
B. thailandensis	Coevolved replicate 5	vgrG							
B. thailandensis	Coevolved replicate 5	BTH_RS06600/BTH_RS066							
B. thailandensis	Monoculture replicate 1	BTH_RS06600/BTH_RS066							
B. thailandensis	Monoculture replicate 1	BTH_RS10750/BTH_RS107							
B. thailandensis	Monoculture replicate 1	BTH_RS35120							
B. thailandensis	Monoculture replicate 1	arsC/BTH_RS12180							
B. thailandensis	Monoculture replicate 1	BTH_RS17640/nuoE							
B. thailandensis	Monoculture replicate 2	BTH_RS10275/BTH_RS304							
B. thailandensis	Monoculture replicate 2	BTH_RS11790							
B. thailandensis	Monoculture replicate 2	tssM							
B. thailandensis	Monoculture replicate 3	BTH_RS04585/BTH_RS045							
B. thailandensis	Monoculture replicate 3	BTH_RS04590							
B. thailandensis	Monoculture replicate 3	BTH_RS12945/gatC							
B. thailandensis	Monoculture replicate 3								
B. thailandensis	Monoculture replicate 3	waaF/BTH_RS15555							
B. thailandensis	Monoculture replicate 3	waaF/BTH_RS15555							
B. thailandensis	Monoculture replicate 4	BTH_RS10750/BTH_RS107							
B. thailandensis	Monoculture replicate 4	mnmE/BTH_RS28660							
B. thailandensis	Monoculture replicate 5	BTH_RS06600/BTH_RS066							
B. thailandensis	Monoculture replicate 5	fliH							
B. thailandensis	Monoculture replicate 5	BTH_RS18425/BTH_RS184							

gene_position
pseudogene (127-133/135 nt)
coding (2789-2797/2877 nt)
coding (595/912 nt)
intergenic (+87/+147)
intergenic (-714/-269)
coding (595/912 nt)
coding (77-122/681 nt)
intergenic (+337/-191)
coding (326/1593 nt)
2475
intergenic (-453/-72)
intergenic (-453/-72)
intergenic (-143/-13) coding (221-229/477 nt)
intergenic (-222/-297)
intergenic (+143/-19)
intergenic (-41/-276)
coding (33-58/276 nt)
coding (1364-1369/3906 nt)
intergenic (-79/-33)
coding (595/912 nt)
intergenic (-176/-188)
coding (105/207 nt)
intergenic (-84/+44)
intergenic (-88/+40)
intergenic (-143/-13)
intergenic (-281/-58)
intergenic (-453/-72)
coding (77-122/681 nt)
intergenic (-213/-254)

gene_product 6-phosphofructokinase type VI secretion system ATPase TssH TetR/AcrR family transcriptional regulator helix-turn-helix transcriptional regulator/hypothetical protein type VI secretion system baseplate subunit TssF/penicillin acylase family protein TetR/AcrR family transcriptional regulator flagellar assembly protein FliH EscU/YscU/HrcU family type III secretion system export apparatus switch protein/PepSY-asso MBL fold metallo-hydrolase type VI secretion system tip protein VgrG amidohydrolase family protein/efflux RND transporter periplasmic adaptor subunit amidohydrolase family protein/efflux RND transporter periplasmic adaptor subunit GNAT family N-acetyltransferase/GntR family transcriptional regulator hypothetical protein arsenate reductase (glutaredoxin)/AAA family ATPase NADH-quinone oxidoreductase subunit D/NADH-quinone oxidoreductase subunit NuoE helix-turn-helix domain-containing protein/H-NS histone family protein hypothetical protein type VI secretion system membrane subunit TssM GNAT family N-acetyltransferase/GntR family transcriptional regulator tRNA uridine-5-carboxymethylaminomethyl(34) synthesis GTPase MnmE/transcriptional regu amidohydrolase family protein/efflux RND transporter periplasmic adaptor subunit flagellar assembly protein FliH MFS transporter/LysR substrate-binding domain-containing protein

mutation_category	new_seq	position	position_end	position_start	size	snp_type
small_indel		3545222	3545228	3545222	7	
small_indel		1012569	1012577	1012569	9	
small_indel	TGCAGGC	1039294	1039294	1039294		
small_indel		1519708	1519714	1519708	7	
small_indel	ACAGGCG	725350	725350	725350		
small_indel	TGCAGGC	1039294	1039294	1039294		
small_indel		232548	232593	232548	46	
small_indel		239205	239212	239205	8	
small_indel	TCGGCGC	1476934	1476934	1476934		
snp_synonymous	G	153747	153747	153747	NC_00765	synonymou
snp_intergenic	Α	1539855	1539855	1539855	NC_00765	intergenic
snp_intergenic	Α	1539855	1539855	1539855		intergenic
snp_intergenic	Α	2581752	2581752	2581752		intergenic
small_indel		2713058	2713066	2713058	9	
small_indel	GTTGGC	2908216	2908216	2908216		
snp_intergenic	T	1206554	1206554	1206554		intergenic
small_indel		2458559	2458559	2458559	1	
small_indel		2815276	2815301	2815276	26	
small_indel		3397661	3397666	3397661	6	
snp_intergenic		1038667	1038667	1038667		intergenic
small_indel	TGCAGGC	1039294	1039294	1039294		
small_indel		177802	177804	177802		
small_indel	ATCGGC	728113	728113	728113		
snp_intergenic		757464	757464	757464		intergenic
snp_intergenic	G	757468	757468	757468		intergenic
snp_intergenic	Α	2581752	2581752	2581752		intergenic
snp_intergenic	Α	3686634	3686634	3686634		intergenic
snp_intergenic	Α	1539855	1539855	1539855		intergenic
small_indel		232548	232593	232548	46	
large_deletion		1371337	1371387	1371337	51	

type DEL DEL INS DEL INS INS DEL DEL INS SNP SNP SNP SNP DEL INS SNP DEL DEL DEL SNP SNP SNP

DEL DEL

Summary of result	Summary of results from breseq							
Organism	Evolved line and replicate	aa_new_s	aa_positio	aa_ref_sec	clone			
B. thailandensis	Coevolved replicate 1							
B. thailandensis	Coevolved replicate 2							
B. thailandensis	Coevolved replicate 2							
B. thailandensis	Coevolved replicate 2							
B. thailandensis	Coevolved replicate 2							
B. thailandensis	Coevolved replicate 3							
B. thailandensis	Coevolved replicate 3							
B. thailandensis	Coevolved replicate 3							
B. thailandensis	Coevolved replicate 4							
B. thailandensis	Coevolved replicate 5	Р	825	Р				
B. thailandensis	Coevolved replicate 5							
B. thailandensis	Monoculture replicate 1							
B. thailandensis	Monoculture replicate 1							
B. thailandensis	Monoculture replicate 1							
B. thailandensis	Monoculture replicate 1							
B. thailandensis	Monoculture replicate 1							
B. thailandensis	Monoculture replicate 2							
B. thailandensis	Monoculture replicate 2							
B. thailandensis	Monoculture replicate 2							
B. thailandensis	Monoculture replicate 3							
B. thailandensis	Monoculture replicate 3							
B. thailandensis	Monoculture replicate 3							
B. thailandensis	Monoculture replicate 3							
B. thailandensis	Monoculture replicate 3							
B. thailandensis	Monoculture replicate 3							
B. thailandensis	Monoculture replicate 4							
B. thailandensis	Monoculture replicate 4							
B. thailandensis	Monoculture replicate 5							
B. thailandensis	Monoculture replicate 5							
B. thailandensis	Monoculture replicate 5							

codon_nev	codon_nur	codon_pos	codon_pos	codon_ref	gene_name
					BTH_RS35420
					tssH
					BTH_RS04590
					BTH_RS06525/BTH_
					tssF/BTH_RS15400
					BTH_RS04590
					fliH
					BTH_RS13245/BTH_
					BTH_RS06340
CCG	825	3		CCA	vgrG
					BTH_RS06600/BTH_
					BTH_RS06600/BTH_
					BTH_RS10750/BTH_
					BTH_RS35120
					arsC/BTH_RS12180
					BTH_RS17640/nuoE
					BTH_RS10275/BTH_
					BTH_RS11790
					tssM
					BTH_RS04585/BTH_
					BTH_RS04590
					BTH_RS12945/gatC
					BTH_RS33635
					waaF/BTH_RS1555
					waaF/BTH_RS1555!
					BTH_RS10750/BTH_
					mnmE/BTH_RS2866
					BTH_RS06600/BTH_
					fliH
					BTH_RS18425/BTH_

gene_position	gene_product	gene_strai	genes_inactiva
pseudogene (127-133/135 nt)	6-phosphofructokinase	>	
coding (2789-2797/2877 nt)	type VI secretion system ATPas	<	
coding (595/912 nt)	TetR/AcrR family transcriptiona	>	BTH_RS04590
intergenic (+87/+147)	helix-turn-helix transcriptional ı	>/<	
intergenic (-714/-269)	type VI secretion system basep		
coding (595/912 nt)	TetR/AcrR family transcriptiona	>	BTH_RS04590
coding (77-122/681 nt)	flagellar assembly protein FliH	<	fliH
intergenic (+337/-191)	EscU/YscU/HrcU family type III	>/>	
coding (326/1593 nt)	MBL fold metallo-hydrolase	>	BTH_RS06340
2475	type VI secretion system tip pro	>	
intergenic (-453/-72)	amidohydrolase family protein/		
intergenic (-453/-72)	amidohydrolase family protein/		
intergenic (-143/-13)	GNAT family N-acetyltransfera		
coding (221-229/477 nt)	hypothetical protein	>	BTH_RS35120
intergenic (-222/-297)	arsenate reductase (glutaredox		
intergenic (+143/-19)	NADH-quinone oxidoreductase :	>/>	
intergenic (-41/-276)	helix-turn-helix domain-contain		
coding (33-58/276 nt)	hypothetical protein	<	BTH_RS11790
coding (1364-1369/3906 nt)	type VI secretion system memb	>	tssM
intergenic (-79/-33)	Tm-1-like ATP-binding domain-		
coding (595/912 nt)	TetR/AcrR family transcriptiona		BTH_RS04590
intergenic (-176/-188)	rod shape-determining protein/		
coding (105/207 nt)	hypothetical protein		BTH_RS33635
intergenic (-84/+44)	lipopolysaccharide heptosyltran		
intergenic (-88/+40)	lipopolysaccharide heptosyltran		
intergenic (-143/-13)	GNAT family N-acetyltransfera		
intergenic (-281/-58)	tRNA uridine-5-carboxymethyla		
intergenic (-453/-72)	amidohydrolase family protein/		
coding (77-122/681 nt)	flagellar assembly protein FliH	<	fliH
intergenic (-213/-254)	MFS transporter/LysR substrate		

genes_overlapping	genes_promoter	insert_position			locus_tags
BTH_RS35420			BTH_RS35	420	BTH_RS35
tssH			BTH_RS04	485	BTH_RS04
		1	BTH_RS04	BTH_RS04	590
	BTH_RS06530			525/BTH_R	
		1		395/BTH_R	
		1		BTH_RS04	
				BTH_RS13	
	BTH_RS13250		_	245/BTH_R	
		1		BTH_RS06	
vgrG			BTH_RS00		BTH_RS00
				<mark>600/BTH_R</mark>	
				600/BTH_R	
	BTH_RS10750			750/BTH_R	
				BTH_RS35	
		1		175/BTH_R	
	nuoE			640/BTH_R	
	BTH_RS10275			275/BTH_R	
				BTH_RS11	
				BTH_RS27	
	BTH_RS04585				
		1			
				945/BTH_R	
		1			
	waaF				
	waaF			550/BTH_R	
	BTH_RS10750			750/BTH_R	
				655/BTH_R	
				600/BTH_R	
				BTH_RS13	
			BTH_RS18	425/BTH_R	S18430

locus_tags	mutation_ mutator_s	new_seq	population	position	position_e	position_s	ref_seq
420	small_indel			3545222	3545228	3545222	GCGGCAA
485	small_indel			1012569	1012577	1012569	CGTTGGG
	small_indel	TGCAGGC	GGCGCTCG	1039294	1039294	1039294	G
BTH_RS06	small_indel			1519708	1519714	1519708	CCATCCG
	small_indel	ACAGGCG		725350	725350	725350	G
	small_indel	TGCAGGC	GGCGCTCG	1039294	1039294	1039294	G
	small_indel			232548	232593	232548	46-bp
BTH_RS13	small_indel			239205	239212	239205	ACCGGAT(
	small_indel	TCGGCGC		1476934	1476934	1476934	С
660	snp_synonymous	G		153747	153747	153747	Α
	snp_intergenic	A		1539855	1539855	1539855	Т
	snp_intergenic	Α		1539855	1539855	1539855	Т
BTH_RS10	snp_intergenic	Α		2581752	2581752	2581752	G
	small_indel			2713058	2713066	2713058	GTAATGC(
	small_indel	GTTGGC		2908216	2908216	2908216	С
BTH_RS17	snp_intergenic	T		1206554	1206554	1206554	G
BTH_RS10	small_indel			2458559	2458559	2458559	Α
	small_indel			2815276	2815301	2815276	26-bp
	small_indel			3397661	3397666	3397661	CGCTCG
BTH_RS04	snp_intergenic			1038667	1038667	1038667	Α
		TGCAGGC		1039294	1039294	1039294	G
				177802	177804	177802	GCG
		ATCGGC		728113	728113	728113	С
BTH_RS15	snp_intergenic			757464	757464	757464	С
BTH_RS15	snp_intergenic			757468	757468	757468	С
BTH_RS10	snp_intergenic	Α		2581752	2581752	2581752	
	snp_intergenic	Α		3686634	3686634	3686634	
	snp_intergenic	Α		1539855	1539855	1539855	Т
	small_indel			232548	232593	232548	46-bp
	large_deletion			1371337	1371387	1371337	51-bp

repeat_ler	repeat_ne	repeat_ref_c	repeat_seq	seq	_id	size	snp_type	time
7	13	14	GCGGCAA	NC_	_00765	7		-1
9	8	9	CGTTGGGCG	NC_	00765	9		-1
					_00765			-1
7	8	9	CCATCCG		00765			-1
7	8	7	ACAGGCG	_	00765			-1
				_	00765	0		-1
				_	_00765	46		-1
8	5		ACCGGATC	_	_00765			-1
7	2	1	TCGGCGC	NC_	00765			-1
							synonymo:	-1
							intergenic	-1
				_	00765		intergenic	-1
				_	00765		intergenic	-1
9	6	7	GTAATGCGG					-1
6	4	3	GTTGGC		00765			-1
					_00765		intergenic	-1
				_	_00765			-1
				_	_00765			-1
6	2	3	CGCTCG	_	00765	6		-1
							intergenic	-1
								-1
3								-1
6			ATCGGC					-1
							intergenic	-1
				_	00765		intergenic	-1
			G		00765		intergenic	-1
			G	_	_00765		intergenic	-1
					00765		intergenic	-1
				_	_00765			-1
				NC_	_00765	51		-1

title	transl_tab	treatment	type
output			DEL
output			DEL
output			INS
output			DEL
output			INS
output			INS
output			DEL
output			DEL
output			INS
output	11		SNP
output			DEL
output			INS
output			SNP
output			DEL
output			DEL
output			DEL
output			SNP
output			INS
output			
output			INS
output			SNP
output			DEL
output			DEL

Organism	Strain	Replicate
Burkholderia thailandensis	Ancestor	0
Burkholderia thailandensis	Ancestor	0
Burkholderia thailandensis	Ancestor	0
Burkholderia thailandensis	Coevolved	1
Burkholderia thailandensis	Coevolved	1
Burkholderia thailandensis	Coevolved	1_
Burkholderia thailandensis	Coevolved	2
Burkholderia thailandensis	Coevolved	2
Burkholderia thailandensis	Coevolved	2
Burkholderia thailandensis	Coevolved	3
Burkholderia thailandensis	Coevolved	3
Burkholderia thailandensis	Coevolved	3
Burkholderia thailandensis	Coevolved	4
Burkholderia thailandensis	Coevolved	4
Burkholderia thailandensis	Coevolved	4
Burkholderia thailandensis	Coevolved	5
Burkholderia thailandensis	Coevolved	5
Burkholderia thailandensis	Coevolved	5
Burkholderia thailandensis	Monoculture evolved	1
Burkholderia thailandensis	Monoculture evolved	1
Burkholderia thailandensis	Monoculture evolved	1
Burkholderia thailandensis	Monoculture evolved	2
Burkholderia thailandensis	Monoculture evolved	2
Burkholderia thailandensis	Monoculture evolved	2
Burkholderia thailandensis	Monoculture evolved	3
Burkholderia thailandensis	Monoculture evolved	3
Burkholderia thailandensis	Monoculture evolved	3
Burkholderia thailandensis	Monoculture evolved	4
Burkholderia thailandensis	Monoculture evolved	4
Burkholderia thailandensis	Monoculture evolved	4
Burkholderia thailandensis	Monoculture evolved	5
Burkholderia thailandensis	Monoculture evolved	5
Burkholderia thailandensis	Monoculture evolved	5_
Flavobacterium johnsoniae	Ancestor	0
Flavobacterium johnsoniae	Ancestor	0
Flavobacterium johnsoniae	Ancestor	0
Flavobacterium johnsoniae	Coevolved	1
Flavobacterium johnsoniae	Coevolved	1
Flavobacterium johnsoniae	Coevolved	1
Flavobacterium johnsoniae	Coevolved	2
Flavobacterium johnsoniae	Coevolved	2
Flavobacterium johnsoniae	Coevolved	2
Flavobacterium johnsoniae	Coevolved	3
Flavobacterium johnsoniae	Coevolved	3
Flavobacterium johnsoniae	Coevolved	3
Flavobacterium johnsoniae	Coevolved	4
Flavobacterium johnsoniae	Coevolved	4
Flavobacterium johnsoniae	Coevolved	4
Flavobacterium johnsoniae	Coevolved	5
Flavobacterium johnsoniae	Coevolved	5

Flavobacterium johnsoniae	Coevolved	5
Flavobacterium johnsoniae	Monoculture evolved	1
Flavobacterium johnsoniae	Monoculture evolved	1
Flavobacterium johnsoniae	Monoculture evolved	1
Flavobacterium johnsoniae	Monoculture evolved	2
Flavobacterium johnsoniae	Monoculture evolved	2
Flavobacterium johnsoniae	Monoculture evolved	2
Flavobacterium johnsoniae	Monoculture evolved	3
Flavobacterium johnsoniae	Monoculture evolved	3
Flavobacterium johnsoniae	Monoculture evolved	3
Flavobacterium johnsoniae	Monoculture evolved	4
Flavobacterium johnsoniae	Monoculture evolved	4
Flavobacterium johnsoniae	Monoculture evolved	4
Flavobacterium johnsoniae	Monoculture evolved	5
Flavobacterium johnsoniae	Monoculture evolved	5
Flavobacterium johnsoniae	Monoculture evolved	5
Flavobacterium johnsoniae	tolc_33bp_recombinant	0
Flavobacterium johnsoniae	tolc_33bp_recombinant	0
Flavobacterium johnsoniae	tolc_33bp_recombinant	0

File	% reads Q>: ı	reads	% mapped
Burk_anc_S87_R1_001_paired	99.6	1782341	99.9
Burk_anc_S87_R1_001_unpaired	92.9	101358	99.8
Burk_anc_S87_R2_001_paired	99.1	1781191	95.4
Burk_coevo_R1_S93_R1_001_paired	99.6	1456068	99.9
Burk_coevo_R1_S93_R1_001_unpaired	93.7	113336	99.8
Burk_coevo_R1_S93_R2_001_paired	98.8	1454980	95.2
Burk_coevo_R2_S94_R1_001_paired	99.6	1171980	99.9
Burk_coevo_R2_S94_R1_001_unpaired	93.7	90937	99.8
Burk_coevo_R2_S94_R2_001_paired	98.8	1171047	95.6
Burk_coevo_R3_S95_R1_001_paired	99.6	1203099	99.9
Burk_coevo_R3_S95_R1_001_unpaired	94	100148	99.8
Burk_coevo_R3_S95_R2_001_paired	98.8	1201991	96.4
Burk_coevo_R4_S96_R1_001_paired	99.6	10181397	99.9
Burk_coevo_R4_S96_R1_001_unpaired	93.8	84656	99.8
Burk_coevo_R4_S96_R2_001_paired	98.8	1080524	94.2
Burk_coevo_R5_S97_R1_001_paired	99.6	1517293	99.9
Burk_coevo_R5_S97_R1_001_unpaired	93	102422	99.8
Burk_coevo_R5_S97_R2_001_paired	99	1516104	95.6
Burk mono R1 S88 R1 001 paired	99.6	1240546	99.9
Burk_mono_R1_S88_R1_001_unpaired	93.5	87509	99.8
Burk_mono_R1_S88_R2_001_paired	98.9	1239531	95.3
Burk_mono_R2_S89_R1_001_paired	99.6	1141925	99.3
Burk_mono_R2_S89_R1_001_unpaired	93.9	89352	99.5
Burk_mono_R2_S89_R2_001_paired	98.8	1140884	95.9
Burk_mono_R3_S90_R1_001_paired	99.6	1239128	99.9
Burk_mono_R3_S90_R1_001_unpaired	93.5	87335	99.8
Burk_mono_R3_S90_R2_001_paired	98.9	1238229	95.3
Burk_mono_R4_S91_R1_001_paired	99.6	1533822	99.9
Burk_mono_R4_S91_R1_001_unpaired	93.8	117734	99.8
Burk_mono_R4_S91_R2_001_paired	98.8	1532619	96.1
Burk_mono_R5_S92_R1_001_paired	99.6	1518053	99.9
Burk_mono_R5_S92_R1_001_unpaired	93.8	113007	99.8
Burk_mono_R5_S92_R2_001_paired	98.9	1516767	98
Fj_anc_S47_R1_001_paired	99.7	1086306	99.9
Fj_anc_S47_R1_001_unpaired	94.4	207587	99.7
Fj_anc_S47_R2_001_paired	99.1	1085767	99.9
Fj_co1_S48_R1_001_paired	99.8	844209	99.9
Fj_co1_S48_R1_001_unpaired	94.7	164471	99.8
Fj_co1_S48_R2_001_paired	99	843838	99.9
Fj_co2_S49_R1_001_paired	99.7	1187836	99.9
Fj_co2_S49_R1_001_unpaired	94.4	169960	99.7
Fj_co2_S49_R2_001_paired	99.3	1187195	99.9
Fj_co3_S50_R1_001_paired	99.7	989588	99.9
Fj_co3_S50_R1_001_unpaired	94.5	142475	99.8
Fj_co3_S50_R2_001_paired	99.3	989036	99.9
Fj_co4_S51_R1_001_paired	99.7	948034	99.9
Fj_co4_S51_R1_001_unpaired	94.1	136839	99.7
Fj_co4_S51_R2_001_paired	99.3	947580	99.9
Fj_co5_S52_R1_001_paired	99.5	864002	99.9
Fj_co5_S52_R1_001_unpaired	93.7	108985	99.6

F:F (F2 P2 001	00.2	062565	00.0
Fj_co5_S52_R2_001_paired	99.2	863565	99.9
Fj_mc1_S53_R1_001_paired	99.6	930277	99.9
Fj_mc1_S53_R1_001_unpaired	93.8	115078	99.8
Fj_mc1_S53_R2_001_paired	99.3	929848	99.9
Fj_mc2_S54_R1_001_paired	99.7	1126329	99.9
Fj_mc2_S54_R1_001_unpaired	93.9	151560	99.7
Fj_mc2_S54_R2_001_paired	99.3	1125752	99.9
Fj_mc3_S55_R1_001_paired	99.7	1167708	99.9
Fj_mc3_S55_R1_001_unpaired	94	150160	99.7
Fj_mc3_S55_R2_001_paired	99.3	1167069	99.9
Fj_mc4_S56_R1_001_paired	99.7	611216	99.9
Fj_mc4_S56_R1_001_unpaired	94.4	87941	99.7
Fj_mc4_S56_R2_001_paired	99.3	610912	99.9
Fj_mc5_S57_R1_001_paired	99.7	648699	99.9
Fj_mc5_S57_R1_001_unpaired	94.2	82410	99.8
Fj_mc5_S57_R2_001_paired	99.4	648407	99.9
Flavo_33bp_eng_S98_R1_001_paired	99.7	1360293	100
Flavo_33bp_eng_S98_R1_001_unpaired	88.4	45693	99.9
Flavo_33bp_eng_S98_R2_001_paired	99.3	1359576	97.2

78.4	87.2
57	61
3,	
 53.7	56.3
55.9	63.6
70.5	79.6
 61.8	77.6
71.2	72.3
 55	60.5
58.3	53.4
53.3	51.2
67.1	74.9
49.3	
38.6	
47.2	
 43.8	
 42.1	

38.4
41.2
50.3
51.2
27.6
29.1
66.4